Doctoral theses at NTNU, 2020:155

Fahim Abid

Characteristics of Switching Arc in Ultrahigh-pressure Nitrogen

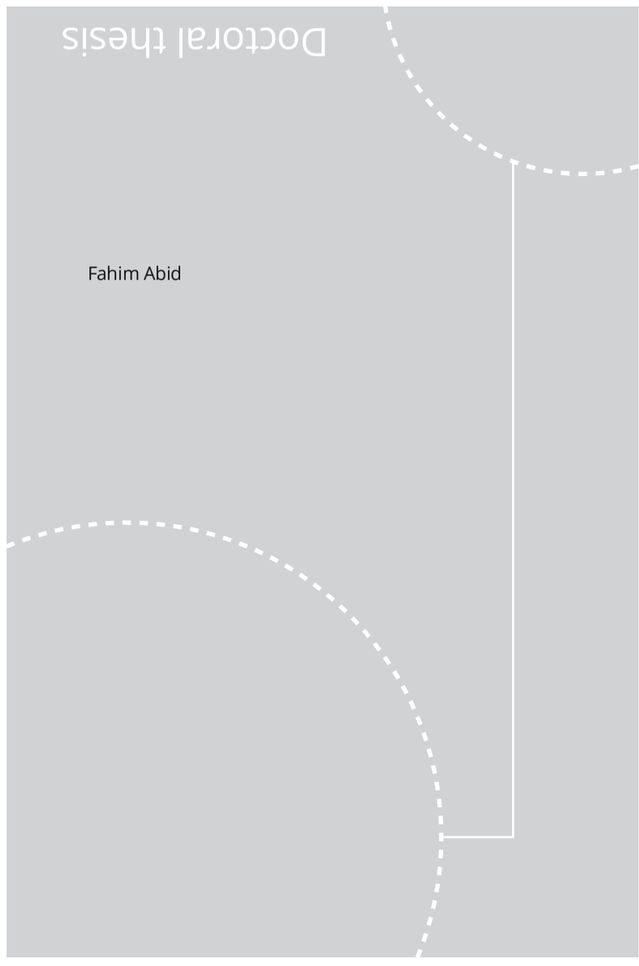

ISBN 978-82-326-4658-6 (printed ver.)
ISBN 978-82-326-4659-3 (electronic ver.)
ISSN 1503-8181

NTNU
Norwegian University of
Science and Technology

NTNU
Norwegian University of Science and Technology
Thesis for the Degree of
Philosophiae Doctor
Faculty of Information Technology and Electrical
Engineering
Department of Electric Power Engineering

Doctoral theses at NTNU, 2020:155

NTNU
Norwegian University of
Science and Technology

Fahim Abid

Characteristics of Switching Arc in Ultrahigh-pressure Nitrogen

Thesis for the Degree of Philosophiae Doctor

Trondheim, May 2020

Norwegian University of Science and Technology
Faculty of Information Technology and Electrical Engineering
Department of Electric Power Engineering

NTNU
Norwegian University of
Science and Technology

NTNU
Norwegian University of Science and Technology

Thesis for the Degree of Philosophiae Doctor

Faculty of Information Technology and Electrical Engineering
Department of Electric Power Engineering

ISBN 978-82-326-4658-6 (printed ver.)
ISBN 978-82-326-4659-3 (electronic ver.)
ISSN 1503-8181

Doctoral theses at NTNU, 2020:155

Printed by NTNU Grafisk senter

To my parents

Abstract

An increasing number of wind farms and mining operations located far off the coast will lead to the development of offshore substations. To avoid the large costs associated with platforms and floaters, such a substation can be placed on the seabed and controlled remotely. The conventional solution is to place the power components, e.g. switchgear placed inside thick-walled pressure-proof vessels to protect them from water and high pressure on the seabed. For current switching in medium voltage applications, there are mainly two options: vacuum circuit breakers or gas circuit breakers (filled at atmospheric or slightly elevated pressure). Whichever option is chosen, power cable feed-throughs or penetrators from the high-pressure water environment into the low pressure inside the vessel are required. These features add substantial technical complexity and costs, in particular at large sea depths. A novel concept is used in this thesis, where the interruption chamber of the circuit breaker can be gradually filled as the switchgear is lowered until finally reaching the same pressure as on the seabed. Reducing the differential pressure on the encapsulation will reduce the overall cost and complexity of such subsea substations. The gas pressures in this case may be in the range of up to tens of bars.

If the temperature and pressure of a gas exceed its critical point, it enters a supercritical state. In this state, the physical properties are between that of a gas and a liquid. The properties include high diffusivity, high heat conductivity, high heat capacity, high dielectric strength and an absence of vapour bubbles. These properties of the supercritical fluid are believed to be in favour of a successful current interruption medium. However, there is a distinct lack of knowledge on arc properties and the current interruption capability of extremely high-pressure gasses as well as on the supercritical region. In this thesis, nitrogen (N_2) is chosen for its low critical point (33.5 bar, 126 K), good insulation strength and environment-friendly nature. As the critical temperature of N_2 is lower than room temperature, the transition to supercritical state can be achieved by pressurizing N_2 above 33.5 bar.

This thesis reports on the experimental investigation of the characteristics of N_2 arc as a function of filling pressure as well as in the supercritical state. For the bulk of the study, filling pressures of 1, 20, 40 and 80 bar are investigated, the latter two being in the supercritical state. A fixed electrode arrangement is used where the arc is initiated by the melting of a copper ignition wire. The investigated arc current amplitude is in the range of 85 A to 450 A at a frequency of 190 Hz to 950 Hz. Based on the focus area of different phases of the arc, this thesis can primarily be divided into three major parts. First, the arc properties during the high-current phase, i.e. during current peak time, are investigated for free-burning and tube-constricted arcs. In the second phase, the investigation is focused near the current zero (CZ) where the thermal phase of the arc is studied. In the final phase, the post-arc dielectric recovery characteristics are studied. The effect of the forced gas flow is investigated in both the thermal and dielectric phase of the arc.

Based on the experimental results, the arc voltage is found to increase with the filling pressure without any abrupt change during the transition from gas

to the supercritical state. Increased current density due to the constriction of the arc at high filling pressure turned out to be the dominant factor for the high arc voltage. When the free-burning arc is physically constricted by means of burning inside a tube, an inverse relation between the arc voltage and the inner tube diameter is observed at 1 bar, as expected. At higher filling pressures, however, such a simple relationship does not exist. The reduced arc radius and the increased absorption of radiation at high filling pressures may limit the interaction between the arc and the tube.

The energy deposition in the arc increases while the arc radius decreases with increasing filling pressure. The arc gets constricted and as a result the temperature of the arc core increases. In the free-burning arc, in the absence of forced cooling, the arc core fails to dissipate the stored thermal energy quickly. As a result, without efficient cooling a high post-arc current is often observed at a high filling pressure compared to at 1 bar. The high energy deposition in the post-arc channel due to increased post-arc current causes an early re-ignition at high N_2 pressure compared to at 1 bar. A forced gas flow, however, significantly enhances cooling at high filling pressures and improves the interruption performance.

In the free-burning arc arrangement, the post-arc dielectric strength of the gap increases rapidly with increasing filling pressure, only after a critical time delay following CZ. This critical time delay is probably linked to the temperature decay of the gap. Below the critical time delay, however, the dielectric strength of the gap is lower at a higher filling pressure in contrast to at 1 bar, similar to what is observed in the thermal re-ignitions of the free-burning arc. Forced gas flow significantly enhances the dielectric recovery of the arc channel at a high filling pressure, also in the thermal phase. The experiments indicate that although the thermal phase is the critical phase of the ultrahigh-pressure N_2 arc interruption, the dielectric phase is inherently superior at a high filling pressure compared to atmospheric pressure. With the help of efficient cooling, the thermal phase can be improved, and hence the ultrahigh-pressure N_2 reveals its potential to be used as a current interruption medium.

Preface

The work on this thesis was carried out in the period between September 2016 and December 2019. It is submitted as a paper collection, partially fulfilling the requirements for the Degree of Philosophiae Doctor (Ph.D.) at the Department of Electric Power Engineering at Norwegian University of Science and Technology (NTNU). This work has been supported by the NTNU, the Research Council of Norway and SINTEF Energy Research. Professor Kaveh Niayesh has been the main supervisor for this work with Chief Scientist Magne Runde from SINTEF Energy acting as co-supervisor.

Acknowledgments

I express my heartfelt gratitude to my supervisor, Professor Kaveh Niayesh, for his guidance throughout the whole Ph.D. process. Your advice on research and writing was invaluable. Whenever and wherever I needed your guidance during my Ph.D., your door for discussion was always open. I could not have imagined having a better supervisor than you during my Ph.D. study.

I would like to thank SINTEF Energy Research for providing me access to the unique laboratory facility in Tiller. Special thanks to Chief Scientist Magne Runde for his support, and particularly for introducing me to SINTEF Energy in the early days of the project when I could not see the light at the end of the tunnel. Nina Støa-Aanensen from SINTEF Energy helped me from the very first day until the end, spent her valuable time fixing issues, accompanied me in the laboratory and helped immensely with the writing process. Without your help, it would not have been possible to finish this Ph.D. on time. Erik Jonsson from SINTEF Energy helped during the initial laboratory setup. Thanks to Camilla Espedal from SINTEF Energy. Discussion of various aspects of the project from time to time with Ali Kadivar, Henning Taxt, Emre Kanter, Hans Kristian Meyer, Naghme Dorraki and Milad Mohammadhosein were very fruitful.

This Ph.D. project involved building a new test setup to experimentally investigate the arc discharge at extremely high filling pressure. Many people at the Department of Electric Power Engineering at NTNU and SINTEF Energy Research have largely contributed throughout the project. I would like to thank Aksel Andreas Reitan Hanssen, Morten Flå, Dominik Häger, Bård Almås, Vladimir Klubicka, Horst Forster, Oddgeir Rokseth and Oddgeir Kvien. Contributions from M.Sc. student Shashidhara Basavapura Thimmappa and summer internship student Egil Viken are highly acknowledged in this thesis.

Last, but not least, I would like to thank my parents, my wife Arik Subhana and the two lovely families I am part of; without their support it would have been impossible for me to pursue my dreams. When I was a child, it was my father who whispered into my ears that I should be a researcher, it was you who showed me dreams. I dedicate this thesis to my parents.

Fahim Abid
Trondheim, December 2019

List of Publications and the Candidate's Contribution

I. Fahim Abid, Kaveh Niayesh, Erik Jonsson, Nina Støa-Aanensen and Magne Runde, "*Arc Voltage Characteristics in Ultrahigh-Pressure Nitrogen Including Supercritical Region*," in IEEE Transactions on Plasma Science, vol. 46, no. 1, pp. 187–193, Jan. 2018.

Fahim Abid planned the experiment, built the test setup together with Erik Jonsson, carried out the experiments together with Erik Jonsson and Nina Støa-Aanensen, post-processed, plotted and interpreted the results and wrote and edited the paper. All the co-authors contributed through discussion of the results and provided feedback to improve presentation and language.

II. Fahim Abid, Kaveh Niayesh, Nina Støa-Aanensen, "*Ultrahigh-Pressure Nitrogen Arc Burning Inside Cylindrical Tubes*," in IEEE Transactions on Plasma Science, vol. 47, no. 1, pp. 754–761, Jan. 2019.

Fahim Abid planned the experiment, carried out the experiments together with Nina Støa-Aanensen, post-processed, plotted and interpreted the results and wrote and edited the paper. All the co-authors contributed through discussion of the results and provided feedback to improve presentation and language.

III. Fahim Abid, Kaveh Niayesh, Nina Sasaki Støa-Aanensen, '*Nozzle wear and pressure rise in heating volume of self-blast type ultra-high pressure nitrogen arc*', in Journal of Plasma Physics and Technology, vol. 6, no.1, pp 23–26, 2019.

Fahim Abid planned the experiment, designed and built the passive transient recovery voltage (TRV) circuit and the model switch, carried out the experiments together with Nina Støa-Aanensen, post-processed, plotted and interpreted the results and wrote and edited the paper. All the co-authors contributed through discussion of the results and provided feedback to improve presentation and language.

IV. Fahim Abid, Kaveh Niayesh, Camilla Espedal, Nina Støa-Aanensen, "*Current Interruption Performance of Ultra-high Pressure Nitrogen Arc*," in Journal of Physics D: Applied Physics, vol. 53, 2020.

Fahim Abid planned the experiment, designed and built the passive TRV circuit, carried out the experiments together with Camilla Espedal and Nina Støa-Aanensen, post-processed, plotted and interpreted the results and wrote and edited the paper. All the co-authors contributed through discussion of the results and provided feedback to improve presentation and language.

V. Fahim Abid, Kaveh Niayesh, Egil Viken, Nina Støa-Aanensen, Erik Jonsson, and Hans Kristian Meyer, "*Effect of Filling Pressure on Post-Arc Gap Recovery of N_2*," accepted in IEEE Transactions on Dielectrics and Electrical Insulation.

Fahim Abid planned the experiment, designed and built the high voltage pulse injection circuit, carried out the experiments together

with Egil Viken, Nina Støa-Aanensen, Erik Jonsson and Hans Kristian Meyer, post-processed, plotted and interpreted the results and wrote and edited the paper. Erik Jonsson built the puffer arrangement. All the co-authors contributed through discussion of the results and provided feedback to improve presentation and language.

VI. Fahim Abid, Kaveh Niayesh, Shashidhara Basavapura Thimmappa, Camilla Espedal, Nina Sasaki Støa-Aanensen, "*Thermal Interruption Performance of Ultrahigh-Pressure Free-burning Nitrogen Arc*," in Lecture Notes in Electrical Engineering, Springer, vol. 599, pp 663–671, 2019.

Fahim Abid planned the experiment, designed and built the passive TRV circuit, carried out the experiments together with Shashidhara Basavapura Thimmappa, Camilla Espedal and Nina Støa-Aanensen, post-processed, plotted and interpreted the results and wrote and edited the paper. All the co-authors contributed through discussion of the results and provided feedback to improve presentation and language.

VII. Fahim Abid, Kaveh Niayesh, Nina Sasaki Støa-Aanensen, '*Arc Voltage Distribution Measurement in Tube Constricted Ultrahigh-Pressure Nitrogen Arc*', in Lecture Notes in Electrical Engineering, Springer, vol. 599, pp 672–679, 2019.

Fahim Abid planned the experiment, designed the probe measurement system, carried out the experiments together with Nina Støa-Aanensen, post-processed, plotted and interpreted the results and wrote and edited the paper. All the co-authors contributed through discussion of the results and provided feedback to improve presentation and language.

VIII. Fahim Abid, Kaveh Niayesh, Nina Støa-Aanensen, Erik Jonsson, Magne Runde, "*Arc Voltage Measurements of Ultrahigh-Pressure Nitrogen Arc in Cylindrical Tubes*," in 22nd international conference on gas discharge and their application, Novi Sad, Serbia, Sep 2–7, 2018.

Fahim Abid planned the experiment, carried out the experiments together with Nina Støa-Aanensen, post-processed, plotted and interpreted the results and wrote and edited the paper. All the co-authors contributed through discussion of the results and provided feedback to improve presentation and language.

IX. Fahim Abid, Kaveh Niayesh, Nina Sasaki Støa-Aanensen, '*Post-arc Dielectric Recovery Characteristics of Free-burning Ultrahigh-Pressure Nitrogen Arc*', in 5th International conference on Electric Power Equipment- Switching Technology, Kitakyushu, Japan, Oct 13–16, 2019.

Fahim Abid planned the experiment, built the high voltage pulse injection circuit, carried out the experiments together with Nina Støa-Aanensen, post-processed, plotted and interpreted the results and wrote the paper. All the co-authors contributed through discussion of

the results and provided feedback to improve presentation and language.

Contents

1. Introduction 1
   1.1. Problem Description 2
   1.2. Scope of the Work and Limitations 3
2. Theory and Methodology 5
   2.1 The Electric Arc 5
   2.2 Method 6
      2.2.1 High-current Phase 6
      2.2.2 Thermal Phase 7
      2.2.3 Dielectric Recovery Characteristics 9
3. Experimental Setup 11
   3.1 Electrode and Nozzle Arrangement 11
      3.1.1 Free-burning Arc 12
      3.1.2 Tube-constricted Arc 12
      3.1.3 Self-blast Arrangement 14
      3.1.4 Puffer Arrangement 14
   3.2 Measured Parameters 15
4 Publications 17
5. Summary of the Results and Conclusions 105
   5.1 High-current Phase 105
   5.2 Thermal Interruption Performance 108
   5.3 Post-arc Dielectric Recovery Characteristics 109
   5.4 Conclusions 111
   5.5 Suggestions for Future Work 112
References 115

Chapter 1

1. Introduction

Approximately 71% of the world's surface is covered by water. Due to the depletion of available mining resources on land, experts believe that there is a huge potential for offshore mining [1]. Furthermore, there is an increasing trend of wind farms being built far away from the shore. The need to transfer power to and from offshore installations will lead to the development of offshore substations. To materialise such a substation, there are two possible paths to follow: one path is to place the electrical equipment on a platform or floater above sea level. Another path is to directly place the equipment on the seafloor and control it remotely. Among these two options, the latter is more economically viable [2]. The major benefit of building the substation on the seabed is that it is safe from hazards such as icebergs and hurricanes, and the labor cost can be dramatically reduced as the operation will be controlled remotely [3]. The conventional solution is to use a thick-walled steel pressure-proof vessel to provide an environment for the power components (e.g. switchgear) like that of onshore installations [3]. To transfer power from the high-pressure water environment at the seabed to the low pressure inside the pressure vessel, different feed-throughs or penetrators are used, as shown in Fig. 1.1(a). These features add substantial technical complexity and costs, in particular at large sea depths. A novel concept is developed in this thesis, where the interruption chamber can be filled with high-pressure gas to reduce the differential pressure exerted on the encapsulation, see Fig. 1.1(b). Reducing the differential pressure will substantially reduce the cost and complexity of the encapsulations and feed-throughs.

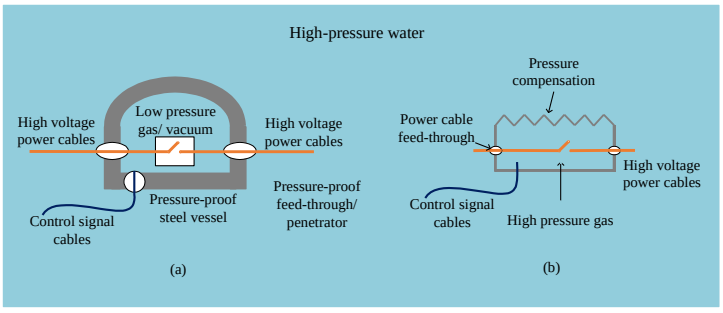

Fig. 1.1. Subsea switchgear. (a) Conventional solution. (b) The concept of filling the chamber with high-pressure gas.

If the temperature and pressure of a gas exceed a critical point, it enters into the supercritical (SC) region [4], [5]. In this SC region, liquid and gas states are united and indistinguishable [6]. For example, an SC fluid has a high density, while the viscosity is low like that of a gas. Other important properties

of an SC fluid include high diffusivity, high heat conductivity, high heat capacity, high dielectric strength and an absence of vapour bubbles [7]. In power switching applications, the switchgear must fulfil extreme demands, such as high dielectric strength when in the open position, low resistance when in the closed position, high current handling capability, high voltage rating, fast switching time, fast recovery after switching and long lifetime. The properties of an SC fluid are believed to be in favour of a successful current interruption medium [5]. Although it is difficult to use the SC fluid for land-based applications due to the extremely high pressure required, it nonetheless has a high potential for the subsea environment where high pressure already exists.

1.1. Problem Description

Medium voltage gas circuit breakers are typically filled at atmospheric or slightly elevated pressure and are sealed at the manufacturing site [8]. Increasing the gas pressure improves the dielectric strength as well as the current interruption capability [9]. For high voltage applications, the gas circuit breakers are often filled with pressures of 6–10 bar [10]. Among the different gases, sulphur hexafluoride (SF_6) has shown to have the best insulating and current interruption performance. However, the environmental concerns of SF_6 are driving the electric power industry to look for alternatives [11]. Although SC fluids are known in chemical applications, and some recent studies illustrate their favourable dielectric withstand and recovery properties, there is still no study of the arc characteristics and current interruption in those mediums [5]. SC fluid can be one possible alternative to SF_6, especially in the subsea applications.

One of the main reasons for the lack of experimental investigation on electrical discharge inside an SC medium is the need for an unusually high-pressure environment to generate the SC state. Among the works published on arc discharge at extremely high pressures, some are focused on the application in underwater welding [12], [13]. Other studies address fundamental properties of the discharge in the range of 1-mm or smaller interelectrode gaps inside SC carbon dioxide [14]–[16], helium [17] or nitrogen [7], [18], [19] under low-energy dissipation, typically in the range of millijoules. However, the energy dissipations in switching arcs are normally up to hundreds of kilojoules [20]. Although satisfying dielectric strength and dielectric recovery after low-energy spark gaps have been reported [18], [19], there is still no data available on arc quenching capabilities of such SC fluids.

The difference between properties of the best available gas, SF_6, and relevant alternatives like air, carbon dioxide (CO_2) or nitrogen (N_2) is large. For example, CO_2 exhibits fairly good current interruption performance; nonetheless, to have a comparable performance with SF_6, the filling pressure of CO_2 is often increased [9]. When choosing between different alternative gases, CO_2 is not considered in this thesis, due to its high critical pressure (72.9 bar) compared to N_2 (33.5 bar). Moreover, N_2 is environmentally benign and has good insulation strength. At room temperature when N_2 is pressurised above the critical pressure of 33.5 bar, it enters into the SC region.

1.2. Scope of the Work and Limitations

Investigating the arc properties in ultrahigh-pressure N_2 including the SC region is a novel field of research. Studying arc discharges at extremely high filling pressures is challenging because of the sudden energy deposition in a high-pressure environment. As a result, building the ultrahigh-pressure arc discharge setup to conduct the tests in a safe and secure manner is the first objective in the thesis.

Based on the investigations carried out at different phases of the arcing, the focus area in this thesis can be split into three main parts: arc characteristics near high-current phase, in the thermal phase (immediately after CZ) and post-arc dielectric recovery characteristics.

First, the free-burning arc voltage during the high-current phase of the arc as a function of filling pressure (1 bar to 98 bar) is investigated. The influence of amplitude and frequency of the arc current and the arc length on the characteristics of the free-burning arc at different filling pressures are also investigated and reported in Paper I [21]. For current interruption applications, however, the arcs are not free-burning in nature, rather a forced gas flow mechanism is used to cool the arc near CZ. To guide the gas flow through the arc, an insulating nozzle is often used, where the arc burns inside the nozzle. As a result, after investigating the free-burning arc, the effect of tube constriction on the ultrahigh-pressure N_2 arc during the high-current phase is studied and presented in Papers II and VIII [22], [23]. To investigate the effect of ablation, arcs burning inside ablating polytetrafluoroethylene (PTFE) and non-ablating alumina (ceramic) tubes are compared. The inner diameter of the tube is varied from 15 mm to 2 mm and the results are compared to the free-burning arc.

The investigation later addresses the thermal phase of the current interruption process as a function of N_2 filling pressure. To do so, a passive transient recovery voltage (TRV) circuit is used to control the initial rate of rise of the recovery voltage (IRRRV). First, the free-burning arc is studied in the absence of forced gas flow at different filling pressures, which is reported in Paper VI [24]. To study the effect of the forced gas flow near CZ, a self-blast arrangement with a heating volume is used. The effect of forced gas flow on the cooling of the different axial sections of the arc is studied by independently measuring the arc voltage at different sections of the arc and is presented in Paper VII [25]. A comparative study of the interruption performance of free-burning, tube-constricted and self-blast arrangements at different filling pressures is reported in Paper IV [26]. Furthermore, the effect of different filling pressures on nozzle mass loss and the interruption performance for different self-blast designs is illustrated in Paper III [27].

In the last and final stage of this thesis, the post-arc dielectric recovery characteristics of N_2 as a function of filling pressure is investigated by applying a 10 kV high voltage (HV) pulse at different instants after CZ. The breakdown or hold voltage as a function of time after CZ is analysed to study the recovery characteristics of the ultrahigh-pressure N_2 arc. The recovery characteristic of the free-burning arc is first studied and reported in Paper IX [28]. Finally, the effect of forced gas flow on the recovery process is

investigated by using two arrangements: a self-blast and a puffer arrangement, and is presented in Paper V [29].

In a gas circuit breaker, a moving contact is used to draw the arc. However, in this thesis, to eliminate the complexity associated with the contact movement, all the tests are conducted in a fixed electrode arrangement, and the arc is initiated by melting a thin copper wire. As a result, after each test the pressure vessel needs to be opened and the ignition wire mounted by hand. This manual procedure limited the number of tests performed under different test conditions. The arc current is generated by capacitive discharge using an *LC* circuit. The current amplitude is varied from 85 A to 450 A depending on the investigation. Due to the limitations of having high capacitances and inductances, the frequency of the arc current is in the range of 190 Hz to 950 Hz, and not the power frequency.

The structure of this thesis is as follows: first, the theory and different methods used to study different phases of the arc are briefly discussed in Chapter 2. Thereafter, a description of the experimental setup is presented in Chapter 3. In Chapter 4, the main works consisting of nine papers are presented. Finally, in Chapter 5, a summary of the results, conclusions and suggestions for further work are briefly provided.

Chapter 2

2. Theory and Methodology

2.1 The Electric Arc

As previously mentioned, a fixed electrode arrangement where the arc is initiated by melting a thin copper wire is used throughout this thesis. Once the arc is formed the plasma conducts the current, resulting in a voltage drop across the electrodes called the arc voltage. The arc voltage can be divided into three distinct regions, namely cathode drop, anode drop and the arc column [30]. For the arc surrounded by gas, the cathode and the anode drop strongly depend on the electrode material while the voltage drop in the arc column depends primarily on the type of gas, the arc current, the gas pressure and the length of the column itself [30].

In the free-burning arrangements, the arc burns freely between the electrodes without any forced gas flow. The arc properties vary considerably depending on the current level due to the dominance of different physical mechanisms at different current levels [31]. For the low currents, i.e. less than 30 A, the radiation is negligible and natural convection is the dominant cooling process due to the low temperature in the arc. High-current (>30 A) arc properties are mainly determined by magnetically induced convection. The self-magnetic field of the arc current produces a compressive force directed inward on the arc. A smaller arc cross-section results in a higher pressure near the electrodes where the current density is the highest. A strong convective flow is induced by this axial pressure gradient. The radiation emission coefficient increases rapidly with the temperature, so that for high currents the radiation dominates the conduction. When the filling pressure is increased the arc radius is constricted, which results in a higher current density. As a result, the arc voltage increases with the increase of the filling pressure [32].

Compared to the free-burning arc, when an arc burns inside a tube the tube also constricts the diameter of the arc based on the tube material and the inner diameter of the tube. As a result, the arc voltage increases due to the constriction of the arc. The radiation from the high-temperature arc core has different frequency components. A part of the radiation from the arc core transparently leaves the tube, while a part is absorbed into the boundary of the arc [33], [34]. The rest of the radiation reaches the inner surface of the tube, causing ablation. The ablation depends, among many other factors, on the total arc energy [34], [35]. As the cylinder ablates, a high-pressure stagnation region is formed at the centre of the tube, which expels the plasma out from both ends of the tube [36].

The arc can be considered as a resistive element with strong temperature-dependent resistivity. When the current approaches zero, the arc temperature decreases and the resistivity increases. Near CZ crossing the power injected into the arc also decreases to zero, and the circuit breaker uses this opportunity

to interrupt the current. When the temperature drops below a certain level, the ionised atoms or molecules start to recombine and the number of free charge carriers decreases. However, the temperature decay of the arc channel at CZ is not instantaneous. As a result, there are still charge carriers present even in the absence of arc current at natural CZ crossing. Due to the energy-storing elements in the grid or the test circuit, just after CZ a voltage across the electrodes is developed, known as transient recovery voltage (TRV). The remaining free charge carriers accelerate under the influence of the TRV. This causes a small post-arc current to flow between the electrodes. The post-arc current deposits thermal energy into the electrode gap, which slows down the recombination of the plasma. If the energy deposition is higher than the cooling of the medium, the arc re-ignites. The re-ignition caused by the post-arc current is often termed thermal re-ignition. Thermal re-ignition occurs almost immediately (up to some tens of microseconds) after CZ [37]. Thermal re-ignition is reported to be greatly dependent on the IRRRV and the steepness of the current (d*i*/d*t*) before CZ [20]. To successfully pass the thermal phase, gas circuit breakers use forced gas flow to effectively cool the arc.

After the post-arc current the dielectric phase begins, and the TRV continues to increase across the contact gap. A new race is started and if the switch does not manage to increase its dielectric strength across the contact gap faster than the electric field increases due to the TRV, an electric flash-over will re-ignite the arc. A dielectric restrike typically occurs several hundred microseconds after CZ, when the TRV reaches its peak value [17].

2.2 Method

Based on the investigations carried out at different phases of the arc, this thesis can be divided into three distinct parts: investigation during the high-current phase, thermal phase, and the post-arc dielectric recovery characteristics. The methods followed during different phases of the investigation are summarised here.

2.2.1 High-current Phase

In this thesis, the high-current phase is defined as the phase when the arc current amplitude is highest in the alternating current (AC) cycle. The rate of change of current at this stage is low and hence the arc during the current peak can be considered as a quasi-static arc.

A capacitive discharge circuit is used to generate the arc current by LC oscillation as shown in Fig. 2.1. The C is kept fixed at 4.8 µF capacitance while the inductor, L, and the charging voltage of the capacitor are varied to control the frequency and amplitude of the arc current. During the high-current phase, both the free-burning arc and the tube-constricted arc are studied. Either a triggered vacuum switch (TVS) or a mechanical knife switch is used to initiate the capacitive discharge, see Fig. 2.1. The TVS allows only half a cycle of the current to flow through the arcing chamber, thus minimising the energy deposition in the arc [21].

For the free-burning arc, the arc voltage as a function of nitrogen filling pressure is investigated from one bar (atmospheric pressure) up to 98 bar. The arc voltage dependency on the amplitude and frequency of the arc current as well as on the arc length at different filling pressures is studied. To investigate the effect of the arc duration on the arc voltage at various filling pressures, experiments with a fixed current amplitude and current half-cycle with current durations of 0.59 ms, 1.43 ms and 2.17 ms have been performed. Current amplitudes of 150 A, 300 A, and 450 A are used with a half-cycle current duration of 1.43 ms to study the relationship between arc voltage and arc current. For pressure dependency, arc duration dependency and current dependency measurements, the distance between the electrodes in the arcing chamber is kept fixed at 20 mm. Finally, to investigate the correlation between the interelectrode gap and the arc voltage, experiments have been carried out at a fixed current amplitude and current duration with different interelectrode gaps varied from 5 mm to 30 mm with a 5 mm increment. Four different pressure levels are used: atmospheric pressure (1 bar), 15 bar, 30 bar and 45 bar for arc duration dependency, current dependency and distance dependency measurements.

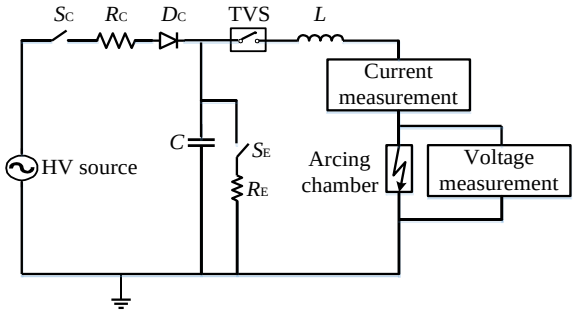

Fig. 2.1. schematics of the test setup to investigate the ultrahigh-pressure N_2 arc during high current phase.

For the tube-constricted arc arrangement, the arc voltages for arcs burning inside cylindrical tubes at different filling pressures of N_2 from 1 bar to 80 bar are studied. To analyse ablation effects further, two different tube materials have been investigated: ablating polytetrafluoroethylene (PTFE) and a less-ablating ceramic material (alumina). The insulating cylindrical tubes with a length of 20 mm and different inner diameters are held in position by insulating supports at a 5-mm distance from the electrodes. The inner diameter is varied from 2 mm to 4 mm, 8 mm and 15 mm. Corresponding experiments with free-burning arcs (without tube) are also carried out.

2.2.2 Thermal Phase

The thermal phase of the current interruption starts immediately after CZ when the temperature of the arc channel is very high. The thermal phase is a race between the rate of cooling of the contact gap and the rate of temperature rise due to the energy deposition in the post-arc channel. IRRRV after CZ and the slope of the current before CZ heavily influence the thermal phase [5]. In

this thesis, the steepness of the current before CZ is kept constant while the IRRRV is varied [38]. To vary the IRRRV, a passive TRV circuit is added in parallel to the arcing chamber, as shown in Fig. 2.2. By changing the value of R_{TRV}, the IRRRV is varied from 9.8 V/µs to 84.8 V/µs.

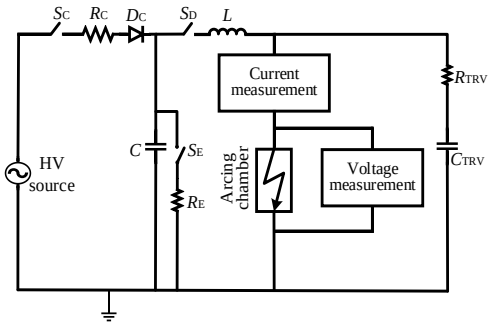

Fig. 2.2. Schematics of the test circuit to generate different IRRRVs to evaluate the thermal interruption performance.

As the arc resistance varies with the filling pressure and the type of arc (free-burning or tube-constricted), the amplitude of the arc current also changes. The arc-current amplitude varies from 130 A for the minimum arc voltage (free-burning, 1 bar) to 120 A for the maximum arc voltage (self-blast, 40 bar). One possible solution to overcome the challenge of slightly different arc current amplitudes would be to increase the charging voltage of the capacitor. However, changing the charging voltage would also influence the capacitor's stored energy and the IRRRV. Hence, in this thesis the charging voltage of the capacitor is kept constant while the slight change in the arc current amplitude is considered as a property of different types of arcs.

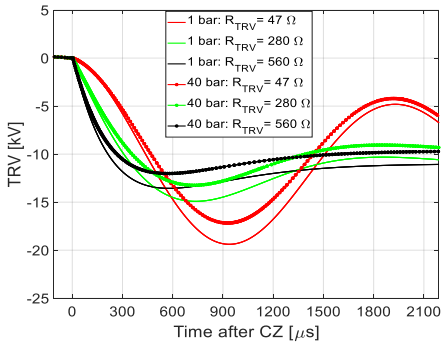

Fig. 2.3. Influence of the arc voltage on the TRV shapes for different R_{TRV}.

The arc resistance also plays a role in the shape of the TRV. The circuit is simulated in MATLAB Simulink to calculate the current amplitude, IRRRV, TRV peak and time to TRV peak from CZ. The TRV shape is first simulated considering the arc voltages for different filling pressures. The simulated TRV as a function of three different R_{TRV} for two different filling pressures is plotted in Fig. 2.3. It can be seen that the TRV amplitude is highest when R_{TRV}

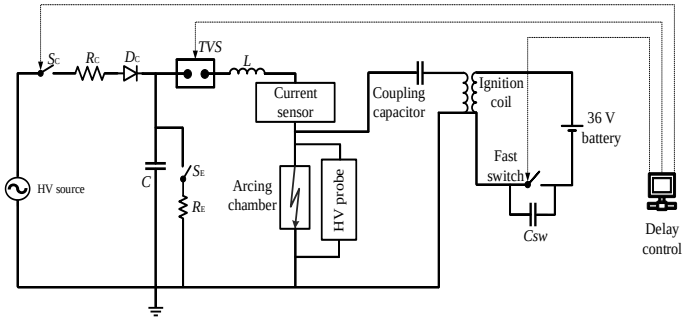

Fig. 2.4 Schematics of the test circuit to study post-arc dielectric recovery characteristics. An ignition coil is used to generate a 10-kV pulse which is applied after a controlled time delay following CZ.

is lowest. The TRV peak gradually decreases as R_{TRV} increases. The filling pressure, on the other hand, reduces the TRV peak due to the high arc voltage.

Three different filling pressures are used: 1, 20 and 40 bar, the latter being in the SC state. Different electrode arrangements and nozzle configurations are used: free-burning, tube-constricted and self-blast, which will be briefly discussed in Chapter 3.

2.2.3 Dielectric Recovery Characteristics

To evaluate the post-arc dielectric recovery characteristics, an HV pulse is applied at different instants after CZ [39]. In this thesis, a 10-kV HV pulse with a rise time of approximately 70 µs is supplied using the circuit shown in Fig. 2.4. The TVS interrupts the arc current at first natural CZ. The right part of the test circuit in Fig. 2.4 is a voltage pulse generator circuit using an ignition coil. To study the breakdown voltage as a function of time after CZ, the time between CZ and the HV pulse is precisely controlled in the order of microseconds. The time delay is varied from 10 µs after CZ to 10 ms after CZ. Both the free-burning arc without forced gas flow and the effect of forced gas flow on the dielectric recovery characteristics are studied.

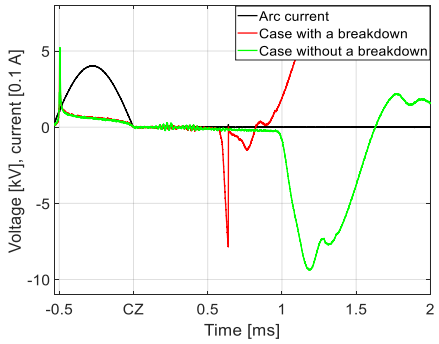

Fig. 2.5. Typical measurement showing a case of a breakdown (red line) and a case without a breakdown (hold) (green line) after applying pulses after CZ.

Two different cases, one with breakdown and one without breakdown, are shown in Fig. 2.5. The red line represents a test where the HV pulse was applied approximately 700 µs after CZ, resulting in a breakdown. The breakdown is detected by a voltage collapse at 7.8 kV. The test without a breakdown (pulse applied at 1 ms after CZ) shows the full HV pulse and following oscillations from the ignition coil (green line). For the cases where a breakdown occurred, the value of the breakdown voltage is recorded. For the cases without a breakdown, the peak of the voltage pulse is recorded.

Due to the stray capacitance in the setup, there are voltage oscillations with a voltage peak of approximately 400 V just after CZ, which are not part of the applied HV pulse. The rate of rise of these voltage oscillations is 125 V/µs. As the breakdown strength of the contact gap is very low just after CZ, a breakdown may occur due to such voltage oscillations. In this thesis, the breakdowns caused by these voltage oscillations are also considered when evaluating the recovery characteristics.

3. Experimental Setup

The actual test setup is shown in Fig. 3.1. Industrial grade N_2 bottles are used to fill the pressure vessel with the help of remotely controllable valves. A 15.7-litre steel pressure tank of 500 bar rating without any optical window is used as the arcing chamber. A miniature HV cable of the rated voltage of 24 kV is fed through the pressure tank using techniques described elsewhere [40]. The HV cable is held in position by several insulating supports and the ignition wire is attached between fixed arc-resistant copper-tungsten (Cu-W) electrodes. The return path of the current is through the supporting metal structure and through the flange of the pressure vessel. The test cell is designed in such a way that in case of a sudden pressure rise inside the cell, the weakest part will blow out (the glass door at the back of the cell).

Fig. 3.1. Test setup.

The capacitive discharge circuit is used to generate the arc current, which can be seen in Fig. 3.1. The capacitors and various switches (TVS and knife switches) are mounted on a movable pallet. The inductor, L, is built in such a way that the overall inductance can be varied from 6 mH to 96 mH. Depending on the desired current amplitude and frequency, the charging voltage of the capacitor and the inductance values are varied.

3.1 Electrode and Nozzle Arrangement

Different electrode and nozzle arrangements are used throughout the thesis, namely, free-burning arc, tube-constricted arc, self-blast arrangement and finally a puffer setup. All the different configurations used for different investigations are briefly discussed.

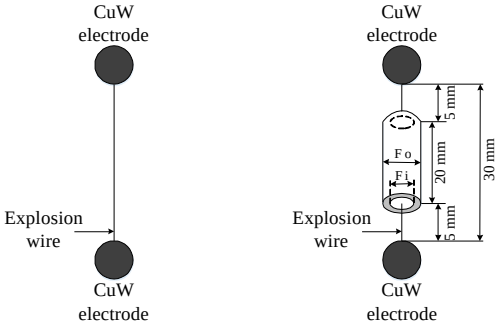

Fig. 3.2. Spherical electrodes. (a) Free-burning arrangement. (b) Arc burning inside a tube arrangement.

3.1.1 Free-burning Arc

In this arrangement, the arc burns freely between two fixed electrodes without any forced gas flow, hence, the name free-burning. Two identical spherical electrodes of 10 mm diameter made of arc resistant copper-tungsten (Cu-W) are used for the investigation of arc properties during the high-current phase in Papers I, II and VIII, see Fig. 3.2(a). The free-burning arrangement using spherical electrodes is shown in Fig. 3.3. In the latter part of this thesis, a pin and a ring electrode arrangement is used, as shown schematically in Fig. 3.4(a). The interelectrode gap between the electrodes varied from 5 mm to 50 mm depending on the investigation.

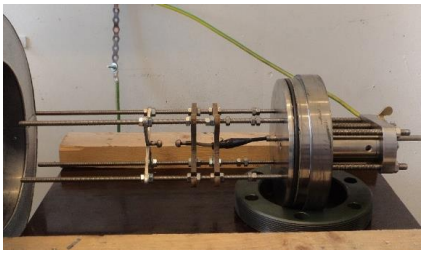

Fig. 3.3. Free-burning arc configuration using spherical electrodes.

3.1.2 Tube-constricted Arc

Two different tube-constricted arc arrangements are used in this thesis. For the first type, both ends of the tube are kept open and the 10 mm diameter spherical electrodes are placed 5 mm apart from the end of the tube, see Fig. 3.2(b). In this arrangement, the inner diameter of the tube is varied from 2 mm to 4mm, 8mm and 15 mm. In the ‘both ends open configuration’, the flow stagnation point lies in the middle of the tube. The first type of arrangement, as shown in Fig. 3.2(b), is used to study the effect of tube constriction on arc burning at different filling pressures in Papers II and VIII.

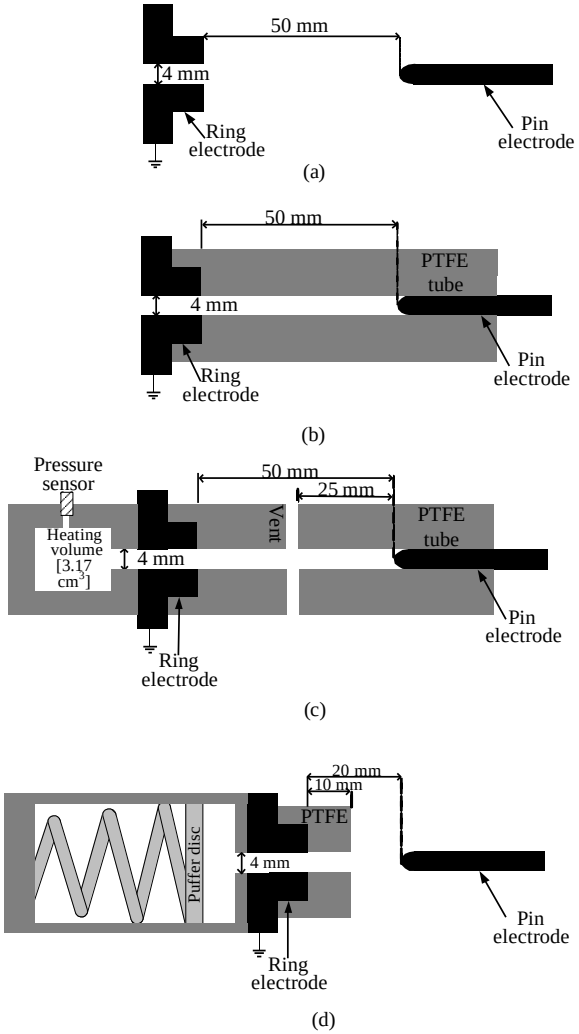

Fig. 3.4 A ring and a pin electrode arrangement. (a) Free-burning arrangement. (b) Tube-constricted arrangement. (c) Self-blast arrangement. (d) Puffer arrangement.

In the second type, the thermal interruption performance of the tube-constricted arc is studied, as shown in Fig. 3.4(b). In this configuration, a PTFE tube with an inner diameter of 4 mm is mounted on the ring electrode. The ignition wire is passed through the PTFE tube and attached to the electrodes. Afterwards, the pin electrode is pushed inside the tube to allow the ablated gas to flow out of the tube through the ring electrode outlet only. The interelectrode gap is kept fixed at 50 mm. In this configuration, the flow stagnation point lies near the pin electrode as it blocks the gas flow out through the pin electrode end.

3.1.3 Self-blast Arrangement

In order to generate a forced gas flow near CZ to cool the arc, a simple self-blast arrangement is used. In this configuration, a heating volume of 3.17 cm^3 is attached behind the ring electrode, as shown in Fig. 3.4(c). The holes in the middle of the interelectrode gap act as vents. For the bulk of the study in a self-blast arrangement, two opposite holes of 3 mm diameter are used.

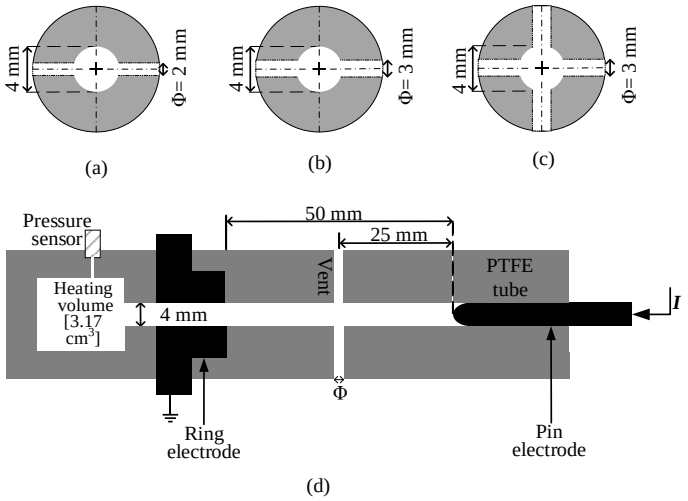

Fig. 3.5. Cross sectional view of the vent of three designs. (a) design a, (b) design b, (c) design c.

In Paper III, however, the effect of vent design on the interruption performance is studied, where three different vent dimensions are used: two opposite holes of 2 mm diameter (design *a*), 2 opposite holes of 3 mm diameter (design *b*) and 4 opposite holes of 3 mm diameter (design *c*), as shown in Fig. 3.5. During the high-current phase, some of the ablated PTFE exits through the vents while the rest is stored in the heating volume. At CZ, the over-pressure built up in the heating volume generates a back-flow of relatively cold gas from the heating volume and through the vent to cool the arc. As the arc energy is utilised to generate the forced gas flow, this arrangement is termed the self-blast type. The interelectrode gap is kept fixed at 50 mm. When a PTFE tube is used (tube and self-blast arrangement), the PTFE tube is changed after ten tests.

3.1.4 Puffer Arrangement

The last test arrangement is a puffer-type configuration, as shown schematically in Fig. 3.4(d). The puffer mechanism works by pre-charging a spring which is kept in position with the help of an electromagnet. A 10 mm long, 4 mm diameter PTFE nozzle is mounted with the ring electrode. The total interelectrode gap in the puffer setup is kept fixed at 20 mm. As the filling pressure increases, the density and the viscosity also increase. As a result, for the same pre-charging of the spring, the travel curve of the piston varies at

different filling pressures. In this thesis, the spring is released in such a way that a similar blowing pressure at CZ can be obtained for different filling pressures. The puffer arrangement is used to study the post-arc dielectric recovery characteristics under forced gas flow in Paper V only.

3.2 Measured Parameters

HV probes are used to measure the arc voltage, the TRV across the electrodes and the HV pulse (for dielectric recovery experiments). For the bulk of the measurements, a Tektronix P6015A-1000X (bandwidth 75 MHz) is used. However, the HV probe has a ratio of 1000:1, and hence saturates the optical fibre transmitter for any voltage above 5 kV. To measure the voltage above 5 kV, a North Start PVM-3 (bandwidth 25 MHz) with a ratio of 10000:1 is used. To measure the axial voltage distribution of the arc, two HV probes are used to measure the voltage drop at a distance of 20 mm and 30 mm from the pin electrode with respect to the ground. These probes were inserted into the pressure vessel and were subjected to high filling pressures. A TT-HVP15HF-HV Probe (bandwidth 50 MHz) is used when the probes are inserted into the pressure vessel. To measure the axial voltage distribution, thin tungsten wire is inserted into the tube through a tiny hole. To avoid the gas flow through the tiny hole, the hole is closed from the outside of the tube.

A shunt resistor is used to measure the arc current. To measure the small post-arc current near CZ, a post-arc current sensor is used [41]. A post-arc current sensor is essentially a clamped resistive shunt with antiparallel diodes [42]. The diodes bypass the resistor shunt when the current is high. When the current is low, and thus the voltage lower than the diodes' forward voltage, all current flows through the resistor shunt. Both current sensors are connected on the high voltage side of the arcing chamber on a floating potential.

In some cases, the pressure rise in the heating volume of the self-blast arrangement is measured. To do so, a piezoelectric pressure sensor is mounted on the heating volume to measure the pressure rise, as seen in Fig. 3.4(c). The pressure sensor is recess-mounted, and vinyl electrical tape is used to protect it from the thermal blast. For the puffer arrangement, the movement of the piston is recorded by a linear displacement sensor while the blow pressure is recorded by a differential piezoelectric pressure sensor mounted at the throat of the puffer.

All the data is sent to the control room via a transmitter (LTX-5510-T) through fibre optic and converted into an analog signal using a receiver (LTX-5510-R). The bandwidth of the fibre optic transmitter and receiver is 12.5 MHz. The data is recorded in a Tektronix MSO 2024 (bandwidth 200 MHz) digital oscilloscope for further analysis. The sampling rate of measured data is 10 MHz.

4 Publications

Paper I

Arc Voltage Characteristics in Ultrahigh-Pressure Nitrogen Including Supercritical Region

Fahim Abid, Kaveh Niayesh, Erik Jonsson, Nina Støa-Aanensen and Magne Runde

IEEE Transactions on Plasma Science, vol. 46, no. 1, pp. 187–193, Jan. 2018.

In Paper I the effect of filling pressure (1 bar to 98 bar) of N_2 and SC state on the arc voltage during high-current phase are investigated for an arc peak current of 150 A at 350 Hz. This paper investigates the arc burning in the free-burning arrangement, without any forced gas flow. The current (150 A to 450 A), frequency (230 Hz to 850 Hz) and distance dependence of the arc voltage are also studied at four different filling pressures (1, 15, 30 and 45 bar).

The arc voltage increased with the filling pressure without any abrupt change during the transition from gas to SC state. No significant change in arc voltage is observed for the investigated current amplitudes and frequencies. Electrode drop is found to be fixed and independent of the filling pressure.

Paper II

Ultrahigh-Pressure Nitrogen Arc Burning Inside Cylindrical Tubes

Fahim Abid, Kaveh Niayesh, Nina Støa-Aanensen

IEEE Transactions on Plasma Science, vol. 47, no. 1, pp. 754–761, Jan. 2019.

Paper II focuses on the effect of tube constriction on the arc. The arc voltage variation for the arcs burning inside cylindrical tubes is studied for different filling pressures: 1, 20, 40 and 80 bar, thus covering the SC region.

The arc voltage is found to increase with a decreasing inner diameter of the tube at atmospheric pressure. At higher filling pressures (i.e., 20, 40 and 80 bar), however, such a simple relationship is not observed. The arc temperature and radius have been calculated based on the “simple theory of free-burning arcs” and the “two-zone ablation arc model.” The calculated arc radius decreases with increasing gas pressure. Due to increased absorption of radiation at high filling pressures, ablation is found to be less significant for ultrahigh-pressure nitrogen arcs compared to atmospheric pressure arcs. This is in line with the observations from optical micrographs of the inner surfaces of the tubes exposed to arcs at different filling pressures.

Paper III

Nozzle Wear and Pressure Rise in Heating Volume of Self-Blast Type Ultrahigh-Pressure Nitrogen Arc

Fahim Abid, Kaveh Niayesh, Nina Sasaki Støa-Aanensen
Journal of Plasma Physics and Technology, vol. 6, no.1, pp 23–26, 2019.

The effect of filling pressure on nozzle mass loss and pressure rise in the heating volume of self-blast arrangement is investigated under different vent designs.

The energy deposited in the arc increases with the filling pressure. It is observed that the pressure rise in the heating volume is linked to the filling pressure, while the vent size plays a crucial role in the blow pressure near the CZ. The nozzle mass loss per unit energy deposited in the arc is found to be less dependent on the filling pressure.

Paper IV

Current Interruption Performance of Ultrahigh-Pressure Nitrogen Arc

Fahim Abid, Kaveh Niayesh, Camilla Espedal, Nina Støa-Aanensen
in Journal of Physics D: Applied Physics

Paper IV focuses on the thermal interruption performance of the ultrahigh-pressure N_2 arc. In this paper, the interruption performance of three different electrode and nozzle arrangements are compared: a simple contact configuration with a free-burning arc, a contact and a cylindrical nozzle setup (tube-constricted arc) and finally a self-blast arrangement where the arc is cooled by a forced gas flow. The initial rate of rise of recovery voltage just after CZ is varied from 9.8 V/µs to 84.9 V/µs.

It is observed that the interruption performance deteriorates with increased filling pressure in the absence of forced gas flow. Higher post-arc current is observed for the arcs burning at high filling pressures (i.e. 20 bar and 40 bar) compared to at atmospheric pressure in cases with no or little forced cooling. On the other hand, a forced gas flow near CZ reduces the post-arc current and also improves the interruption performance at high filling pressures. Little effect of the supercritical state on the interruption performance of N_2 is observed. Under the above-mentioned test conditions, the majority of the failures at high filling pressure is observed to be of the thermal re-ignition type.

Paper V

Effect of Filling Pressure on Post-Arc Gap Recovery of N_2

Fahim Abid, Kaveh Niayesh, Egil Viken, Nina Støa-Aanensen, Erik Jonsson, and Hans Kristian Meyer
Accepted in *IEEE Transactions on Dielectrics and Electrical Insulation.*

The dielectric recovery characteristics of an N_2 arc as a function of filling pressure are reported in this paper. A 10-kV high voltage pulse is applied across the electrodes followed by a controlled time delay after CZ (from 10

µs to 10 ms). First, the free-burning arc is studied. In the free-burning arrangement, the current and distance dependence of the dielectric recovery is also studied. Finally, self-blast and puffer arrangements are used to investigate the effect of forced gas flow on the recovery characteristics.

Experimental results show that, even in the absence of forced gas flow, the dielectric strength of the post-arc channel increases faster with the increase of the filling pressure, only after a critical time instant. The critical time instant is perhaps linked with the temperature decay of the post-arc channel. Just after CZ and until the critical time of approximately 300 µs, the dielectric strength at high filling pressure is observed to be lower than 1 bar. A longer gap recovers faster whereas the current dependency on the dielectric recovery is not observed. The forced gas flow, however, significantly enhances the dielectric recovery of the arc channel at a high filling pressure, even in the thermal phase.

Paper VI

Thermal Interruption Performance of Ultrahigh-Pressure Free-Burning Nitrogen Arc

Fahim Abid, Kaveh Niayesh, Shashidhara Basavapura Thimmappa, Camilla Espedal, Nina Sasaki Støa-Aanensen

Lecture Notes in Electrical Engineering, Springer, vol. 599, pp 663–671, 2019.

This paper's aim is to find the effect of filling pressure on thermal interruption performance of a free-burning N_2 arc in a fixed electrode arrangement. The initial rate of rise of recovery voltage (IRRRV) is varied from 9.8 V/µs to 84.8 V/µs.

It is observed that the re-ignition time rises with the decrease of IRRRV at all pressure levels, which is expected. However, in the absence of a forced gas flow, high N_2 filling pressure results in a reduction of the time to re-ignition and the re-ignition voltage, in contrast to atmospheric pressure arcs.

Paper VII

Arc Voltage Distribution Measurement in Tube Constricted Ultrahigh-Pressure Nitrogen Arc

Fahim Abid, Kaveh Niayesh, Nina Sasaki Støa-Aanensen

Lecture Notes in Electrical Engineering, Springer, vol. 599, pp 663–671, 2019.

This paper reports on the effect of gas flow on the axial voltage distribution of the arc burning inside a PTFE tube. To examine the axial voltage distribution in the arc, the arc voltage is independently measured at three different axial positions of the arc. In some cases, a heating volume is attached to the ring electrode, which produces a back-flow of gas. For the cases with a heating volume, the pressure rise in the heating volume is also measured.

It is observed that the pressure rise in the heating volume increases with the filling pressure. In the presence of the heating volume at a high filling pressure

(i.e. 20 bar and 40 bar), the voltage drop increases significantly near the vent due to the relatively cold gas flow compared to 1 bar.

Paper VIII

Arc Voltage Measurements of Ultrahigh-Pressure Nitrogen Arc in Cylindrical Tubes

Fahim Abid, Kaveh Niayesh, Nina Støa-Aanensen, Erik Jonsson, Magne Runde

22nd International Conference on Gas Discharge and their Application, Novi Sad, Serbia, Sep 2–7, 2018

The effect of tube constriction on the arc burning in N_2 at different filling pressures (1 bar to 80 bar) for the current peak of 150 A at 350 Hz is investigated in this paper. To investigate the effect of ablation, ceramic and PTFE tubes with different inner diameters (2 mm, 4 mm, 8 mm, 15 mm, and free-burning) are studied.

At atmospheric pressure, an inverse relation exists between arc voltage and inner tube diameter. At a high filling pressure, such behaviour is not obvious. The arc voltage of arcs burning inside ceramic and PTFE tubes is found to be similar in the investigated current and pressure regions.

Paper IX

Post-Arc Dielectric Recovery Characteristics of Free-Burning Ultrahigh-Pressure Nitrogen Arc

Fahim Abid, Kaveh Niayesh, Nina Sasaki Støa-Aanensen

5th International Conference on Electric Power Equipment-Switching Technology, Kitakyushu, Japan, Oct 13–16, 2019.

Post-arc dielectric recovery characteristics of free-burning nitrogen arcs as a function of gas filling pressure is studied in this paper. To investigate the effect of the inter-electrode gap on the recovery process, two different gap distances are studied: 20 mm and 50 mm. A 10 kV high voltage pulse with a rate of rise of 150 V/μs is applied across the electrodes after current zero. To evaluate the recovery process, the time between current zero and the start of the pulse is varied from 10 μs to 10 ms.

Experimental results show that the dielectric recovery performance improves with the filling pressure even in the absence of forced gas flow after a critical time instant after CZ. The breakdown strength is observed to recover faster for a longer electrode gap.

Paper I

Arc Voltage Characteristics in Ultra-High Pressure Nitrogen Including Supercritical Region

Fahim Abid, Kaveh Niayesh, *Senior Member, IEEE,* Erik Jonsson, Nina Støa-Aanensen, and Magne Runde

***Abstract*—A supercritical fluid is formed when both pressure and temperature of a fluid exceed the critical point, where distinct gas and liquid phases no longer exist. Supercritical fluids demonstrate combined properties of gas and liquid; which makes it interesting to investigate them as an arc extinction medium. This study focuses on the arc voltage characteristics of industrial grade nitrogen subjected to different filling pressures up to 98 bar including supercritical region. Pressure, arc duration, current and distance dependency of the arc are investigated by arc voltage measurement. It has been found that arc voltage increases with filling pressures without any abrupt change during the transition from gas into supercritical region. Arc duration and current dependency of the arc voltage are not significant in the investigated parameter range. Arc voltage measurement with different electrode gaps suggest that electrode voltage drop does not vary with filling pressures.**

***Index Terms*— Arc voltage, free-burning arc, supercritical fluid (SCF), switchgear, ultra-high pressure nitrogen.**

I. Introduction

AN increasing number of windfarms located far off the coasts and also a growing demand for electric power supply to oil and gas installations on the seabed will lead to a development of off-shore substations. The substations (i.e., where all the components except the power cable are gathered) of such a system will be placed on the seabed and be remotely controlled as opposed to building platforms or floaters to avoid large building costs. Placing the equipment on the seabed in many cases implies that it must be protected from the water pressure. For example, switching equipment such as circuit breakers need expensive solutions of encapsulations (to protect the equipment from high ambient pressure at seabed) and feedthroughs (to transfer power from the high-pressure water environment and into the more normal ambient inside [1]). A novel concept based on filling the interrupting chamber with the same surrounding high pressures at seabed can substantially reduce the cost of the encapsulations and feedthroughs.

Air is a well known insulating material, where nitrogen is the main constituent. When the pressure and temperature exceed the critical pressure (P_c) and the critical temperature (T_c) as shown for nitrogen in Fig. 1, then it enters into a so-called supercritical (SC) region. Properties like the density, viscosity, diffusivity, thermal conductivity, and heat capacity of SC nitrogen lies in between the properties of the gaseous and the liquid form of nitrogen [2]. For successful arc interruption, these properties are crucial, and hence, it is believed that SC nitrogen has the potential to be used as interruption medium [3].

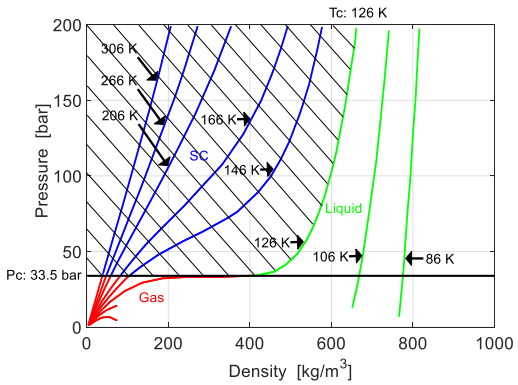

Fig. 1. Phase diagram of N_2, covering pressure up to 200 bar, temperature in the range 86–306K. *P*c = 33.5 bar and *T*c = 126 K [3].

Electric discharge inside SC medium is a poorly studied phenomenon because of the unusually high pressure needed for transition into SC region. Most of the previous works explore small-scale discharges of one millimeter or smaller inter-electrode gaps inside SC carbon dioxide [4]–[9] or SC nitrogen [2], [3], [10] under low energy dissipation, typically in the range of millijoules, while energy dissipations in switching arcs are normally up to hundreds of kilojoules. Exploring the arc properties in ultra-high pressure nitrogen including SC region is a novel field of research. Arc experiments inside a high-pressure chamber can be hazardous without proper estimation of energy dissipation in the arc. As there is clearly a lack of experimental data of arc voltage in SC nitrogen, this work will help to estimate the energy dissipation in the arcing channel for further research of switching arc in SC nitrogen.

This paper explores the arcing voltage between two identical

Fahim Abid and Kaveh Niayesh are with the Department of Electrical Power Engineering, Norwegian University of Science and Technology (NTNU), Trondheim 7491, Norway (e-mail: fahim.abid@ntnu.no).

Nina Støa-Aanensen, Erik Jonsson and Magne Runde are with SINTEF Energy Research, Trondheim 7465, Norway.

fixed electrodes with different filling pressures of nitrogen. Nitrogen is chosen for its low critical temperature (126 K) and pressure (33.5 bar) as well as for its environmentally benign nature [11]. As the room temperature is well above the critical temperature of nitrogen, varying the pressure alone can facilitate the transition into SC region. The arc duration and the current dependency of the arcing voltage are also investigated under different filling pressures. Finally, the electrode gap is varied to estimate the electrode voltage drop at different filling pressures.

II. Experimental Setup and Procedure

A. Test Circuit

The test circuit is shown in Fig. 2, and consists of a charging and a discharging section of a 4.8 µF high voltage (HV) capacitor, *C*. The capacitor can be charged to a predefined charging voltage of up to 20 kV through a diode resistor (D_C-R_C) unit. Once the capacitor is fully charged to the predefined level, switch S_1 can be opened to disconnect the charged capacitor from the grid.

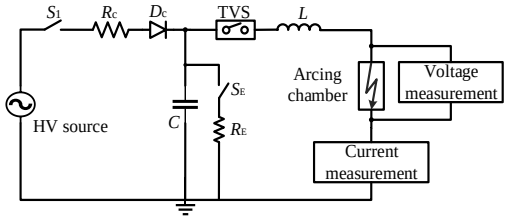

Fig. 2. Test circuit

The capacitor is discharged using a triggered vacuum switch (TVS) through the inductor, *L*, and further through an ignition copper wire inside the arcing chamber, see Fig. 2. An oscillation between the capacitor and the inductor generates a near sinusoidal current. The TVS allows only one-half cycle of the current to pass. Due to manual triggering of the TVS and the decay of the charged voltage through internal stray resistance of the capacitor, a ±5% error in the charging voltage is present. The 25 micron copper ignition wire melts due to adiabatic heating and subsequently creates the arcing channel. The capacitor is grounded using the earthing switch, S_E, once the test is over.

The arcing chamber is a 15.7 litres pressure tank rated for 500 bar and is shown in Fig. 3. A 24 kV miniature HV cable is fed through the flange of the pressure tank (technique described elsewhere [12]) and held in position by several insulating supports. The ignition wire is attached between two identical arc resistant copper-tungsten (CuW) electrodes of 10 mm diameter. The return path of the current is through the supporting metal structure and through the flange of the pressure tank. A HV probe is used for voltage measurement across the electrode gap and a current shunt is used to measure the current flowing through the arc. These data are sent via fiber optics connection to the control room where they are stored in a digital oscilloscope.

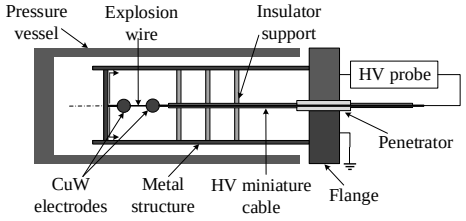

Fig. 3. Schematics of pressure vessel and the components inside.

B. Procedure

The first and main experimental series investigates the arc voltage at different pressures, from atmospheric level and up to 98 bar. The current amplitude was approximately 150 A, and with a current pulse duration of 1.43 ms for all tests. The contact distance was kept constant at 20 mm.

To investigate the influence of arc duration on the arc voltage, a second series with different current pulse durations is performed. Three different pulse durations are used; 0.59 ms, 1.43 ms, and 2.17 ms.

In the third series, the relationship between the arc voltage and the current amplitude is studied. Tests at 150 A, 300 A, and 450 A are performed.

Finally, in the fourth series, the correlation between the electrode gap distance and arc voltage is investigated. Experiments with gap distances from 5 mm to 30 mm are carried out.

For the second, third and fourth series, experiments are performed at four different pressure levels for each configuration; atmospheric pressure (1 bar), 15 bar, 30 bar, and 45 bar. All the test cases are summarized in Table I.

TABLE I
Test Cases and Conditions.

Test series	**Current amplitude [A]**	**Electrode gap distance [mm]**	**Current pulse duration [ms]**	**Nitrogen pressure [bar]**
1. Pressure dependency	150	20	1.43	1 to 98 (at 43 different levels)
2. Arc duration dependency	150	20	0.59, 1.43, 2.17	1, 15, 30, 45
3. Current dependency	150, 300, 450	20	0.59	1, 15, 30, 45
4. Distance dependency	150	5, 10, 15, 20, 25, 30	1.43	1, 15, 30, 45

Prior to each test, the pressure vessel is flushed with industrial grade nitrogen, ensuring that it contains 99% pure nitrogen for all the experiments conducted. After each experiment, the overpressure is released, the pressure vessel opened and a new arc ignition wire is mounted.

In addition to the main scope, the influence of metal vapor

from the arc ignition wire is evaluated since this could be an error source to the above investigations. Tests with three different wire thicknesses are therefore performed.

III. Results

A typical measurement of the arc voltage and the arc current is shown in Fig. 4. First order Savitzky-Golay filtering is used to remove the inherent high frequency noise present in the measurement. Filtering does not affect the results, as during the high current period of an alternating current, arc voltage remains quite stable. Due to triggering of the TVS, a time delay of few tens of microseconds occurs between the trigger and the start of the conduction of current. This time delay is evident in the voltage measurement just after $t = 0$ ms. Due to joule heating, the voltage drop across the copper wire increases until voltage peak just before 0.1 ms. The voltage peak corresponds to the evaporation of the copper wire and formation of arc channel. Once the arc is formed, the voltage drops quickly to a stable value. The arc voltage goes down slowly with time, showing free-burning arc characteristics.

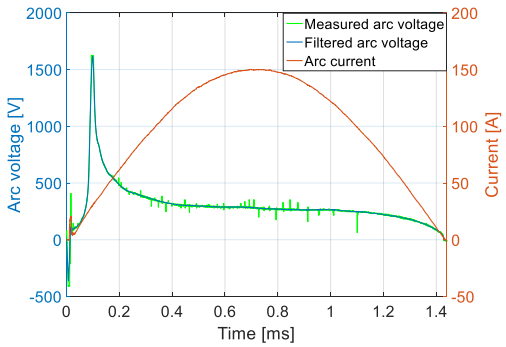

Fig. 4. Measured arc voltage and current at 45 bar filling pressures and 20 mm electrode gap.

A. Pressure Dependency

The main part of this work was to investigate the arc voltage as a function of different filling pressures. In Fig. 5a, measured arc voltages at 20 bar interval of filling pressures are plotted. Clearly, the arc voltage increases with the filling pressure. The arc voltage even at high filling pressures, exhibits free-burning arc characteristics where the arc voltage goes down with time. High arc conductivity due to decrease of the arc voltage before current zero indicates very low interruption capability characteristic of free-burning arcs.

All the experiments from the pressure dependency investigations are plotted in Fig. 5b. Each point represents the arc voltage at current peak. The arc voltage increases from about 60-65 V at atmospheric pressure to approximately 450 V at 98 bar. The energy dissipation in the arc varied from 9 J to 68 J. The rate of increase of arc voltage with filling pressures is higher up to approximately 20 bar compared to after 20 bar. The gas enters into SC region at approximately 34 bar. Considering the stochastic nature of the arc and measurement uncertainty, no abrupt change in arc voltage near critical point is observed.

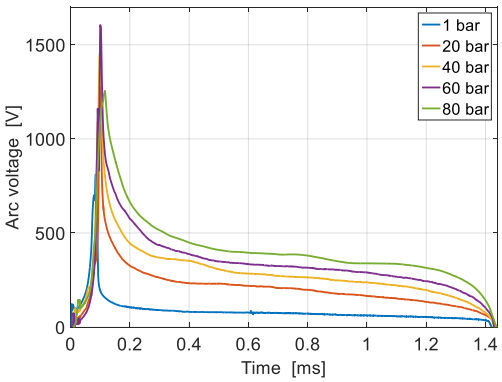

a) Measured arc voltage at 20 bar interval of filling pressures.

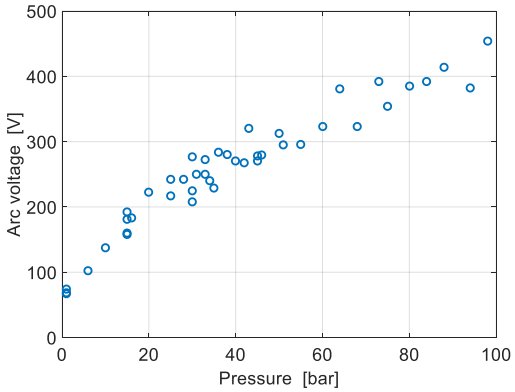

b) Arc voltage at current peak for different filling pressures.

Fig. 5. Arc voltage for arc current of 150 A, for half cycle current duration of 1.43 ms, at 20 mm electrode gap for different filling pressures.

B. Arc Duration Dependency

Fig. 6a shows the arc voltage versus the arc current for three different arc durations at atmospheric pressure. Oscillations after current zero due to stray capacitances are removed when plotted in Fig. 6a, as the focus of this study is on the arcing period and not after current zero. The arc initiation time corresponding to the voltage peak varies with different current durations, which is expected due to the high rate of change of the current at shorter current durations. The arc voltage at the current peak as a function of the current duration for different filling pressures are plotted in Fig. 6b. For the current durations of 0.59 ms, two measurements for each case are tested and the average is plotted with the error bar. Due to the complexity of the test and time associated with it, no statistical data is gathered further in this paper. Nevertheless, for pressure dependency measurements shown in Fig. 5b, same tests were repeated for some cases (e.g., at 1 bar, 15 bar, 30 bar etc.), which can provide an estimation of measurement variations. Based on the results shown in Fig. 6b, no strong arc duration dependency is

observed from the measurement.

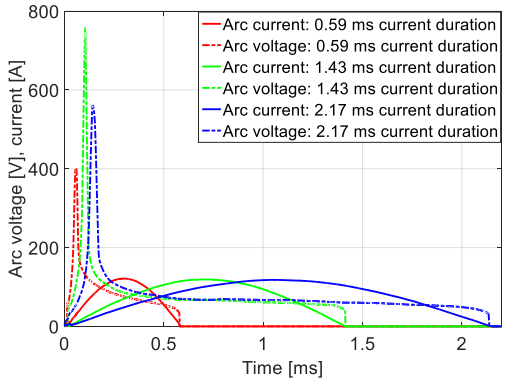

a) Measured arc voltage and current at atmospheric pressure with different current durations.

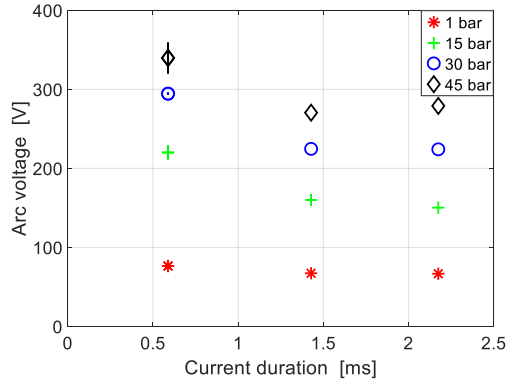

b) Arc voltage at the current peak for different current durations at different filling pressures.

Fig. 6. Arc voltage as a function of the current duration for arc current of 150 A, at 20 mm electrode gap.

C. Current Dependency

The arc voltage as a function of the arc current is illustrated in Fig. 7. The arc voltages for 20 mm electrode gap at atmospheric pressure for three different current levels are found to be 78 V, 80 V, and 87 V, respectively. For higher filling pressures at 45 bar, arc voltages for three different current levels are 358 V, 303 V, and 302 V, respectively. Although at 150 A, measured arc voltage is slightly higher compared to other cases; considering arc voltages for 300 A, and 450 A, no significant current dependency is apparent in the investigated range.

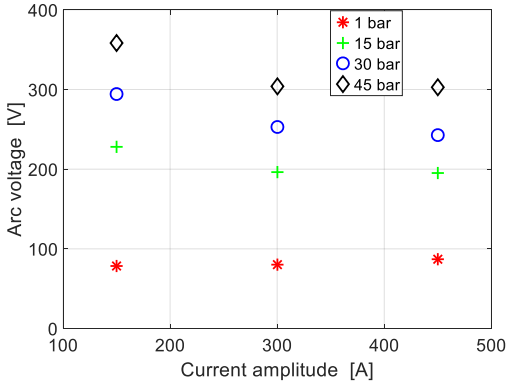

Fig. 7. Current dependency of arc voltage for 20 mm electrode gap for current duration of 0.59 ms.

D. Distance Dependency

The correlation between the electrode gap and the arc voltage is explored by changing the electrode gap from 5 mm to 30 mm with 5 mm increments and is shown in Fig. 8. Considering a linear relation between the arc voltage and the electrode gap, if the data is extrapolated to 0 mm arcing distance, the electrode voltage drop otherwise known as cathode and anode fall of potential can be estimated. This electrode drop is found to be approximately 33-37 V for the tested filling pressures. It is high in comparison to the typical electrode voltage drop of around 16.3 V for 26 mm diameter CuW electrode for arc at atmospheric pressure in air [13]. Such large variation in electrode voltage drop is probably due to presence of non-linear characteristics of arc voltage with electrode gap for smaller arc lengths below 5 mm. However, considering the arc voltage for 5 mm and larger electrode gaps, the experimental results are in line with the literature [13].

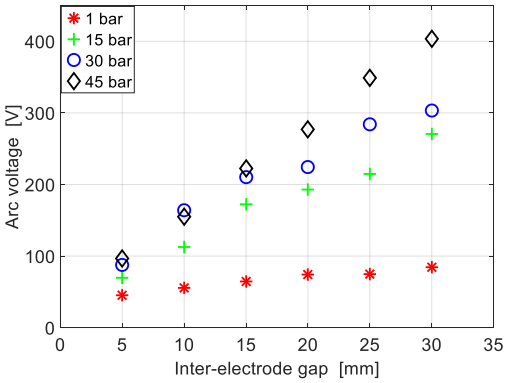

Fig. 8. Distance dependency of arc voltage for 150 A current for 1.43 ms current duration for different filling pressures.

E. Effect of Metal Vapor

To investigate the effect of metal vapor in the measured data, ignition wires of different thicknesses are used and the results are plotted in Fig. 9. It is assumed that the energy dissipated in the ignition wire is responsible for temperature increase and phase transitions of the wire. Time and voltage peak corresponding to ignition wire evaporation are estimated using the temperature dependent resistivity and specific heat of copper from literature [14]–[17]. The estimation of voltage peak corresponding to ignition fits well with the experimental results. The presence of metal vapor generally leads to decrease in the arc temperature due to increase in the radiative emission. The increased electrical conductivity due to metal vapor tends to decrease the arc voltage, however the temperature decrease associated with strong radiative emission has the opposite effect due to temperature dependent conductivity. This may explain the increase of arc voltage observed for 100 micron ignition wire [18]. Considering the arc voltage measured for 25 and 40 micron ignition wires, it can be concluded that metal vapor in the above experiments does not have significant effect on the arc voltage.

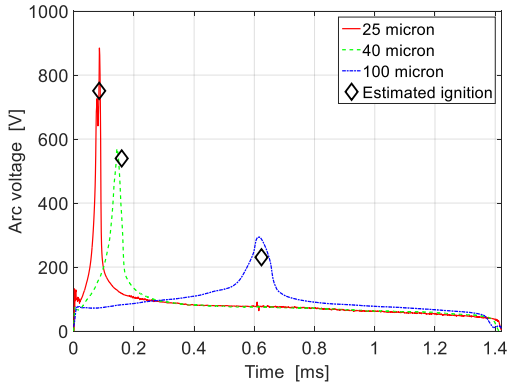

Fig. 9. Measured and estimated ignition time with different thickness of ignition wire at atmospheric pressure for arc current of 150 A at 20 mm electrode gap.

IV. Discussions

The increase of the arc voltage with filling pressure is obvious from the results. Low currents (i.e., less than 30 A) and high currents (i.e., more than 30A) arc properties differ significantly from each other due to different physical processes dominating the arc [19]. In this paper most of the experiments were conducted at current amplitude of 150 A, or higher, which lies in the high current region. Primarily, the arc temperature at the arc center can be determined by the energy balance equation:

$$\frac{I^2}{\sigma A^2} = \frac{4\pi kT}{A} + U, \tag{1}$$

where I is the arc current, σ is the electrical conductivity, A is the arc cross section area, T is the temperature of the arc, k is the thermal conductivity, and U is the net radiation emission coefficient. For low current arcs, due to low temperature in the arc, the radiation is negligible and natural convection is the dominant cooling process. High current arc properties are mainly determined by magnetically induced convection. The magnetic field, B, of the arc produces a compressive force inwards on the arc:

$$(J \times B)_r = -\frac{\mu\sigma E^2}{r}\int_0^r x\sigma dx, \tag{2}$$

where J is the current density, E is the electric field, B is the magnetic flux density, H is the magnetic field strength and $\mu = 1.26\times10^{-8}$ Hcm^{-1}. This compressive force is balanced by an increase in pressure inside the arc:

$$\Delta P = \frac{\mu I^2}{4\pi A}\left(1-\frac{r^2}{R^2}\right), \tag{3}$$

where r the distance towards radial direction, and R is the radius of the isothermal plasma. According to (3), a smaller arc cross section results in a higher pressures near the electrodes where the current density is the highest. A strong convective flow is induced by this axial pressure gradient. The radiation emission coefficient increases rapidly with the temperature, so that for high currents, the term U dominates the conduction term in (1). Based on many assumptions (described elsewhere [19]), Lowke estimated the electric field of the high current arc:

$$E = \frac{I}{\sigma A} = 0.26\left(\frac{h}{\sigma z}\right)^{0.5}\left(\frac{\mu J_0 \rho}{2\pi}\right)^{0.25} I^{0.25} \tag{4}$$

where h is the enthalpy of the plasma, ρ is the density, J_0 is the current density at the cathode, and z is the axial distance from cathode. It can be seen from (4) that the electric field is related to the density of the medium; this explains the high arcing voltage at higher filling pressures.

The arc contracts with filling pressure which results in the high current density and the high electric fields [20]. Radiation coefficient also increases with the filling pressure, resulting in a better cooling at higher filling pressures. Hence, the temperature in the arc core decreases with filling pressure [19]. Reduction of arc temperature decreases the conductivity of arc channel, which increases the voltage drop over the arc. From the simple theory of free-burning arcs given by Lowke [19], the estimated electric field for 10 kA and 10 A arc current from theory and the calculated electric field from the measurements in this paper are plotted in Fig. 10. Here, the electric field is assumed homogeneous in the arc column and by subtracting the electrode voltage drop calculated earlier.

The arc voltage of pressurized air up to 9 bar has been reported in literature where researchers also found an increasing arc voltage with increasing filling pressure [21]. No strong current dependency is reported for currents below 1 kA and the electrode voltage drop was in the range of 30 V to 40 [21]. These findings are in agreement with our measurements. Arc voltages in the range of approximately 100 V has been reported for an electrode gap of 1.81mm at 50 bar filling pressure of nitrogen, which is higher than our observation [22]. However,

the experiments were conducted at frequencies of more than 3 kHz and with currents up to few tens of amperes. Lower currents, higher frequency, and different electrode size, all can have an influence on the arc voltage.

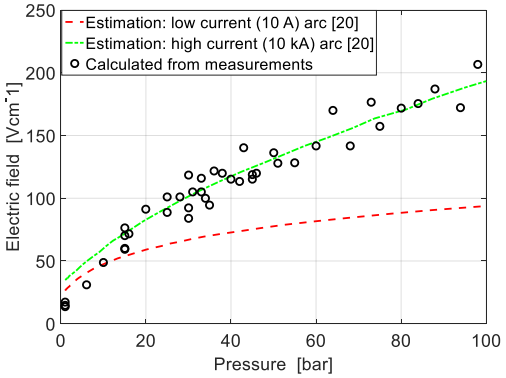

Fig. 10. Estimations from Lowke [20] and calculated electrical field from measured arc voltage with different filling pressures (arc current: 150 A, current duration: 1.43 ms).

The density variation is not abrupt at room temperature when transition to SC happens, as shown in Fig. 1. Researchers found that breakdown field strength of synthetic air, carbon dioxide (CO_2), a mixture of CO_2 and oxygen (O_2), and tetrafluoromethane (CF_4) shows a saturation of the breakdown electric field strength above 20 bar [23]. It was also concluded that, if the gas becomes supercritical, there is no change in the breakdown electric field strength. Although the arc voltage and the breakdown voltage are not directly correlated, both observations are in line.

V. Conclusions

The arc voltage in 99% pure nitrogen at different filling pressures (from atmospheric pressure up to 98 bar) including SC region has been investigated for medium voltage ratings and currents in the range of 150 A to 450 A. Based on the experimental findings, the following conclusions have been drawn:

- The arc voltage increases with filling pressure.
- The arc voltage does not change abruptly when the transition from gas to supercritical happens.
- The arc duration dependency of the arc voltage is not significant for current durations of 0.59 ms up to 2.17 ms for filling pressures up to 45 bar.
- The current dependency of the arc voltage is not strong for currents of 150 A to 450 A and filling pressures up to 45 bar.
- The electrode voltage drop is estimated to be approximately 33-37 V for 10 mm wide CuW contacts for filling pressures up to 45 bar.

References

[1] t. Hazel, h. H. Baerd, j. J. Legeay, and j. J. Bremnes, "Taking power distribution under the sea: design, manufacture, and assembly of a subsea electrical distribution system," *IEEE Ind. Appl. Mag.*, vol. 19, no. 5, pp. 58–67, Sep. 2013.

[2] J. Zhang *et al.*, "Breakdown strength and dielectric recovery in a high pressure supercritical nitrogen switch," *IEEE Trans. Dielectr. Electr. Insul.*, vol. 22, no. 4, pp. 1823–1832, Aug. 2015.

[3] J. Zhang, A. H. Markosyan, M. Seeger, E. M. van Veldhuizen, E. J. M. van Heesch, and U. Ebert, "Numerical and experimental investigation of dielectric recovery in supercritical N_2," *Plasma Sources Sci. Technol.*, vol. 24, no. 2, p. 25008, Feb. 2015.

[4] M. Goto *et al.*, "Reaction in plasma generated in supercritical carbon dioxide," *J. Phys. Conf. Ser.*, vol. 121, no. 8, p. 82009, Jul. 2008.

[5] T. Ito and K. Terashima, "Generation of micrometer-scale discharge in a supercritical fluid environment," *Appl. Phys. Lett.*, vol. 80, no. 16, pp. 2854–2856, Apr. 2002.

[6] E. H. Lock, A. V. Saveliev, and L. A. Kennedy, "Influence of electrode characteristics on dc point-to-plane breakdown in high-pressure gaseous and supercritical carbon dioxide," *IEEE Trans. Plasma Sci.*, vol. 37, no. 6, pp. 1078–1083, Jun. 2009.

[7] H. Tanoue *et al.*, "Shock wave generated by negative pulsed discharge in supercritical carbon dioxide," in *2013 19th IEEE Pulsed Power Conference (PPC)*, 2013, pp. 1–5.

[8] Z. B. Yang, S. H. R. Hosseini, T. Kiyan, S. Gnapowski, and H. Akiyama, "Post-breakdown dielectric recovery characteristics of high-pressure liquid CO_2 including supercritical phase," *IEEE Trans. Dielectr. Electr. Insul.*, vol. 21, no. 3, pp. 1089–1094, Jun. 2014.

[9] H. Tanoue, T. Furusato, K. Takahashi, S. H. R. Hosseini, S. Katsuki, and H. Akiyama, "Characteristics of shock waves generated by a negative pulsed discharge in supercritical carbon dioxide," *IEEE Trans. Plasma Sci.*, vol. 42, no. 10, pp. 3258–3263, Oct. 2014.

[10] J. Zhang, B. van Heesch, F. Beckers, T. Huiskamp, and G. Pemen, "Breakdown voltage and recovery rate estimation of a supercritical nitrogen plasma switch," *IEEE Trans. Plasma Sci.*, vol. 42, no. 2, pp. 376–383, Feb. 2014.

[11] J. V Sengers and J. M. H. L. Sengers, "Thermodynamic behavior of fluids near the critical point," *Annu. Rev. Phys. Chem.*, vol. 37, no. 1, pp. 189–222, Oct. 1986.

[12] J. Aakervik, G. Berg, and S. Hvidsten, "Design of a high voltage penetrator for high pressure and temperature laboratory testing," in *2011 Annual Report Conference on Electrical Insulation and Dielectric Phenomena*, 2011, pp. 267–270.

[13] Y. Yokomizu, T. Matsumura, R. Henmi, and Y. Kito, "Total voltage drops in electrode fall regions of SF_6 , argon and air arcs in current range from 10 to 20 000 A," *J. Phys. D. Appl. Phys.*, vol. 29, no. 5, pp. 1260–1267, 1996.

[14] E. M. Apfel'baum, "Calculation of the electrical conductivity of liquid aluminum, copper, and molybdenum," *High Temp. from Teplofiz. Vysok. Temp.*, vol. 41, no. 4, pp. 466–471, 2003.

[15] J. Brillo and I. Egry, "Density determination of liquid copper, nickel, and their alloys," *Int. J. Thermophys.*, vol. 24, no. 4, pp. 1155–1170, 2003.

[16] G. Lohöfer, "Electrical resistivity measurement of liquid metals," *Meas. Sci. Technol.*, vol. 16, no. 2, pp. 417–425, Feb. 2005.

[17] V. Y. Chekhovskoi, V. D. Tarasov, and Y. V. Gusev, "Calorific properties of liquid copper," *High Temp. Transl. from Teplofiz. Vysok. Temp.*, vol. 38, no. 3, pp. 394–399, May 2000.

[18] J. Haidar, "The dynamic effects of metal vapour in gas metal arc welding," *J. Phys. D. Appl. Phys.*, vol. 43, no. 16, p. 165204, Apr. 2010.

[19] J. J. Lowke, "Simple theory of free-burning arcs," *J. Phys. D. Appl. Phys.*, vol. 12, no. 11, pp. 1873–1886, Nov. 1979.

[20] K. C. Hsu and E. Pfender, "Modeling of a free-burning, high-intensity arc at elevated pressures," *Plasma Chem. Plasma Process.*, vol. 4, no. 3, pp. 219–234, Sep. 1984.

[21] S. Watanabe, K. Kokura, K. Minoda, and S. Sato, "Characteristics of the arc voltage of a high-current air arc in a sealed chamber," *Electr. Eng. Japan*, vol. 186, no. 1, pp. 34–42, Jan. 2014.

[22] J. Zhang, "Supercritical fluids for high power switching," Technische Universiteit Eindhoven, 2015.

[23] M. Seeger, P. Stoller, and A. Garyfallos, "Breakdown fields in synthetic air, CO_2, a CO_2/ O_2 mixture, and CF_4 in the pressure range 0.5–10 MPa," *IEEE Trans. Dielectr. Electr. Insul.*, vol. 24, no. 3, pp. 1582–1591, Jun. 2017.

Fahim Abid received the B.Sc. degree in electrical and electronic engineering from the Islamic University of Technology (IUT), Dhaka, Bangladesh in 2012. He received the M.Sc. degree in electrical engineering combinedly from Royal Institute of Technology (KTH), Stockholm, Sweden and Technical University Eindhoven (TU/e), Eindhoven, Netherlands in 2015. He is currently working as a PhD candidate at the department of electric power engineering in Norwegian University of Science and Technology (NTNU), Trondheim, Norway.

Kaveh Niayesh (S'98–M'01–SM'08) received the B.Sc. and M.Sc. degrees in electrical engineering from the University of Tehran, Tehran, Iran, in 1993 and 1996, respectively, and the Ph.D. degree in electrical engineering from the RWTH-Aachen University of Technology, Aachen, Germany, in 2001. During the last 16 years, he held different academic and industrial positions including Principal Scientist with the ABB Corporate Research Center, Baden-Dattwil, Switzerland; Associate Professor with the University of Tehran; and Manager, Basic Research, with AREVA T&D, Regensburg, Germany. Currently, he is a Professor with the Department of Electric Power Engineering, Norwegian University of Science and Technology (NTNU). He is the holder of 16 patents and has more than 95 journal and conference publications on current interruption and limitation, vacuum and gaseous discharges, plasma modeling and diagnostics, switching transients, and pulsed power technology.

Erik Jonsson received the M.Sc. degree in physics from Uppsala University, Uppsala, Sweden, in 2005 and the Ph.D. degree in electrical power engineering at Norwegian University of Science and Technology (NTNU), Trondheim, Norway, in 2014. From 2006 to 2007, he was with ABB Corporate Research, Västerås, Sweden. Currently, he is with SINTEF Energy Research, Trondheim, Norway, working with medium-voltage switchgear and power cables.

Nina Sasaki Støa-Aanensen received the M.Sc. degree in applied physics and mathematics and the Ph.D. degree in electrical power engineering from the Norwegian University of Science and Technology (NTNU), Trondheim, Norway, in 2011 and 2015, respectively. She is currently working with SINTEF Energy Research, Trondheim, Norway.

Magne Runde received the M.Sc. degree in physics and the Ph.D. degree in electrical power engineering from the Norwegian University of Science and Technology (NTNU), Trondheim, Norway, in 1984 and 1987, respectively. He has been with SINTEF Energy Research, Trondheim, since 1988. From 1996 to 2013, he was an Adjoint Professor of High Voltage Technology, NTNU. His fields of interest include circuit breakers and switchgear, electrical contacts, power cables, diagnostic testing of power apparatus, and power applications of superconductors. Magne Runde has been the convener and member of several CIGRÉ working groups; authored and coauthored more than 45 articles in peer-reviewed international journals and more than 45 conference publications.

Paper II

Ultrahigh-Pressure Nitrogen Arcs Burning inside Cylindrical Tubes

Fahim Abid, Kaveh Niayesh, *Senior Member, IEEE*, Nina Støa-Aanensen

***Abstract*— When the pressure and temperature of a fluid exceed a critical point, the fluid enters into the supercritical region. In this region, the physical properties are believed to be in favor of a good current interruption medium. This study focuses on the arc voltage characteristics of nitrogen arcs burning inside cylindrical tubes at different filling pressures: 1 bar, 20 bar, 40 bar, and 80 bar, thus covering the supercritical region. Two different tube materials have been used in the experiments; alumina and PTFE. Arc voltages are measured for arcs burning inside tubes of 2, 4, 8, and 15 mm inner diameters. In addition, free-burning arcs have been investigated at the same filling pressures. The arc current was 150 A at 350 Hz throughout the study. The arc voltage is found to increase with decreasing inner diameter of the tube at atmospheric pressure. At higher filling pressures (i.e., 20 bar, 40 bar, 80 bar), however, such a simple relationship is not observed. The arc temperature and radius have been calculated based on the 'simple theory of free-burning arcs' and the 'two-zone ablation arc model'. The calculated arc radius decreases with increasing gas pressure. Furthermore, due to increased absorption of radiation at high filling pressures, ablation is found less significant for ultrahigh-pressure nitrogen arcs compared to atmospheric pressure arcs. This is in line with the observations from optical micrographs of the inner surfaces of the tubes exposed to arcs at different filling pressures.**

***Index Terms*— Arc voltage, supercritical nitrogen, switchgear, ultra-high pressure arc, two-zone arc model.**

I. Introduction

An increase of wind farms and mining operations located far off the coast will increase the need for offshore substations in the future. Such substations can be put on the seabed instead of building expensive floaters and platforms [1]. Placing the equipment on the seabed in many cases implies that it must be protected from water and the high ambient pressure at the seabed. Conventional switching equipment such as circuit breakers (vacuum breakers or breakers filled with gases at a few bars) require expensive solutions for encapsulation and feedthroughs to protect them from water and high ambient pressure. A novel concept based on filling the interrupting chamber with a fluid at the same high pressure as the surroundings could substantially reduce the cost of the encapsulations and feedthroughs.

Nitrogen (N_2) is a good insulating gas. When the pressure and temperature of N_2 exceed the critical pressure (33.5 bar) and temperature (126 K), it enters into the supercritical (SC) region [2]. Properties such as the density, viscosity, diffusivity, thermal conductivity, and heat capacity of SC N_2 are believed to be in favor of a good interruption medium [3]. However, electrical discharges inside SC N_2 are not a well-explored field because of the high pressure needed for the transition into the SC region. A few works have reported on electrical discharges inside supercritical fluids in general [4-8]. However, in contrast to the high energy (normally up to hundreds of kilojoules) deposited in switching arcs of medium voltage switchgears, previous studies cover short distance electrical discharges in SC fluids for energy dissipation in the range of millijoules.

The voltage drop across free-burning nitrogen arcs has been found to increase with increasing filling pressure without any abrupt change during the transition from gas to supercritical state [9]. In gas-filled circuit breakers, the arcs are usually not free-burning, but constricted by an insulating nozzle or tube. In contrast to free-burning arcs, a cylindrical tube constricts the diameter of the arc core based on the tube material and the inner diameter of the tube. A part of the radiation from the arc core transparently leaves the tube, while some part is absorbed at the boundary of the arc. The rest of the radiation reaches the inner surface of the tube, causing ablation. As the cylinder ablates, a high-pressure stagnation region is formed at the center of the tube, which expels the plasma out from both ends of the tube. Several works have been reported for such tube-constricted arcs at atmospheric pressure [10-14]. However, little or no work have been reported for arcs burning inside a tube at a very high filling pressure.

This paper focuses on the arc voltage characteristics of arcs burning inside cylindrical tubes at different filling pressures of N_2. The voltage drop for arcs burning in tubes with varied inner diameters are measured alongside those of free-burning arcs. The arcs burning inside tube at higher filling pressures are then compared with arcs burning in air at atmospheric pressure. To analyze ablation effects further, two different tube materials have been studied: ablating Polytetrafluoroethylene (PTFE), and a less-ablating ceramic material (alumina). To qualitatively evaluate the ablation caused by an arc at high filling pressures as well as at atmospheric pressure, the inner surface of the tubes are inspected using an optical microscope. Some of these works have been presented in a conference report [15].

The experimental setup and procedure are explained in chapter II, followed by the experimental results in chapter III. Using well-known semi-analytical arc models, the temperatures

F. Abid and K. Niayesh are with the Department of Electrical Power Engineering, Norwegian University of Science and Technology, 7491 Trondheim, Norway (e-mail: fahim.abid@ntnu.no).

N. S. Støa-Aanensen is with SINTEF Energy Research, 7465 Trondheim, Norway.

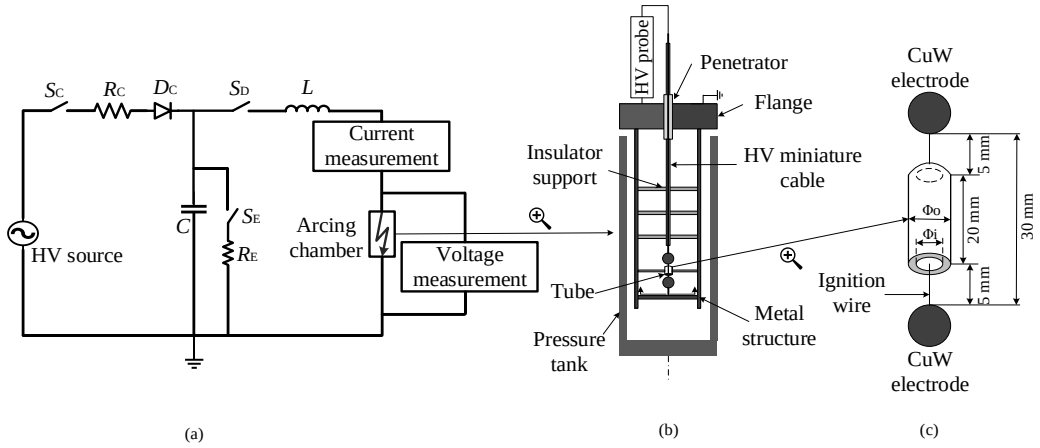

Fig. 1: The experimental setup. (a) The test circuit showing the charging and discharging part of the circuit. (b) Schematics of the high pressure arcing chamber and the inside connections. (c) The configuration of the tube with respect to electrodes inside the arcing chamber.

and radii of the arcs are calculated and discussed in chapter IV. Finally, based on the experimental results and discussions, the conclusions are drawn in chapter V.

II. Experimental Setup And Procedure

The experimental setup is shown schematically in Fig. 1. The test circuit consists of the charging and discharging sections of a 4.8 µF high voltage (HV) capacitor, *C*, shown in Fig. 1(a). The capacitor is charged to a predefined charging voltage of 15 kV through the diode resistor unit R_C-D_C. Once the capacitor is charged, the switch S_C is opened to disconnect the charged capacitor from the grid. Due to the decay of the charged voltage of the capacitor through internal stray resistance, a ±5% error in the charging voltage is present in the system. When the knife switch, S_D, is closed, the capacitor is discharged through the inductor, *L*, and further through an ignition wire in the arcing chamber. The ignition wire melts due to adiabatic heating within 0.1 ms, and the current continues to flow through an arc.

A pressure tank of 15.7-liters rated for 500 bar is used as arcing chamber, this is shown schematically in Fig. 1(b). Prior to each test, the pressure vessel is flushed with industrial grade nitrogen. It is ensured that 99% pure nitrogen is used for all the experiments conducted, except for atmospheric pressure cases, where ambient air is used. A 24 kV miniature HV cable is fed through the pressure tank (the techniques are described in [16]). The miniature cable is held in position by several insulating supports. In a previous study on free-burning arcs, it was reported that the copper vapor did not have a significant effect on the arc characteristics if the thickness of the ignition wire was kept less than 100 µm [9]. Hence, a copper wire with a diameter of 25 µm is used to initiate the arc. The ignition wire is passed through the tube and attached between two identical copper-tungsten (Cu-W) spherical electrodes of 10 mm diameter.

The insulating cylindrical tubes with a length of 20 mm and different inner diameters are held in position by an insulating support at a 5 mm distance from the electrodes, as shown in Fig. 1(c). The return path of the current is through the supporting metal structure and the flange of the pressure tank. An HV probe is used to measure the voltage across the electrodes and a shunt resistor is used to measure the current flowing through the arc.

TABLE I
Test Cases and Conditions.

Tube material	Current [A]	Tube diameter [mm]	Frequency [Hz]	Filling pressure [bar]
Alumina	150	2, 4, 8, 15	350	1, 20, 40, 80
PTFE	150	2, 4, 8, 15	350	1, 20, 40, 80
Free-burning	150	No tube	350	1, 20, 40, 80

Two different tube materials are investigated: PTFE and alumina. The inner diameter, Φ_i, is varied from 2 to 4, 8, and 15 mm. Corresponding experiments with free-burning arcs (without tube) are also carried out. The outer diameter of the tube, Φ_o, is either 15 mm (for the Φ_i= 2, 4, and 8 mm tubes) or 20 mm (for Φ_i= 15 mm tube). After each experiment, the tubes are carefully examined to ensure that no arc traces are found on their outer surfaces. The tubes are tested at four different filling pressures: 1 bar (atmospheric air), 20 bar, 40 bar, and 80 bar. Each test case is repeated three times. All the test cases are summarized in Table I.

The inner surfaces of the tubes are investigated by optical microscopy. After the arcing tests, three types of samples for both PTFE and alumina are studied using microscopy: without any arc (reference), after arcing at 1 bar, and after arcing at 80 bar N_2 for 4 mm inner diameter of the tube. To prepare the samples, the tubes are cut along the axis and cleaned with a soft brush to remove the arcing by-products. The microscopy samples are taken from the middle part of the inner surface of the tube.

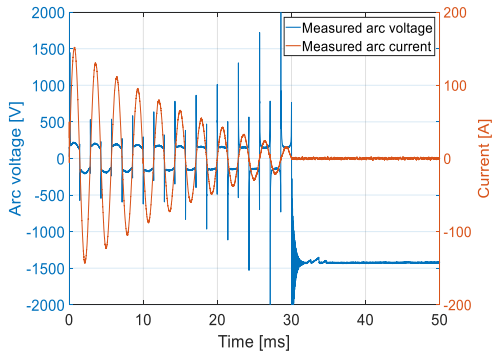

(a)

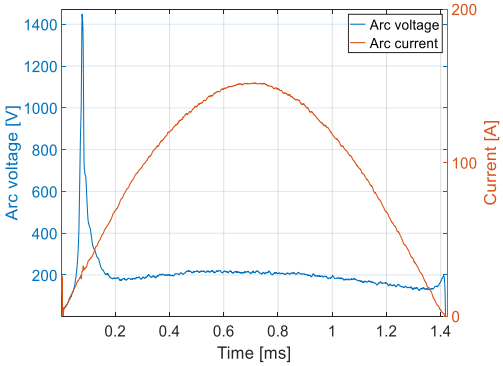

(b)

Fig. 2. Measured arc current and arc voltage waveform for arc burning inside 2 mm PTFE tube at atmospheric pressure. (a) The current is damped out due to the arc resistance. (b) First half cycle of the measured arc current and arc voltage.

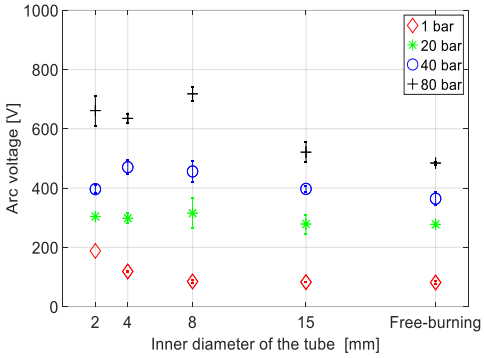

(a)

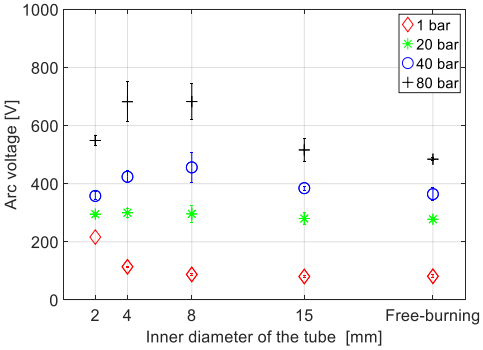

(b)

Fig. 3. Arc voltages at the current peak of 150 A at 350 Hz as a function of inner diameters of the tubes at different filling pressures. (a) Alumina. (b) PTFE.

III. Experimental Results

A typical arcing test with measurements of the arc voltage and the current for an arc burning inside a 2 mm PTFE tube at atmospheric pressure is shown in Fig. 2 (a). Due to the arc resistance, the current damps out with time. It has been reported that the arc resistance changes with gas pressure [9]. Therefore, only the first half cycle of the current is considered for further analysis. The current starts at t = 0, while the arc initiates at around t = 0.1 ms, when the ignition wire has melted (first voltage peak), see Fig. 2 (b). Once the arc is initiated, a stable arc voltage is measured from approximately 0.2 ms until it collapses before current zero. This paper investigates the arc voltage characteristics at the peak current of the first half cycle.

A. Arc Voltage Dependency on Inner Diameter of the Tube at Different Filling Pressures

The arc voltage as a function of the inner diameter of the tube for different filling pressures is plotted in Fig. 3, together with the free-burning arc tests. The average arc voltage of the three tests conducted per test case is plotted with an error bar. Here, the error bar is the maximum deviation from the average arc voltage per test case. Fig. 3(a) shows the arc voltages corresponding to alumina tubes, while the arc voltages inside the PTFE tubes are plotted in Fig. 3(b). At atmospheric pressure, the average free-burning arc voltage is found to be approximately 80 V. As the inner diameter decreases, a gradual increase of the arc voltage is observed for both alumina and PTFE tubes at 1 bar. The average arc voltage increases to 187 V for arcs burning inside a 2 mm wide alumina tube, and to 215 V for arcs burning inside a 2 mm wide PTFE tube at atmospheric pressure.

As the nitrogen filling pressure is increased, the arc voltage increases too. This is expected based on previous investigations [9]. The arc voltages measured for arcs burning inside 15 mm wide tubes are similar to those of corresponding free-burning arcs. The variation in arc voltage for a given case seems to increase somewhat with increasing pressure and decreasing diameter, although the data is limited. The arc voltage dependency on the tube material is not strong at 20, 40, and 80 bar nitrogen filling pressures.

The gradual increase in arc voltage with decreasing tube

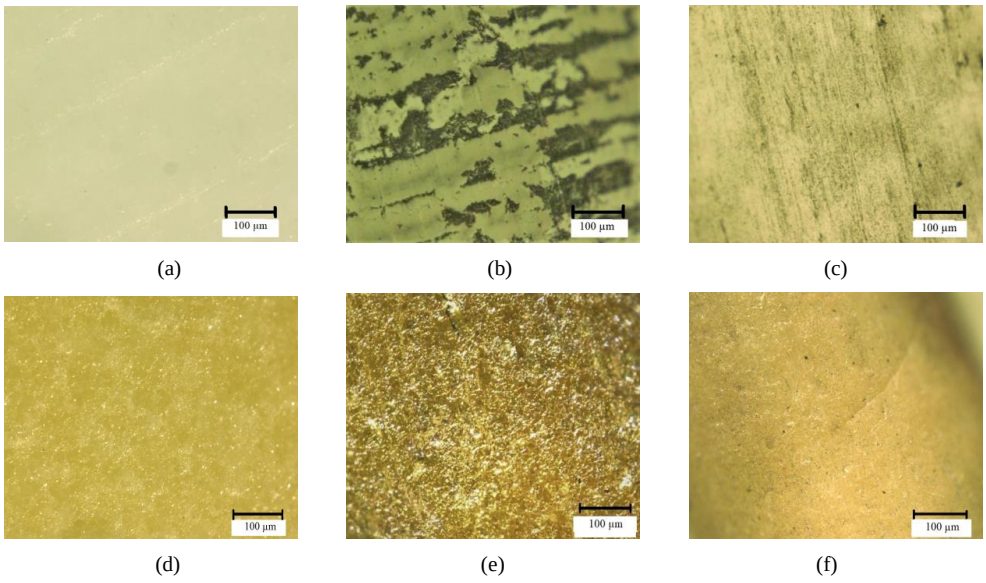

Fig. 4. Optical micrographs of the inner surface of 4 mm diameter tubes. (a) PTFE new (no arc). (b) PTFE, after arc at atmospheric pressure. (c) PTFE, after arc at 80 bar filling pressure. (d) Alumina new (no arc). (e) Alumina, after arc at atmospheric pressure. (f) Alumina, after arc at 80 bar filling pressure.

inner diameter that was observed for arcs at 1 bar pressure is not evident for higher pressures. At a nitrogen filling pressure of 20 bar, the arc voltage (approximately 300 V) seems to be more or less independent of both tube inner diameter and tube material. At 40, and 80 bar nitrogen, the maximum arc voltage is observed not for the smallest inner diameter of the tubes, but rather for 4 or 8 mm tube inner diameters.

B. Optical Microscopy of the Inner Surface of the Tube

Fig. 4 shows the optical micrographs of the investigated inner surfaces of tubes with 4 mm inner diameter before and after arcing. At atmospheric pressure, carbonization and scar marks are visible in the PTFE tube, (Fig. 4(b)). The presence of carbonization marks after arcing at atmospheric pressure could be due to the presence of O_2 and CO_2 in air. The ablation traces are significantly less visible in the PTFE tubes after arcing in 80 bar nitrogen, (Fig. 4(c)). When the arc burns inside alumina tubes at atmospheric pressure (Fig. 4(e)), the surface is changed compared to new alumina (Fig. 4(d)). On the other hand, when the filling pressure is increased to 80 bar, almost no arc traces are observed in the alumina tubes, as shown in Fig. 4(f). Both of the materials show reduced ablation traces at 80 bar nitrogen in contrast to atmospheric air.

IV. Model And Discussions

A. Free-burning Arc

The free-burning arc properties can be calculated based on Lowke's analytical model of free-burning arcs to estimate the effect of constriction due to the filling pressure [17]. The model is validated by comparing the calculated and the measured arc voltages. The peak arc current in this paper is 150 A, which is considered as a high-current arc. According to Lowke's model, the temperature at the arc center can be determined by the energy balance equation

$$\frac{I^2}{\sigma A^2} = \frac{4\pi k T}{A} + U, \tag{1}$$

where I is the arc current, σ is the electrical conductivity, A is the arc cross-sectional area, T is the temperature of the arc, k is the thermal conductivity, and U is the net radiation emission. The arc core is assumed to be a blackbody radiator and the net radiation emission can be expressed as

$$U = \frac{2\beta T^4}{r}\epsilon\,, \tag{2}$$

where β is the Stefan-Boltzmann constant, r is the arc radius, and ϵ is a parameter which characterizes the radiation mechanism inside the arc [12]. The parameter ϵ depends on the pressure and the arc radius and can be written as

$$\epsilon = 1 - \exp[-\gamma(pr)^{0.6}]\,, \tag{3}$$

where p is the pressure. The γ is a constant and has been considered equal to a value 0.025 by Niemeyer for a range of plastic materials [18]. However, for free-burning arcs in air, the constant γ is lower than 0.025. In this paper it is assumed to be 0.007 at atmospheric pressure and 0.023 at 80 bar based on the data for arcs burning in air [18].

The equations that define the arc radius and the electric field in the free-burning arc are taken directly from the expressions for high current arcs deduced by Lowke [17]:

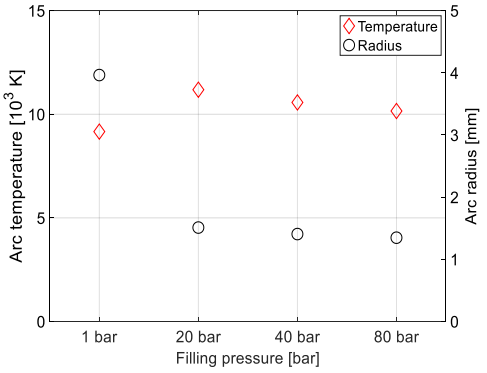

(a)

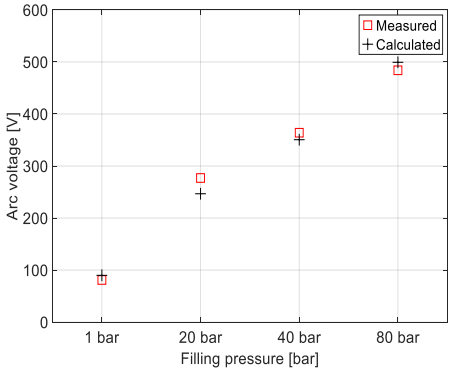

(b)

Fig. 5. Calculated parameters of free-burning arcs as a function of filling pressure for arc current of 150 A (a) Calculated arc temperature and radius. (b) Measured and calculated arc voltage.

$$r = 1.11\left(\frac{z}{h\sigma}\right)^{\frac{1}{4}}\frac{I^{\frac{3}{8}}}{(\mu J_o \rho)^{\frac{1}{8}}}, \tag{4}$$

and

$$E = 0.26\left(\frac{h}{z\sigma}\right)^{\frac{1}{2}} I^{\frac{1}{4}}(\mu J_o \rho)^{\frac{1}{4}}. \tag{5}$$

Here, z is the distance from the cathode, h is the enthalpy of the arc core, μ is the permeability, J_o is the current density at the cathode, ρ is the density, and E is the electric field. Solving equation (1-5) iteratively together with the material data of nitrogen enable calculation of the arc temperature, radius, and the electric field. In some cases, due to scarcity of high pressure material data for nitrogen at high temperature, thermodynamic and transport properties of high pressure air are used [19-21]. From the calculated electric field, the arc voltage can then be estimated by assuming a fixed electrode voltage drop of 17 V for all filling pressures, based on previous works [9], [22].

The calculated arc temperature and radius for free-burning arcs at different filling pressures are plotted in Fig. 5(a). It can be seen that the free-burning arc radius decreases from approximately 4 mm for atmospheric pressure arcs to approximately 1.5 mm and 1.35 mm for arcs burning at 20 bar and 80 bar filling pressures, respectively. The calculated arc temperature for free-burning arcs at different pressure levels lies in the range of 9,000-12,000 K. The temperature in the arc increases when the pressure rises from 1 bar to 20 bar mainly due to constriction. The slight decrease in temperature for 40 bar and 80 bar is due to the increased radiative cooling of the arc [17]. The calculated arc voltages for free-burning arcs, at different filling pressures are in good agreement with the measured values and are plotted in Fig. 5(b).

B. Tube-constricted Arc

Ablation controlled arcs at atmospheric pressure have been studied in the past [11-13]. The contraction factor which is the ratio of the cross sectional area of the arc and the tube is calculated based on the analytical expression described in the works of Kovitya [23]:

$$\frac{A}{Q} = \frac{(1-f)\rho_c a_c}{\left(\frac{f}{h_c} - \frac{1-f}{h-h_c}\right)\rho(h-h_c)a + (1-f)\rho_c a_c}. \tag{6}$$

Here, A is the arc cross sectional area, Q is the cross sectional area of the tube, h is the enthalpy of the arc, a is the speed of sound, ρ is the mass density, and f is the parameter determining the part of radiation causing ablation. The subscript c denotes the properties in the vapor region, while without subscript denotes the arc core. The value of f lies in the range of 0 to 1 and can ideally be determined from the measured mass loss of the tube due to ablation. The mass losses in these cases are believed to be extremely small and were not measured. In this paper, f is chosen in such a way that the calculated arc voltage matches the measured arc voltage. The steady state solution of the two zone model is determined for an arc current of 150 A. Conservation of mass, momentum, and energy along with Ohm's law is used to calculate the arc temperature and radius of the tube-constricted arc [23]. As the arc voltage dependency on tube material was not found to be strong at high filling pressures, only the alumina was considered for the tube-constricted arcs. The two-zone arc model is not valid when the tube diameter is very large compared to the free-burning arc diameter. Hence, only 2 mm, 4 mm, and 8 mm tube inner diameters are considered here. The equations along with the material dependent data of electrical conductivity, density, enthalpy, sonic velocity are solved iteratively [19], [21], [24].

Due to the constriction of the tube, the arc radius decreases and the temperature in the core increases. Fig. 6 shows the calculated arc temperature and radius for the arcs burning inside alumina tube as a function of filling pressure. The free-burning arc radius at atmospheric pressure was previously calculated to be approximately 4 mm with an arc core temperature of approximately 9,000 K. At atmospheric pressure, the tube constricts the arc and subsequently the arc temperature increases up to approximately 19,000 K. An increase in arc temperature generally results in a higher electrical conductivity.

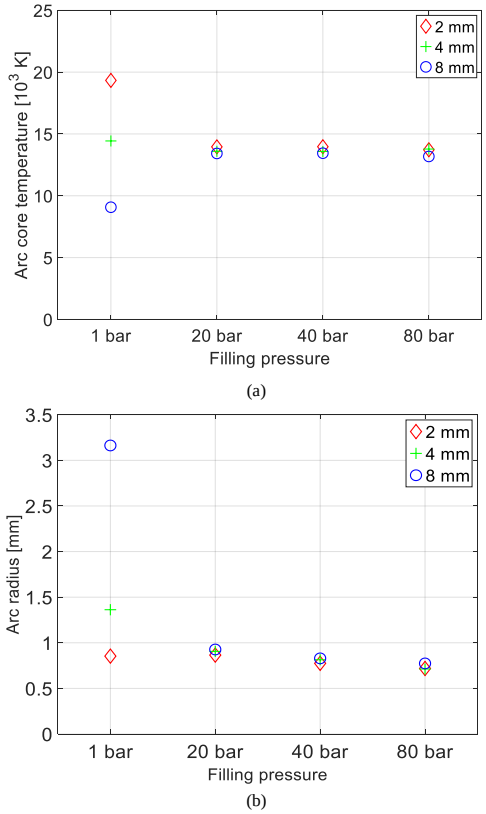

Fig. 6. Calculated arc temperature and radius for arc current of 150 A burning inside different diameter of alumina tube as a function of filling pressures. (a) Arc temperature. (b) Arc radius.

However, due to the tube-constriction at atmospheric pressure, the arc area is reduced. Hence, the arc voltage increases as the tube diameter decreases when the arc burns in atmospheric pressure.

At higher filling pressures (i.e., 20 bar, 40 bar, and 80 bar), the effect of the tube inner diameter on the arc radius and temperature is not as strong as at atmospheric pressure. The filling pressure alone constricts the arc when the pressure is increased, as was seen for the free-burning arcs (see Fig. 5(a)). As a result, the effect of the tube constriction is less significant at higher filling pressures. The arc temperature remains almost constant around 14,000 K for filling pressures above 20 bar irrespective of the tube diameters. The arc radius decreases slightly with filling pressure, while the effect of tube diameter is not strong when the gas pressure is above 20 bar.

From the experimental results, as the filling pressure was increased, the relationship between the arc voltage and tube diameter was not as straightforward as for the atmospheric pressure arcs. As the arc is constricted due to the filling pressure, the radiation emission coefficient increases [25]. For not optically thin plasmas with a radius of 1 mm at 15,000 K, the net emission coefficient becomes approximately 10 times larger when the pressure is increased from 1 bar to 100 bar [25]. However, the increase in filling pressure also accounts for a larger number of molecules outside the arc core, resulting in higher absorption rates of the radiated energy. As a result, the absorption coefficient increases with the filling pressure. The absorption coefficient becomes approximately 100 times larger when the filling pressure is increased from 1 bar to 100 bar at an arc temperature of 15,000 K [25]. This clearly demonstrates the dominant effect of absorption over radiation at high filling pressures. A similar dominance of absorption coefficient over net radiation emission coefficient at elevated pressures has also been reported for hydrogen arcs burning at 20 bar gas pressure [26]. Likewise, a significant reduction of ablation in metal by a laser due to increased pressure of the surrounding gases has been reported in the literature [27]. This agrees with the optical micrographs, where less scar marks were observed at the inner surfaces of the tubes at 80 bar, compared to atmospheric pressure.

For arcs burning in a 2 mm diameter tube, the measured arc voltages were lower than those in 8 mm tube diameters at 40 bar and 80 bar filling pressures. The viscosity could play a vital role in these cases. The fluid flow resistance inside a tube is linearly proportional to viscosity and inversely proportional to the power of four of the tube radius in case of a laminar flow. The type of flow occurred inside the tube is beyond the scope of this study. Nevertheless, the viscosity of air plasma increases approximately 15 times at the calculated arc temperatures when the filling pressure of the air is increased from 1 bar to 80 bar [20]. Consequently, for tubes with inner diameter of 2 mm at 40 and 80 bar filling pressures, a highly conductive plasma may fill the tube due to high flow resistance, which can play a pivotal role to increase the conductivity of the arc channel.

To summarize, the arc radii and temperatures were calculated using Lowke's theory of free-burning arcs. The arc is constricted by increasing gas pressure. The arc radius and the temperature for the arcs burning inside alumina tubes with 2, 4, and 8 mm inner diameters were then calculated for different filling pressures based on the two-zone arc model. The effect of tube constriction is apparent at 1 bar ambient pressure. However, the effect of tube inner diameter (2, 4, 8 mm) on the arc temperature and radius are found less significant at high filling pressures (i.e., 20 bar, 40 bar, and 80 bar). The increased absorption of arc energy by the gas surrounding the arc core reduces the radiation reaching the inner surface of the tube at high filling pressures, which is also consistent with the observation from optical micrographs. Finally, for the tubes with 2 mm inner diameter at gas pressures of 40, and 80 bar, the effect of viscosity could play a crucial role in the reduced arc voltage.

V. Conclusion

Nitrogen arcs burning inside cylindrical tubes of alumina and PTFE have been investigated experimentally by means of arc voltage measurements at different filling pressures, including supercritical region. Moreover, optical microscopy has been used to qualitatively investigate the level of ablation. Based on

the experimental results and calculated arc parameters, the following conclusions have been drawn:

- At atmospheric pressure, the arc voltage increases with decreasing inner diameter of the tube, as expected.
- The measured arc voltage at high filling pressures inside a tube does not have a simple relationship with the inner diameter of the tube. The filling pressure constricts the arc channel, which limits the interaction of the arc core with the tube.
- The optical micrographs show reduced ablation traces in a 4 mm wide tube at 80 bar compared to the 1 bar ambient pressure arcs. The increase in the absorption of radiation by the gas surrounding the arc core at very high pressure reduces the ablation. As a result, ablation may become less significant for ultrahigh-pressure nitrogen arcs in contrast to the atmospheric pressure arcs.

REFERENCES

[1] T. Hazel, H. H. Baerd, J. J. Legeay, and J. J. Bremnes, "Taking power distribution under the sea: design, manufacture, and assembly of a subsea electrical distribution system," *IEEE Industry Applications Magazine*, vol. 19, no. 5, pp. 58-67, 2013.

[2] J. Sengers and J. L. Sengers, "Thermodynamic behavior of fluids near the critical point," *Annual Review of Physical Chemistry*, vol. 37, no. 1, pp. 189-222, 1986.

[3] J. Zhang, A. Markosyan, M. Seeger, E. van Veldhuizen, E. van Heesch, and U. Ebert, "Numerical and experimental investigation of dielectric recovery in supercritical N_2," *Plasma Sources Science and Technology*, vol. 24, no. 2, p. 025008, 2015.

[4] T. Ito and K. Terashima, "Generation of micrometer-scale discharge in a supercritical fluid environment," *Applied physics letters*, vol. 80, no. 16, pp. 2854-2856, 2002.

[5] E. H. Lock, A. V. Saveliev, and L. A. Kennedy, "Influence of electrode characteristics on DC point-to-plane breakdown in high-pressure gaseous and supercritical carbon dioxide," *IEEE Transactions on Plasma Science*, vol. 37, no. 6, pp. 1078-1083, 2009.

[6] H. Tanoue *et al.*, "Characteristics of shock waves generated by a negative pulsed discharge in supercritical carbon dioxide," *IEEE Transactions on Plasma Science*, vol. 42, no. 10, pp. 3258-3263, 2014.

[7] Z. Yang, S. Hosseini, T. Kiyan, S. Gnapowski, and H. Akiyama, "Post-breakdown dielectric recovery characteristics of high-pressure liquid CO_2 including supercritical phase," *IEEE Transactions on Dielectrics and Electrical Insulation*, vol. 21, no. 3, pp. 1089-1094, 2014.

[8] J. Zhang, B. van Heesch, F. Beckers, T. Huiskamp, and G. Pemen, "Breakdown voltage and recovery rate estimation of a supercritical nitrogen plasma switch," *IEEE Transactions on Plasma Science*, vol. 42, no. 2, pp. 376-383, 2014.

[9] F. Abid, K. Niayesh, E. Jonsson, N. S. Støa-Aanensen, and M. Runde, "Arc Voltage Characteristics in Ultrahigh-Pressure Nitrogen Including Supercritical Region," *IEEE Transactions on Plasma Science*, vol. 46, no. 1, pp. 187-193, 2018.

[10] P. Kovitya, "Ablation-stabilized arcs in nylon and boric acid tubes," *IEEE transactions on plasma science*, vol. 15, no. 3, pp. 294-301, 1987.

[11] P. Kovitya and J. Lowke, "Theoretical predictions of ablation-stabilised arcs confined in cylindrical tubes," *Journal of Physics D: Applied Physics*, vol. 17, no. 6, pp. 1197-1212, 1984.

[12] L. Muller, "Modelling of an ablation controlled arc," *Journal of Physics D: Applied Physics*, vol. 26, no. 8, p. 1253, 1993.

[13] C. Ruchti and L. Niemeyer, "Ablation controlled arcs," *IEEE Transactions on Plasma Science*, vol. 14, no. 4, pp. 423-434, 1986.

[14] M. Seeger, J. Tepper, T. Christen, and J. Abrahamson, "Experimental study on PTFE ablation in high voltage circuit-breakers," *Journal of Physics D: Applied Physics*, vol. 39, no. 23, pp. 5016-5024, 2006.

[15] F. Abid, K. Niayesh, E. Jonsson, N. S. Støa-Aanensen, and M. Runde, "Arc Voltage Measurements Of Ultrahigh Pressure Nitrogen Arcs In Cylindrical Tubes," presented at the 22nd International Conference on Gas Discharges and their Applications, Novi Sad, Serbia, 2-7 September, 2018.

[16] J. Aakervik, G. Berg, and S. Hvidsten, "Design of a high voltage penetrator for high pressure and temperature laboratory testing," in *Electrical Insulation and Dielectric Phenomena (CEIDP)*, Cancun, Mexico, 16-19 Oct. 2011, pp. 267-270: IEEE.

[17] J. Lowke, "Simple theory of free-burning arcs," *Journal of physics D: Applied physics*, vol. 12, no. 11, p. 1873, 1979.

[18] L. Niemeyer, "Evaporation dominated high current arcs in narrow channels," *IEEE Transactions on power Apparatus and Systems*, vol. PAS-97, no. 3, pp. 950-958, 1978.

[19] W. Chunlin *et al.*, "Thermodynamic and transport properties of real air plasma in wide range of temperature and pressure," *Plasma Science and Technology*, vol. 18, no. 7, p. 732, 2016.

[20] A. D'Angola, G. Colonna, A. Bonomo, D. Bruno, A. Laricchiuta, and M. Capitelli, "A phenomenological approach for the transport properties of air plasmas," *The European Physical Journal D*, vol. 66, no. 8, p. 205, 2012.

[21] K. Meher, N. Tiwari, and S. Ghorui, "Thermodynamic and transport properties of nitrogen plasma under thermal equilibrium and non-equilibrium conditions," *Plasma Chemistry and Plasma Processing*, vol. 35, no. 4, pp. 605-637, 2015.

[22] Y. Yokomizu, T. Matsumura, R. Henmi, and Y. Kito, "Total voltage drops in electrode fall regions of, argon and air arcs in current range from 10 to 20 000 A," *Journal of Physics D: Applied Physics*, vol. 29, no. 5, p. 1260, 1996.

[23] P. Kovitya and J. Lowke, "Theoretical predictions of ablation-stabilised arcs confined in cylindrical tubes," *Journal of Physics D: Applied Physics*, vol. 17, no. 6, p. 1197, 1984.

[24] P. Kovitya, "Thermodynamic and transport properties of ablated vapors of PTFE, alumina, Perspex, and PVC in the temperature range 5000-30 000 K," *IEEE Transactions on plasma science*, vol. 12, no. 1, pp. 38-42, 1984.

[25] J. Zhong, F. Yang, W. Wang, D. Yuan, and J. D. Yan, "Net Emission Coefficient and Radiation Transfer Characteristics of Thermal Plasma Generated in Nitrogen-PTFE Vapor Mixture," *IEEE Transactions on Plasma Science*, vol. 46, no. 4, pp. 990-1002, 2018.

[26] P. Gueye, Y. Cressault, V. Rohani, and L. Fulcheri, "A simplified model for the determination of current-voltage characteristics of a high pressure hydrogen plasma arc," *Journal of Applied Physics*, vol. 121, no. 7, p. 073302, 2017.

[27] Y. Chivel and V. Nasonov, "Influence of ambient gas pressure on laser induced metal ablation," *Physics Procedia*, vol. 5, pp. 255-259, 2010.

Fahim Abid received the B.Sc. degree in electrical and electronic engineering from the Islamic University of Technology (IUT), Dhaka, Bangladesh in 2012. He received the M.Sc. degree in electrical engineering combinedly from Royal Institute of Technology (KTH), Stockholm, Sweden and Technical University Eindhoven (TU/e), Eindhoven, Netherlands in 2015. He is currently working as a PhD candidate at the department of electric power engineering in Norwegian University of Science and Technology (NTNU), Trondheim, Norway.

Kaveh Niayesh (S'98–M'01–SM'08) received the B.Sc. and M.Sc. degrees in electrical engineering from the University of Tehran, Tehran, Iran, in 1993 and 1996, respectively, and the Ph.D. degree in electrical engineering from the RWTH-Aachen University of Technology, Aachen, Germany, in 2001.

He held different academic and industrial positions including Principal Scientist with the ABB Corporate Research Center, Baden-Dattwil, Switzerland; Associate Professor with the University of Tehran; and Manager, Basic Research, with AREVA T&D, Regensburg, Germany. Currently, he is a Professor with the Department of Electric Power Engineering, Norwegian University of Science and Technology (NTNU). He is the holder of 16 patents and has more than 105 journal and conference publications on current interruption and limitation, vacuum and gaseous discharges, plasma modeling and diagnostics, switching transients, and pulsed power technology.

Nina Sasaki Støa-Aanensen received the M.Sc. degree in applied physics and mathematics and the Ph.D. degree in electrical power engineering from the Norwegian University of Science and Technology (NTNU), Trondheim, Norway, in 2011 and 2015, respectively.

She is currently working with SINTEF Energy Research, Trondheim, Norway.

Paper III

doi:10.14311/ppt.2019.1.23
Plasma Physics and Technology **6**(1):23–26, 2019

NOZZLE WEAR AND PRESSURE RISE IN HEATING VOLUME OF SELF-BLAST TYPE ULTRA-HIGH PRESSURE NITROGEN ARC

F. Abid[a,*], K.Niayesh[a], N. Støa-Aanensen[b]

[a] *Department of Electric Power Engineering, Norwegian University of Science and Technology, 7491, Trondheim, Norway*

[b] *SINTEF Energy Research, 7465, Trondheim, Norway*

[*] fahim.abid@ntnu.no

Abstract. This paper reports on experiments with ultra-high pressure nitrogen arcs in a self-blast type switch design. The effect of filling pressure on nozzle mass loss and pressure-rise in the heating volume is investigated. An arc current peak of 130 A at 190 Hz, and a fixed inter-electrode gap of 50 mm are used. The arc burns inside a polytetrafluoroethylene nozzle with a gas outflow vent in the middle. Three different nitrogen filling pressures were tested: 1, 20 and 40 bar, which also covers the supercritical region. To study the effect of vent size on blow pressure near current zero, three different vent dimensions were investigated. The energy deposited in the arc increases with the filling pressure. It is observed that the pressure-rise in the heating volume is linked to the filling pressure, while the vent size plays a crucial role in the blow pressure near current zero. The nozzle mass loss per unit energy deposited in the arc is found to be independent of the filling pressure.

Keywords: ultrahigh pressure arc, nozzle wear, supercritical fluid, arc discharge.

1. Introduction

The interruption chamber of a medium voltage (MV) gas circuit breaker is generally filled at atmospheric pressure or at a slightly elevated pressure of a few bar. Due to safety reasons, these MV gas circuit breakers are almost never filled with extremely high pressure. For gas circuit breakers, the interruption performance is believed to be related to filling pressure due to the increase of gas flow rate near current zero (CZ) [1]. Switchgears placed at the seabed for subsea power transfer applications have the potential to be filled with extremely high filling pressure. By filling the interrupting chambers of such switchgears at the surrounding pressure, the complexity and cost of the encapsulation can be substantially reduced.

When the pressure and temperature of a gas exceed a critical point, the gas enters into the supercritical (SC) region. High density, high heat conductivity, high diffusivity, absence of vapour bubbles and self-healing properties are some of the unique features of an SC fluid. For gas circuit breakers, the properties of SC fluids are believed to be in favour of improved current interruption performance [2]. For nitrogen (N_2), the critical point is 126 K and 33.5 bar. Nitrogen is chosen in this work due to its environmentally benign nature, good insulation strength and low critical pressure.

There are few publications on gas discharges in ultra-high pressure medium in general, among which almost none of them cover high energy arc discharges typical for power switching applications [2, 3]. Recently, some efforts have been made to investigate arc discharges in SC N_2 at tens of bars filling pressure. The arc voltage is reported to increase with filling pressure, without any abrupt change during the transition from gas to SC state [4]. A higher arc voltage results in an increased energy deposition in the arc channel. Moreover, the arc radius decreases as the filling pressure increases [5].

To investigate the effect of gas flow for very high pressure arc discharges, a self-blast arrangement is adopted in this paper. A self-blast switch design is studied in a fixed electrode arrangement where the arc burns inside a polytetrafluoroethylene (PTFE) nozzle with a gas outflow vent in the middle. During the high current phase, the PTFE nozzle will ablate. Some of the ablated mass escapes through the vent and the rest causes a pressure rise in the heating volume. The compressed gas in the heating volume creates a backflow of relatively cold gas near CZ to cool the arc for current interruption. To study the effect of vent size on blow pressure near CZ, three different vent dimensions are investigated. Experiments are conducted at three different N_2 filling pressures: 1 bar (atmospheric pressure), 20 bar and 40 bar (supercritical region). In this paper, the effect of filling pressure on mass loss of the PTFE nozzle and consecutive pressure rise in the heating volume is reported.

2. Experimental setup

The electrical setup is shown in Figure 1(a). The test circuit consists of the charging and discharging sections of a 7.2 µF high voltage (HV) capacitor bank, C. The capacitor bank is charged through a diode-resistance unit (R_C–D_C) from a HV source. Once the capacitor bank is charged to a predefined voltage, it is disconnected from the grid by switch S_C. Afterwards,

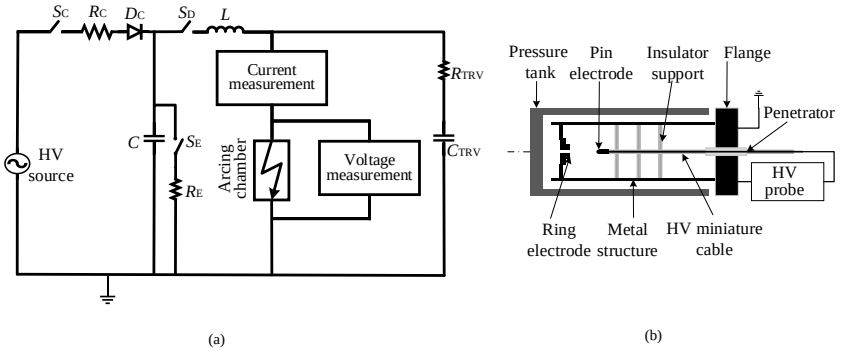

Figure 1. Experiment setup, (a) electrical circuit, (b) interior connection of the pressure tank.

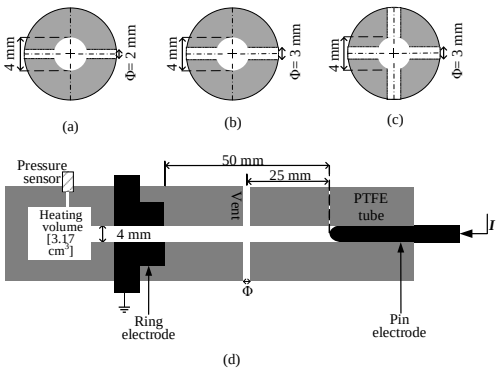

*Figure 2. Cross sectional view of the vent of three designs. (a) design **a**, (b) design **b**, (c) design **c**. Electrode arrangement, nozzle, heating volume, (d) Longitudinal view.*

the switch S_D is closed which results in a current flow through the inductor, L and further through a copper ignition wire (40 µm diameter) inside the arcing chamber. The inductance of L, and the charging voltage of C are kept constant to generate a current amplitude of 130 A in the first half cycle at a frequency of 190 Hz for all the experiments conducted. As the arc resistance varies with the filling pressure, the damping of the LC oscillation also changes. Hence, only the first half cycle is considered for all cases. A parallel resistive-capacitive branch (R_{TRV}–C_{TRV}) is placed across the arc to generate a controlled initial rate of rise of recovery voltage (IRRRV) of 43 V/ µs after CZ, see Figure 1(a).

A pressure tank of 15.7 litres rated for 500 bar, is used as arcing chamber. The interior connection of the pressure tank is shown schematically in Figure 1(b). A HV miniature cable is inserted into the pressure tank using a cable penetrator. The arc burns between the pin and the ring electrode. The arc is initiated by melting of a copper ignition wire. To investigate the effect of gas flow on the arc based on self-blast principle, the arc is ignited inside a 4 mm diameter PTFE nozzle with vents in the middle. The electrode arrangement, nozzle and the heating volume are shown schematically in Figure 2(d). A heating volume of 3.17 cm^3 is attached on the ring electrode where the ablated gas is stored during the high current phase and generates a back-flow of the stored gas near CZ. In this paper, three different vent sizes are investigated: 2 opposite holes of $\Phi = 2$ mm (design **a**), 2 opposite holes of $\Phi = 3$ mm (design **b**), and 4 opposite holes $\Phi = 3$ mm (design **c**), see Figure 2(a-c). Three different filling pressures are investigated in this paper: 1 bar, 20 bar and 40 bar, which also covers the supercritical region. For each filling pressure all three designs are tested with a new nozzle.

A HV probe measures the arc voltage across the electrodes while a current shunt is used to measure the arc current. A piezoelectric pressure sensor is mounted on the heating volume to measure the pressure rise, as can be seen in Figure 2(d). The pressure sensor is recess-mounted, and a vinyl electric tape is used to protect it from the thermal blast. All the data are sent to the control room via optical fibre links and stored in a digital oscilloscope with a sampling rate of ten samples per microsecond. For mass loss measurement, weight measurement with an accuracy of 0.1 mg is carried out before and after five tests of all the new nozzles.

3. Results and discussions

A typical measurement of the arc voltage, arc current, and pressure rise in the heating volume for design **a** at 40 bar filling pressure is shown in Figure 3. The ignition wire melts at approximately 0.2 ms marked by a voltage peak. The pressure in the heating volume starts building from approximately 0.5 ms. The pressure rises to a maximum of 13.5 bar at approximately 0.8 ms. Afterwards, the back-flow of stored gas from heating volume starts and flows out completely at approximately 2.9 ms. The CZ occurs approximately

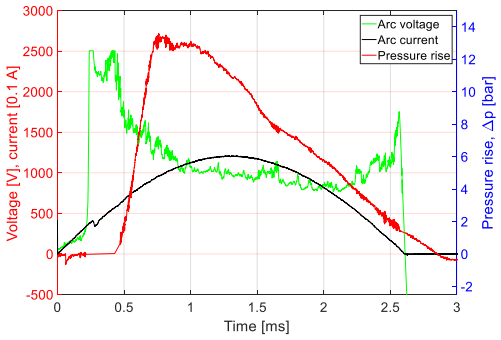

Figure 3. Arc voltage, current and pressure rise in heating volume for design **a** *at a filling pressure of 40 bar.*

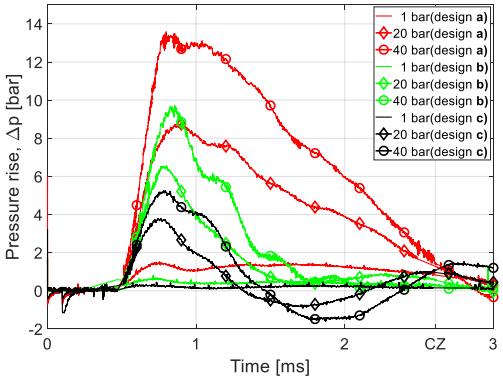

Figure 4. Pressure rise in the heating volume as a function of filling pressure for different designs.

at 2.61 ms where the current is interrupted by the self-blast test switch. The over-pressure in the heating volume at CZ in this case is approximately 1.64 bar. The back-flow of stored gas in heating volume near CZ cools the arc, which can be seen by the extinction peak of the arc voltage.

3.1. Pressure rise in heating volume

The measured over-pressures in the heating volume for three designs at three different filling pressures are plotted in Figure 4. The measured pressure-rise in the heating volume is different for different vent dimensions. As the hole size in the vent is increased, more ablated PTFE vapour leaves the arcing zone through the vent instead of contributing to the pressure build up in heating volume. As a result, design **a** shows higher pressure rise in comparison with design **b** and **c** for any specific filling pressure.

The vent dimension also plays a crucial role in the outflow of the stored gas. The heated N_2 and PTFE vapour flows out more slowly in design **a** compared to other designs. In contrast to design **a**, the stored gas leaves completely in design **b** at approximately 1.75 ms. As a result the over-pressure at CZ is low for design **b**. For design **c** however, a negative pressure rise in the heating volume is observed at 20 bar and 40 bar filling pressure, indicating a gas intake through the hole.

The filling pressure also has a significant effect on the pressure-rise in the heating volume. For all designs, the highest pressure rise is observed for 40 bar filling pressure, followed by 20 bar and 1 bar. The rate of change of over-pressure in the heating volume around CZ determines the gas flow rate, hence, the effective cooling of the arc. The measured over-pressures at CZ for all the cases tested are presented in Table 1.

3.2. Mass loss of PTFE nozzle

Five tests were conducted for each filling pressure and for each design. Among them, the only design that resulted in successful current interruption in the first two CZ was design **a**. The current interruption in design **b** and **c** happened after first, second or several half cycles. Consequently, only design **a** is considered for mass loss analysis.

Filling pressure [bar]	**1**	**20**	**40**
Design **a**	0.81	1.31	1.64
Design **b**	0.27	0.53	0.28
Design **c**	0.15	0.96	1.07

Table 1. Over-pressure in the heating volume at CZ [bar].

As the filling pressure increases, the energy deposition in the arc increases too as a result of the increased arcing voltage. From the measured arc voltage and arc current, the energy deposited in each test is calculated until the current is interrupted. At 1 bar, a total nozzle mass loss of 9.2 mg was measured after five tests, while the total energy deposition of five tests was approximately 313 J. For 20 bar and 40 bar, the mass losses measured after 5 tests were 31.1 mg (851 J) and 42.3 mg (1186 J), respectively. Afterwards, the mass loss per unit energy deposited in the arc at different filling pressure is calculated, which is shown in Table 2. It can be seen that although the overall mass loss in PTFE nozzle increases with the filling pressure, the mass loss per unit energy deposition is not strongly dependent on the gas pressure.

3.3. Current interruption performance

The number of successful interruptions after first half cycle among the five tests conducted for each case are plotted in Figure 5. For design **a** at 1 bar pressure, the current was interrupted 4 times among the 5 tests conducted. The number of successful interruption increased to 5 out of 5 for both 20 bar and 40 bar filling pressure using design **a**. For design **b**, however, the interruption performance deteriorated for all filling pressures. Interruption performance is observed to

Filling pressure [bar]	**1**	**20**	**40**
Total energy deposited [J]	313	851	1186
Mass loss [mg]	9.2	31.1	42.3
Mass loss/energy [mg/kJ]	29.4	36.5	35.7

Table 2. Nozzle mass loss as a function of filling pressure.

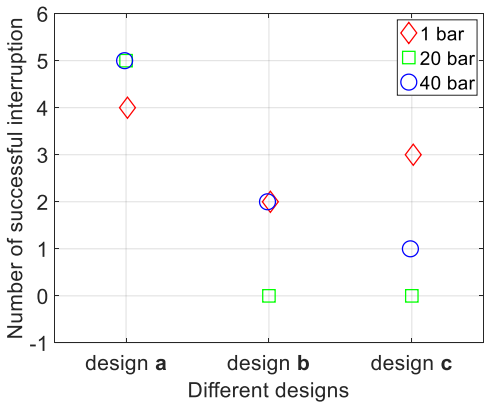

Figure 5. Number of successful interruption among the five tests conducted at different filling pressures for three designs.

deteriorate as the filling pressure increases for design **c**.

For a successful current interruption, effective cooling of the arc is necessary. The arc resistance build-up just before CZ is a key parameter for a successful current interruption [6]. As the gas filling pressure is increased, the arc radius decreases, while the temperature of the arc column increases. Without the sufficient flow at a higher filling pressure (i.e., 20 bar, 40 bar), the arc resistance fails to build up before CZ resulting in a poor interruption performance. The rate of change of overpressure near CZ is high in design **a** for all the filling pressures tested in comparison to other designs, see Figure 4. The gas flow due to high rate of change of over-pressure near CZ results in an improved cooling of the arc and hence, better interruption performance for design **a**. The filling pressure also affects the flow field near CZ [7]. Without sufficient cooling of the arc, the high filling pressure can deteriorate the interruption performance, in this case design **b**, and **c**. This paper underpins the importance of gas flow near CZ for ultra-high pressure N_2 arc for current interruption application.

4. Conclusions

The mass loss of PTFE nozzle, pressure rise in the heating volume and interruption performance for arc burning at different filling pressure of nitrogen are reported in this paper. To study the effect of vent size on blow pressure near current zero, three different vent dimensions are studied. Based on the experimental results following conclusions have been drawn.

1. The pressure rise in the heating volume increases with the filling pressure. The outlet vent dimension plays a decisive role in both the pressure rise in the heating volume and the back-flow near CZ. With proper designing the interruption performance can be improved for ultra-high pressure nitrogen arcs.

2. Total nozzle mass loss is found to increase with the filling pressure. A high filling pressure also constitutes for a high energy deposition in the arc as a result of high arcing voltage. Nevertheless, the mass loss per unit energy deposition in the arc is found to be less dependent on filling pressures.

Acknowledgements

This work is supported by the Research Council of Norway, project number 280539.

References

[1] W. Hermann and K. Ragaller. Theoretical description of the current interruption in HV gas blast breakers. *IEEE Transactions on Power Apparatus and systems*, 96(5):1546–1555, 1977. doi:10.1109/T-PAS.1977.32483.

[2] J. Zhang, E. van Heesch, F. Beckers, A. Pemen, R. Smeets, T. Namihira, and A. Markosyan. Breakdown strength and dielectric recovery in a high pressure supercritical nitrogen switch. *IEEE Transactions on Dielectrics and Electrical Insulation*, 22(4):1823–1832, 2015. doi:10.1109/TDEI.2015.005013.

[3] T. Kiyan, A. Uemura, B. C. Roy, T. Namihira, M. Hara, M. Sasaki, M. Goto, and H. Akiyama. Negative DC prebreakdown phenomena and breakdown-voltage characteristics of pressurized carbon dioxide up to supercritical conditions. *IEEE transactions on plasma science*, 35(3):656–662, 2007. doi:10.1109/TPS.2007.896774.

[4] F. Abid, K. Niayesh, E. Jonsson, N. S. Støa-Aanensen, and M. Runde. Arc voltage characteristics in ultrahigh-pressure nitrogen including supercritical region. *IEEE Transactions on Plasma Science*, 46(1):187–193, 2018. doi:10.1109/TPS.2017.2778800.

[5] F. Abid, K. Niayesh, and N. S. StÃÿa-Aanensen. Ultrahigh-pressure nitrogen arcs burning inside cylindrical tubes. *IEEE Transactions on Plasma Science*, 47(1):754–761, Jan 2019. doi:10.1109/TPS.2018.2880841.

[6] M. Seeger, B. Galletti, R. Bini, V. Dousset, A. Iordanidis, D. Over, N. Mahdizadeh, M. Schwinne, P. Stoller, and T. Votteler. Some aspects of current interruption physics in high voltage circuit breakers. *Contributions to Plasma Physics*, 54(2):225–234, 2014. doi:10.1002/ctpp.201310067.

[7] Z. Guo, X. Li, Y. Zhang, X. Guo, and J. Xiong. Investigation on the influence of gas pressure on CO_2 arc characteristics in high-voltage gas circuit breakers. *Plasma Physics and Technology*, 4(1):95–98, 2017.

Paper IV

Current Interruption Performance of Ultrahigh-Pressure Nitrogen Arc

Fahim Abid[1], Kaveh Niayesh[1], Camilla Espedal[2] and Nina Støa-Aanensen[2]

[1] Department of Electric Power Engineering, Norwegian University of Science and Technology, Trondheim, Norway
[2] SINTEF Energy Research, Trondheim, Norway

E-mail: fahim.abid@ntnu.no

Received xxxxxx
Accepted for publication xxxxxx
Published xxxxxx

Abstract

In this paper, the influence of gas filling pressure on the current interruption performance of different switch configurations with electric arcs burning in nitrogen has been experimentally investigated. A synthetic circuit generating a current of 130 A at 190 Hz is used and the initial rate of rise of recovery voltage just after current zero is varied from 9.8 V/µs to 84.9 V/µs. To evaluate the effect of forced gas flow on current interruption performance, three different test arrangements are investigated: a simple contact configuration with a free-burning arc, a contact and a cylindrical nozzle setup (tube-constricted arc), and finally a self-blast arrangement where the arc is cooled by a gas flow near current zero. In each arrangement, three different filling pressures are mainly studied: 1, 20, and 40 bar, the latter being in the supercritical region. In all cases, the interelectrode gap is fixed at 50 mm. It is observed that the interruption performance deteriorates with increased filling pressure in the absence of forced gas flow. A higher post-arc current is observed for the arcs burning at high filling pressures (i.e., 20 and 40 bar) compared to at atmospheric pressure in cases with no or little forced cooling. On the other hand, a forced gas flow near the current zero reduces the post-arc current and improves the interruption performance also at high filling pressures. Little effect of the supercritical state on the interruption performance of nitrogen is observed. Under the above-mentioned test conditions, the majority of the failures at high filling pressure are observed to be of thermal re-ignition type.

Keywords: supercritical fluid, arc discharge, current interruption.

1. Introduction

An increasing number of offshore wind farms as well as other activities located far off the coast lead to the need for offshore substations. To avoid the large costs associated with platforms and floaters, power switching equipment and other components of such an offshore substation can be placed on the seabed and controlled remotely [1]. The conventional solution is to use thick-walled pressure-proof vessels to provide an environment for the power components like that of onshore installations [2]. Power cable feed-throughs or penetrators from the high-pressure water environment and into the low gas pressure inside the vessel are also required. These features add substantial technical complexity and cost, in particular at large sea depths. However, filling the interrupting chamber of the switchgear with high-pressure gas will reduce the differential pressure over the metal enclosure. The interruption chamber can be filled gradually as the switchgear is lowered and finally reaching the same pressure as is present at the seabed. Reducing the differential pressure will reduce the cost of the encapsulations and feed-throughs.

If the temperature and pressure of a gas exceed a critical point, it enters into the supercritical (SC) region. The physical properties of an SC fluid are somewhere between gas and liquid. For example, an SC fluid has a high density, while the

viscosity is low like a gas. Other important properties of an SC fluid include high diffusivity, high heat conductivity, high heat capacity, and an absence of vapor bubbles. In power switching applications, the switchgear must fulfill extreme demands, such as high dielectric strength during off time, low resistance during on time, high current handling capability, high voltage rating, fast switching time, fast recovery after switching, and long lifetime. An SC fluid is believed to have favorable properties in this regard [3].

To study SC arc discharges, nitrogen (N_2) is chosen due to its environmentally benign nature, good insulation strength and low critical pressure. The critical point of N_2 is at 126 K and 33.5 bar [4]. Thus, at room temperature when N_2 is pressurized to more than 33.5 bar, it enters into the SC region. Arc discharges at extremely high gas pressures have rarely been investigated in the past. Among the works published, some focus on underwater welding applications [5], [6] whereas some focus on the fundamental understanding of electrical discharges inside SC carbon dioxide or SC N_2 [7]–[11]. These fundamental works investigate very small energy discharges in the range of millijoules with interelectrode gap distances in the millimeter range. However, for circuit breaker applications, the energy deposition in the arc are normally up to hundreds of kilojoules. Recently, efforts have been made to experimentally investigate the characteristics of high energy N_2 arc discharges at different filling pressures, up to 98 bar [12]. The free-burning arc voltage is reported to increase with filling pressure of N_2 without any abrupt change during the transition from gas to SC state [12]. The arc radius decreases as the filling pressure increases [13], [14].

To the author's knowledge, there is no experimental work published regarding current interruption in ultrahigh-pressure N_2 for circuit breaker applications. To be able to interrupt the current, the breaker must successfully handle both the thermal and dielectric phases [15]. A finite post-arc current is often observed in the contact gap just after CZ due to the remaining electrical conductivity and the voltage stress due to transient recovery voltage (TRV) [15]. If the energy deposited in the post-arc channel due to the post-arc current is high enough, a thermal re-ignition may occur. Thermal re-ignition occurs almost immediately (up to some tens of microseconds) after CZ [16]. Re-ignition is reported to be greatly dependent on the initial rate of rise of recovery voltage (IRRRV) and the steepness of the current (di/dt) before CZ [15]. Moreover, even after successfully passing the thermal phase, a dielectric restrike may occur if the TRV exceeds the dielectric strength of the switching gap. A dielectric restrike typically occurs several hundred microseconds after CZ when the TRV reaches its peak value [17].

In this paper, the current interruption performance of N_2 as a function of filling pressure is reported. To evaluate the effect of forced gas flow on the current interruption performance, three different test arrangements are adopted. First, a free-burning arc (without any forced gas flow) at different filling pressure is studied. Afterward, to explore the effect of tube-constriction on the arc, the arc burning inside a cylindrical polytetrafluoroethylene (PTFE) tube is investigated. Finally, to investigate the effect of forced flow near CZ, a self-blast arrangement is adopted with a heating volume attached to the PTFE tube. The test circuit can generate a current of 130 A at 190 Hz. To investigate the interruption performance, the IRRRV is varied from 9.8 V/µs to 84.9 V/µs. Mainly, three different filling pressures are tested: 1 bar (atmospheric pressure), 20 bar, and 40 bar, the latter being in the SC region. To study the effect of the SC state on the interruption performance, some tests are conducted at 30 bar (subcritical) and 35 bar filling pressure (supercritical) in the self-blast arrangement.

2. Experimental setup

2.1 Test circuit

The test setup is shown schematically in Figure 1. It consists of a charging and a discharging section of a 7.2 µF high voltage (HV) capacitor bank, C, shown in Figure 1(a). The capacitor C is charged to a predefined charging voltage of 15 kV by closing the switch S_C. Once the capacitor C is fully charged, S_C is opened to disconnect the test circuit from the grid. The capacitor C is discharged by closing the switch, S_D. Once S_D is closed, current starts flowing through the inductor, L, and further through an ignition copper wire inside an arcing chamber. Once the switch S_D is closed, it remains in closed position until the test is over.

A pressure tank of 15.7-liters rated for 500 bar is used as an arcing chamber, shown schematically in Figure 1(b). A 24-kV miniature HV cable is fed through the flange of the pressure tank and held in position by several insulating supports. The ignition wire is mounted on two arc-resistant copper-tungsten (Cu-W) electrodes which are kept at a fixed distance of 50 mm. Once the current starts flowing, the ignition wire melts due to adiabatic heating and initiates the arc. The current continues to flow until CZ where the current is momentarily interrupted. A controlled voltage stress across the electrodes is applied after CZ. The TRV shaping capacitor, C_{TRV} is kept fixed at 1.2 µF. By changing the resistance R_{TRV}, the IRRRV is varied [18]. In this paper, the IRRRV is defined as the rate of change of TRV from CZ up to 50 µs after CZ. As the arc resistance varies with the filling pressure and the type of the arc (free-burning or tube constricted), the amplitude of the arc current also changes. The arc-current amplitude varies from 130 A for the minimum arc voltage (free-burning, 1 bar) to 120 A for the maximum arc voltage (self-blast, 40 bar). One possible solution to overcome the challenge of slightly different arc current amplitudes would be to increase the charging voltage of the capacitor. However, changing the charging voltage would also influence the stored energy of the capacitor and the IRRRV. Hence, in this paper, the charging voltage of the capacitor is kept constant while the slight change of the arc current amplitude is considered as the

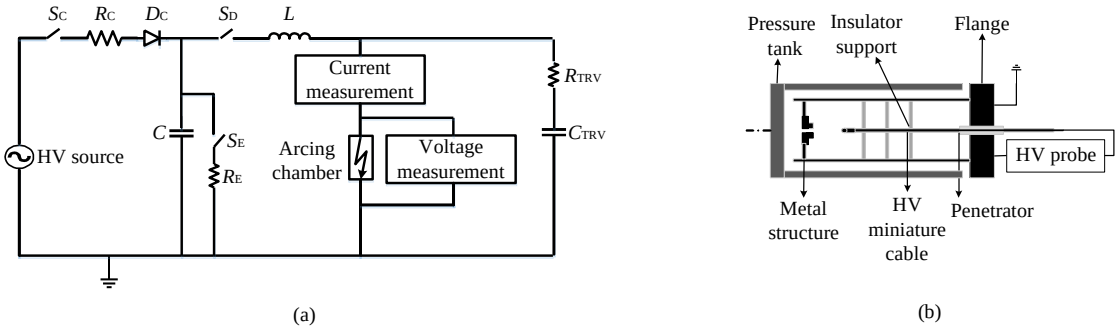

Figure 1. Test circuit. (a) Electrical setup, (b) schematics of the arcing chamber (pressure vessel).

property of different types of arc.

The arc resistance also plays a role in the shape of the TRV. The rate of rise of recovery voltage (RRRV) is defined as the rate of change of 20% of the TRV_{peak} to 80% of the TRV_{peak} [19]. The IRRRV is less influenced by the arc resistance. The circuit is simulated in MATLAB Simulink to calculate the current amplitude, IRRRV, RRRV, TRV_{peak} and time to TRV_{peak} from CZ. The TRV shape is first simulated considering the arc voltages for different test cases. A test case is defined as the tests performed at a particular nozzle arrangement, filling pressure, and IRRRV value. The simulated TRV as a function of three different R_{TRV} for two different filling pressures is plotted in Figure 2. It can be seen that the TRV amplitude is highest when R_{TRV} is lowest. The TRV peak gradually decreases as R_{TRV} increases. The filling pressure, on the other hand, reduces the TRV peak due to the high arc voltage. The voltage measurement in the existing setup saturates above 5 kV. All the simulated TRV shapes are

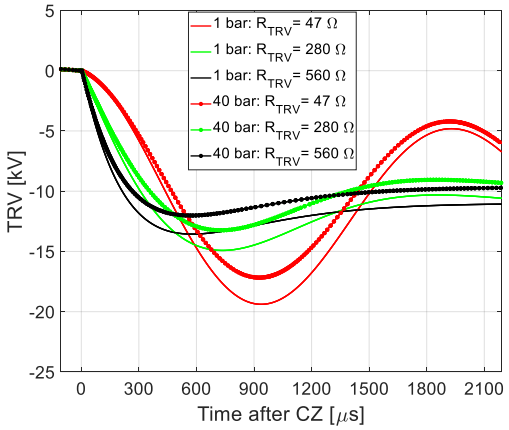

Figure 2. Influence of the arc voltage on the TRV shapes for different R_{TRV} S.

Table 1. Circuit parameter and calculated IRRRV, RRRV, TRV_{peak} an time to TRV_{peak} from CZ for different test cases.

Pressure [bar]	R_{TRV} [Ω]	IRRRV [V/µs]	RRRV [V/µs]	TRV_{peak} [kV]	Time to TRV peak from CZ [µs]
01	47	9.8	33.8	22.1	890
	140	22.4	30.9	19.3	842
	280	43.0	32.9	17.0	720
	420	63.9	39.9	15.9	628
	560	84.8	46.6	15.4	542
20	47	9.8	30.9	20	880
	140	22.4	28.1	17.4	810
	280	43.0	31.3	15.2	704
	420	63.9	38.1	15.1	620
	560	84.8	43.3	14.5	530
40	47	9.8	29.6	17.3	770
	140	22.4	24.4	14.2	790
	280	43.0	31.0	14.9	680
	420	63.9	37.0	14.3	616
	560	84.8	39.6	13.3	510

matched with the measured TRV to calculate the IRRRV, RRRV, TRV_{peak} and the time to TRV_{peak} from CZ. The circuit parameter and the respective TRV parameters for all the test cases are presented in Table 1.

2.2 Test object

Three different contact and nozzle configurations are tested, as shown in Figure 3. In the first design, the arc burns freely between two fixed electrodes (a ring and a pin electrode) kept at 50 mm apart without any forced gas flow. The electrode tips are made of arc resistant copper tungsten (Cu-W). An arc in this configuration is termed as free-burning. Some of the results from the thermal interruption performance

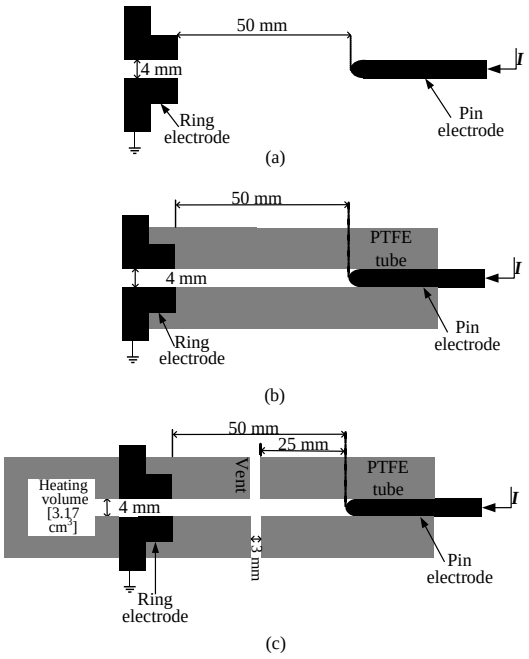

Figure 3: Electrode setup and nozzle arrangement, (a) free-burning arc, (b) tube constricted arc (without heating volume), (c) self-blast arrangement (with heating volume).

of free-burning arcs in ultrahigh-pressure N_2 have been reported in a recent conference publication [20].

In the second configuration, a PTFE tube with inner diameter of 4 mm is mounted on the ring electrode, as shown in Figure 3(b). Based on the Lowke's theory of free-burning arc, the arc radius at different filling pressures were calculated and reported in an earlier publication [14]. The free-burning arc diameter for the current of 150 A was calculated to be 8 mm, 3 mm, and 2.7 mm at 1 bar, 20 bar and 40 bar, respectively [14]. If the inner diameter of the tube is too large compared to the arc diameter, this reduces the interaction between the arc and the tube. Whereas, if the tube diameter is too small, it affects the flow of gas inside the tube. In this study, 4 mm tube diameter is considered which ensures the interaction of the arc and the tube without affecting the gas flow severely as the current interruption is considered as the objective in this study. The ignition wire is passed through the PTFE tube and attached to the electrodes. Afterward, the pin electrode is pushed inside the tube to allow the ablated gas to flow out of the tube through the ring electrode outlet only. The interelectrode gap is kept fixed at 50 mm.

In the final configuration, a heating volume of 3.17 cm^3 is attached behind the ring electrode (termed as self-blast arrangement), as shown in Figure 3(c). Two holes (diameter=3 mm) in the middle of the interelectrode gap act as vents. During the high-current phase, some of the ablated fluid leaves through the vents while the rest is stored in the heating volume. At CZ, the over-pressure built up in the heating volume generates a backflow of relatively cold fluid from the heating volume and through the vent to cool the arc. The interelectrode gap is kept fixed at 50 mm, as seen in Figure 3 (c). When a PTFE tube is used (tube and self-blast arrangement), the PTFE tube is changed after 10 tests.

2.3 Measured parameters

Two HV probes with different voltage ranges are used to measure the arc voltage and the TRV across the electrodes. The HV probes are connected to the current path before and after the pressure tank, as shown in Figure 1 (a). A shunt resistor is used to measure the arc current. Moreover, a post-arc current sensor is used to measure the small currents near CZ. The post-arc current sensor is essentially a clamped resistive shunt with antiparallel diodes [21]. The diodes bypass the resistor shunt when the current is high. When the current is low, and thus, the voltage is lower than the diodes' forward voltage, all current flows through the resistor shunt. Both current sensors are connected on the high voltage side of the arcing chamber on a floating potential, see Figure 1 (a). All the data is sent to the control room via optical fiber links and recorded in a digital oscilloscope for further analysis. The sampling rate is 10 MHz.

Two different kinds of pressure measurements are carried out. One is the static pressure or the filling pressure of the pressure vessel and the other is the dynamic pressure rise in the heating volume of the self-blast arrangement. The filling pressure is measured with a static pressure sensor. The static pressure of the pressure vessel increases when N_2 from the gas bottle enters in the pressure tank through the valve. Once the desired filling pressure is reached, the valve is closed. For dynamic pressure inside the tank, a piezoelectric sensor is placed inside the tank and the electrical signals from sensor are taken out of the tank through signal penetrator. For dynamic pressure measurements, only few tests are carried which is reported elsewhere [22].

In the free-burning arc and tube-constricted arc configurations, ten tests are conducted for all three pressure levels at IRRRV of 9.8 V/µs. For the rest of the IRRRV values, at least five tests are performed for each filling pressure. In total, 90 tests are conducted for both the free-burning arc and tube constricted arc arrangement. For the self-blast arrangement, ten tests are conducted for IRRRV of 43.0 V/µs at 1 bar, 20 bar, 30 bar, 35 bar, and 40 bar. For the rest of the R_{TRV} settings, five tests are conducted at 1 bar, 20 bar, and 40 bar filling pressures. In total, 110 tests are carried out using the self-blast arrangement.

2.4 Procedure

For all R_{TRV} settings, experiments at three different filling

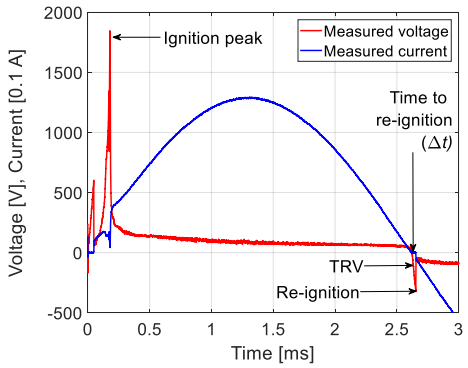

Figure 4: Measured arc voltage and arc current for atmospheric pressure nitrogen arc with an arc peak current of 130 A and an IRRRV of 9.8 V/µs.

pressures are conducted: 1, 20 and 40 bar. Additionally, for the self-blast arrangement and the R_{TRV} giving an IRRRV of 43 V/µs, experiments are also conducted at 30 bar (subcritical) and 35 bar (supercritical) N_2. Before each test, the ignition wire is mounted by hand and the pressure vessel is closed. Afterward, the pressure vessel is flushed and then filled with industrial-grade N_2 to ensure more than 99% pure N_2 inside the pressure tank. After the test, the procedure is repeated. The gas handling and the circuit are remotely controlled from a separate room located at a safe distance.

3. Experimental results

A typical measurement of the arc voltage and the arc current during a test is shown in Figure 4. The voltage peak at approximately 0.2 ms marks the melting of the copper wire and initiation of the arc. Due to the high voltage rise during the melting of the copper wire, some of the energy in capacitor C goes to charge the TRV shaping capacitor, C_{TRV}. Such a case of charging the TRV shaping capacitor can be seen in Figure 4 by the collapse of the arc current during the melting of the ignition wire at approximately 0.2 ms. The current continues to flow in the ignited arc until CZ (at approximately 2.6 ms), where the current is momentarily interrupted. The temperature of the arc can not change instantaneously. As a result, some charge carriers are still present in the post-arc channel. Just after CZ, these remaining charge carriers are accelerated by the transient recovery voltage stress. Such a movement of charge carriers after CZ is often observed as a post-arc current. If the post-arc current is high enough, sufficient energy may deposit in the post-arc current column to re-establish the arc, seen as re-ignition in Figure 4. The re-ignition is marked by the collapse of the TRV and by the sudden increase of the arc current. The re-ignition shown in Figure 4 is due to the thermal failure. Thermal re-ignitions are initiated by the presence of high post-arc current whereas the dielectric restrikes are caused mainly due to the low dielectric strength compared to TRV. The dielectric restrike occurs typically after several hundred of microseconds and when the TRV is very high. The dielectric restrikes are also considered when the interruption performance is analyzed. In this paper, the time between CZ and the re-ignition caused by thermal or dielectric failure is defined as the time to re-ignition (Δt).

3.1 Interruption Performance

Table 2 lists the number of successful current interruptions compared to the number of tests conducted. The successful interruption means when the current is interrupted at the first natural CZ, i.e. after first half cycle. The arcing time in the first half cycle is fixed and is equal to approximately 2.4 ms. First, for the free-burning arc configuration, among the 90 tests conducted at different IRRRVs, no successful current interruptions were observed.

Table 2. Number of successful current interruptions compared to the number of tests conducted at different IRRRVs for different filling pressures and test arrangements.

Test arrangement	Filling Pressure [bar]	Number of successful interruptions / the number of tests conducted				
		IRRRV 9.8 V/µs	IRRRV 22.4 V/µs	IRRRV 43 V/µs	IRRRV 63.9 V/µs	IRRRV 84.8 V/µs
Free burning	1	0/10	0/5	0/5	0/5	0/5
	20	0/10	0/5	0/5	0/5	0/5
	40	0/10	0/5	0/5	0/5	0/5
Tube constricted	1	5/10	0/5	0/5	0/5	0/5
	20	0/10	0/5	0/5	0/5	0/5
	40	10/10	0/5	0/5	0/5	0/5
Self-blast (with a heating volume)	1	3/5	2/5	6/10	3/5	2/5
	20	5/5	1/5	1/10	1/5	1/5
	40	5/5	5/5	6/10	2/5	2/5
	30	-	-	5/10	-	-
	35	-	-	5/10	-	-

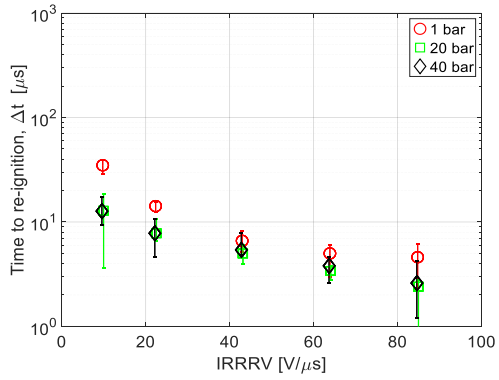

(a)

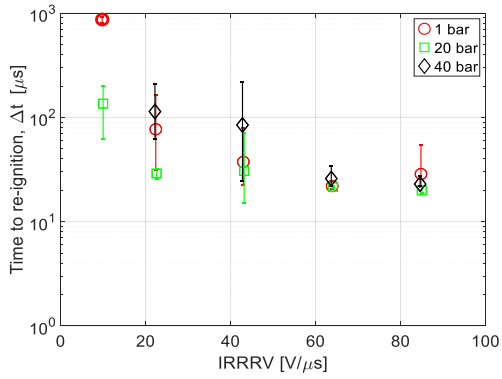

(b)

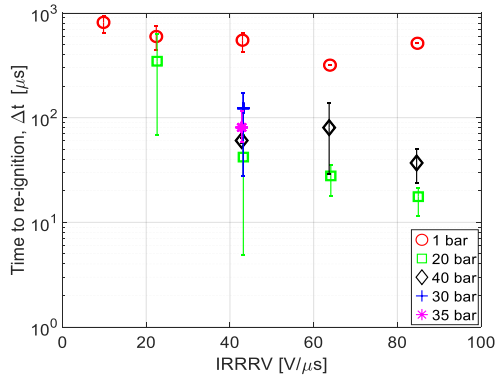

(c)

Figure 5: Re-ignition time as a function of IRRRV for different filling pressures and at different electrode and nozzle configurations. (a) Free-burning arc. (b) Tube constricted arc. (c) Self-blast arrangement.

For tube-constricted arcs, at all pressure levels, when the IRRRV was higher than 9.8 V/µs, no successful current interruption was recorded. However, at 9.8 V/µs, the arc was interrupted 5 times at 1 bar, 0 times at 20 bar and 10 times at 40 bar out of the 10 tests conducted at each filling pressure.

The number of successful interruptions compared to the number of tests conducted is highest for the self-blast arrangement. In this arrangement, at 1 bar filling pressure, the percentage of successful interruptions is found to be 40-60% depending on the IRRRV. At 20 bar filling pressure, the percentage of successful interruptions is found to be 100% when the IRRRV is 9.8 V/µs, decreasing to 20% or lower when the IRRRV is higher. At 40 bar filling pressure, the ratio of successful interruptions is 100% when the IRRRV is 22.3 V/µs or less. The ratio of successful interruptions went to 40% for IRRRVs of 63 V/µs and 84.8 V/µs. No change in current interruption performance is observed when transitioning from gas to the SC state. For both the 30 bar (subcritical) and 35 bar (supercritical) filling pressure, the percentage of successful interruption was measured to be 50%. It is observed that the interruption performance at 40 bar filling pressure is better than at atmospheric pressure when the IRRRV is 22.3 V/µs or less. Moreover, at 20 bar filling pressure, the interruption performance is better than at atmospheric pressure only when the IRRRV is 9.8 V/µs.

3.2 Time to Re-ignition

The time to re-ignition (Δt) as a function of IRRRV for different filling pressures is plotted in Figure 5. The free-burning arc configuration is presented in Figure 5 (a). Each data point represents the average of ten (IRRRV = 9.8 V/µs) or five tests (IRRRV ≠ 9.8 V/µs). The error bar corresponds to the highest and lowest measured values of Δt. For an IRRRV of 9.8 V/µs, the average time to re-ignition at 1 bar is approximately 35 µs. The re-ignition time goes down to approximately 13 µs when the filling pressure is 20 bar or 40 bar. A shorter time to re-ignition at high filling pressures (20 bar or 40 bar) compared to 1 bar is observed for all the measured IRRRV values. The difference in time to re-ignition for arcs burning in 20 bar and 40 bar N_2 is less prominent.

The times to re-ignition for the tube-constricted arc at different filling pressures are shown in Figure 5 (b). Similar to the free-burning arc arrangement, in the tube-constricted arc configuration, the time to re-ignition is observed to decrease as the IRRRV increases. However, compared to free-burning arcs, the time to re-ignition is significantly longer for all filling pressures when the arc burns inside a PTFE tube. The average time to re-ignition at atmospheric pressure with an IRRRV of 9.8 V/ µs increases from 35 µs to 955 µs. Moreover, at 1 bar and with IRRRV of 9.8 V/µs, 5 out of 10 tests were successful interruptions. The average of the 5 failed cases at 1 bar pressure with an IRRRV =9.8 V/µs is shown in Figure 5 (b). For all successful interruptions in a test case, no data point is

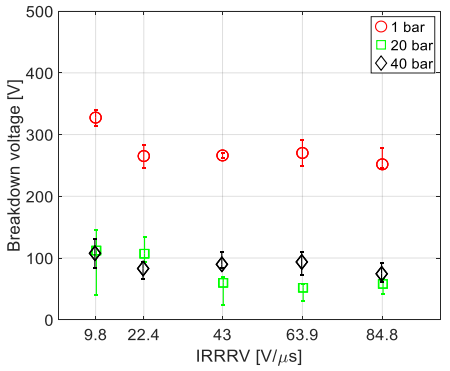

(a)

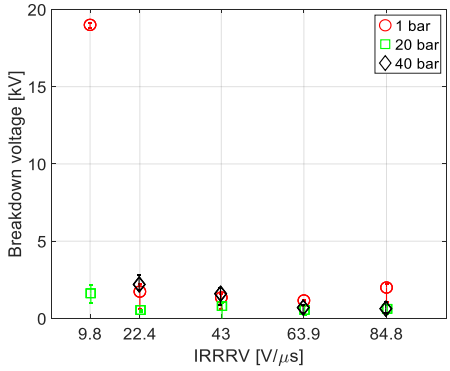

(b)

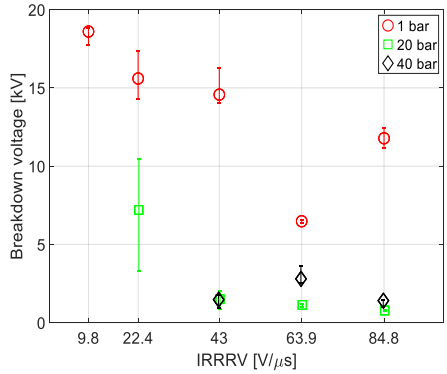

(c)

Figure 6: Breakdown voltage as a function of IRRRV for different filling pressures and at different electrode and nozzle configurations. (a) Free-burning arc. (b) Tube-constricted arc. (c) Self-blast arrangement. The scale of the Y axis is not same for three different configurations.

shown, as the case of 40 bar filling pressure at an IRRRV of 9.8 V/ µs. It is observed that in tube-constricted configuration, at 40 bar filling pressure, the time to re-ignition is slightly longer compared to the tests at 1 bar.

For the self-blast arrangement, the average time to re-ignition as a function of the IRRRV is plotted in Figure 5 (c). At 40 bar filling pressure, 5 successful interruptions are recorded out of 5 tests performed for both the IRRRV of 9.8 and 22.4 V/µs, whereas at 20 bar filling pressure 5 successful interruptions are recorded out of 5 tests performed for an IRRRV of 9.8 V/µs. Hence, these data points are not shown in Figure 5 (c). At 1 bar filling pressure, the average time to re-ignition among the failed interruptions are observed to be more than 300 µs. In general, the time to re-ignition is found to be the longest for the self-blast arrangement among all three electrode and nozzle arrangements. The time to re-ignition in the self-blast arrangement is also found to decrease with the increase of the IRRRV, as expected. In the self-blast arrangement, apart from when IRRRV is 9.8 V/ µs, the re-ignition happens faster for 20 bar filling pressure compared to 1 bar and 40 bar. No significant change in time to re-ignition is observed between 30 bar (subcritical) and 35 bar (supercritical) filling pressure (IRRRV=43 V/ µs).

3.3 Breakdown Voltage

The breakdown voltage as a function of filling pressure for different IRRRVs at different electrode and nozzle configurations is shown in Figure 6. In free-burning arrangement, the breakdown voltage is less dependent on the IRRRVs for all filling pressures. The breakdown voltages at a higher filling pressure (e.g., 20 bar, 40 bar) is observed to be lower than at 1 bar. In tube-constricted arrangement, the average breakdown voltage at 1 bar for the IRRRV of 9.8 V/µs is observed to be approximately 19 kV, which is a dielectric failure. For the rest of the cases, the breakdown voltage is less than 2.5 kV and are of thermal failures. In the self-blast arrangement, the breakdown voltages at 1 bar are found highest for all three filling pressures. At 20 bar filling pressure, when the IRRRV is 22.4 V/µs, the average breakdown voltage is approximately 7.2 kV. Whereas, for the IRRRV of 43 V/µs and higher, the breakdown voltage is observed to be less than 4 kV for 20 bar and 40 bar filling pressures.

3.4 Post-arc Current

A comparison of the average post-arc current in the free-burning, tube-constricted and the self-blast type arrangements as a function of filling pressure for different IRRRV is plotted in Figure 7. Each data point represents the average of the experiments conducted in that test case. The post-arc current measurement saturates at 1000 mA. For all cases, a post-arc current higher than 1000 mA leads to failed interruption. In the case, when there are some successful and some failed

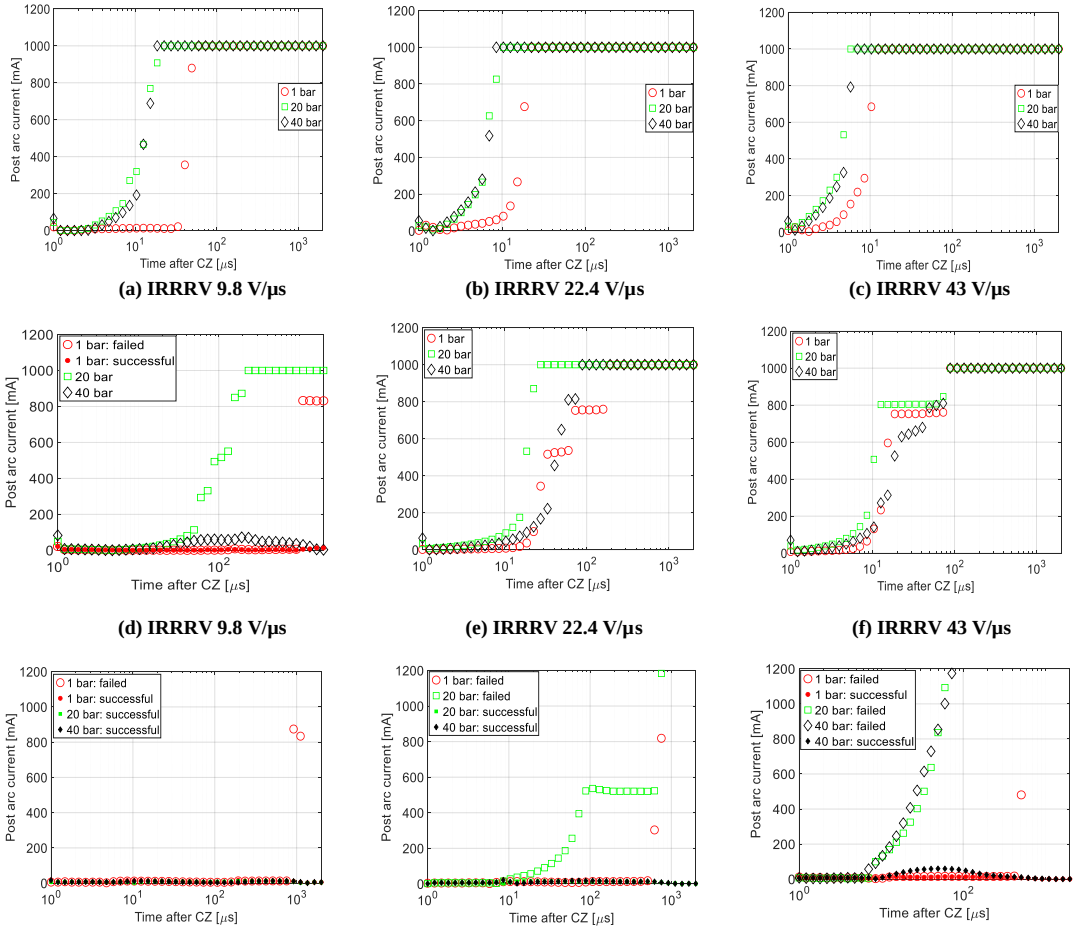

(a) IRRRV 9.8 V/µs **(b) IRRRV 22.4 V/µs** **(c) IRRRV 43 V/µs**

(d) IRRRV 9.8 V/µs **(e) IRRRV 22.4 V/µs** **(f) IRRRV 43 V/µs**

(g) IRRRV 9.8 V/µs **(h) IRRRV 22.4 V/µs** **(i) IRRRV 43 V/µs**

Figure 7: Average post-arc current for different configuration (a-c) free-burning, (d-f) tube constricted, (g-i) self-blast arrangement. The filled markers are for successful

interruptions, a filled marker represents the average of the successful current interruptions. Whereas, an empty marker represents the average of the failed interruptions for any particular test case, see Figure 7 (d).

First, the post-arc current of the free-burning arc as a function of different IRRRV is plotted in Figure 7 (a-c). It can be observed that the post-arc current increases with the increase of the IRRRV, see 10 µs after CZ in Figure 7 (a-c), which is expected. When compared with different filling pressures, for any particular IRRRV, the average post-arc current at 20 bar and 40 bar is higher than at atmospheric pressure, see up to time of re-ignition in Figure 7 (a-c). No significant difference in post-arc current is observed between 20 bar and 40 bar filling pressure for different IRRRVs. From Figure 7 (a-c) it can be seen that the re-ignition happens faster at higher filling pressures in comparison to the atmospheric pressure.

The post-arc current for tube-constricted arcs at different filling pressures and IRRRVs is shown in Figure 7 (d-f). At the lowest IRRRV of 9.8 V/µs, the post-arc current at 1 bar is observed to be the lowest among all the filling pressures, see Figure 7 (d). The failed interruption at 1 bar is probably a dielectric restrike (approximately 1 ms after CZ). Hence, no significant change in post-arc current is observed between successful and failed tests at 1 bar, see Figure 7 (d). The high post-arc current at 40 bar flows for a relatively long time

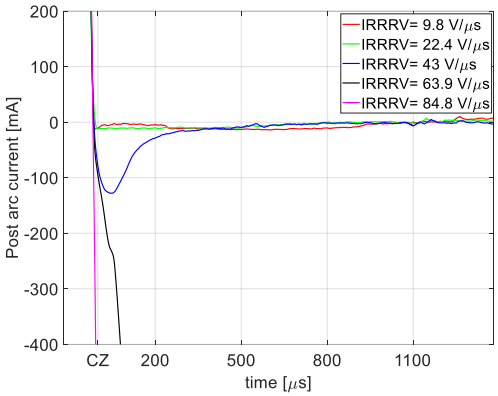

Figure 8: Post-arc current at 40 bar filling pressure in the self blast arrangement for different IRRRV.

(approximately 1500 µs) and gradually diminishes. No re-ignition is observed for 40 bar filling pressure when the arc burns inside a PTFE tube for an IRRRV of 9.8 V/µs. However, at 20 bar filling pressure, all the experiments conducted with an IRRRV of 9.8 V/µs resulted in a re-ignition, see Figure 7 (d). The post-arc current measured for 20 bar filling pressure is found to be the highest for different IRRRV settings when the arc burns inside the PTFE tube. In general, the post-arc current increases as the IRRRV increases, see Figure 7 (d-f), which is expected.

The average post-arc current measured for the self-blast arrangement at different filling pressures and IRRRVs is shown in Figure 7 (g-i). For the lowest IRRRV setting of 9.8 V/µs, the self-blast arrangement shows significantly lower post-arc currents compared to the free-burning and tube-constricted arrangements, see Figure 7 (g). All the experiments conducted with the self-blast arrangement, at 20 bar and 40 bar filling pressure were successful current interruptions at the lowest IRRRV. When the IRRRV was increased to 22.3 V/µs, the post-arc currents at 1 bar and 40 bar were still found to be low. In contrast, a significantly higher post-arc current is recorded for 20 bar. At an IRRRV of 43 V/µs, the post-arc current again increases for higher filling pressures (20 bar and 40 bar) compared to at atmospheric pressure arc.

The post-arc current for the self-blast arrangement at different IRRRVs for 40 bar is shown in Figure 8. At IRRRVs of 9.8 V/µs and 22.3 V/µs, the measured post-arc current is low. At an IRRRV of 43 V/µs, the measured post-arc current is more than 100 mA, but still, the current is successfully interrupted. However, at IRRRVs of 63.9 V/µs and 84.8 V/µs, the post-arc current was more than 200 mA and resulted in a thermal re-ignition.

4. Discussions

For the free-burning arc, the increase of the pressure inside the arc is greatest at the cathode-spot where the current density is the highest [23]. This increase of pressure near cathode-spot induces an axial flow. For a lower current (<30 A), however, the axial flow reduces, and the natural convection plays the dominant role. For tube-constricted arc, the inner surface of the PTFE tube ablates when the arc current is high. The intensity of the ablation reduces when the current approaches the CZ. Nonetheless, even after the arc is extinguished, the nozzle continues to ablate for a few milliseconds after CZ [24]. When a heating volume is used, in self-blast arrangement, during the high current phase, the pressure rises in the heating volume. The overpressure in the heating volume of the self-blast arrangements is measured for few tests, which are reported elsewhere [22]. The pressure rise in the heating volume is observed to increase with the filling pressure.

The arc current is momentarily interrupted at each CZ crossing. Just after CZ, due to the energy-storing elements (capacitors and inductors) in the circuit, voltage stress is developed across the electrodes. As the stored thermal energy of the arc channel is not dissipated instantaneously, some charge carriers may still remain in the electrode gap. These charge carriers get accelerated by the voltage difference between the electrodes and are observed as a measurable post-arc current. If the energy dissipation in the arc channel due to the post-arc current is high compared to the cooling of the medium, a thermal re-ignition may occur [15]. Under the simplifying assumption of a homogeneous post-arc channel, the post-arc current can be written as

$$I = nqvA, \qquad (1)$$

where n is the number of charge carriers per volume, q is the charge, v is the velocity of the charge carriers and A is the cross-sectional area of the post-arc channel. The velocity of the charge carriers is linearly proportional to the applied voltage stress between the electrodes after CZ. As the IRRRV is increased, the rate of change of TRV increases. In other words, for a given time after CZ, the voltage stress across the electrodes is high for high IRRRV. The high electric field will accelerate the remaining charge carriers faster which would increase the post-arc current. A high post-arc current increases the energy deposition in the post-arc channel and increases the possibility of early re-ignition. This causes the time to BD to go down as the IRRRV is increased. As a result, a faster time to re-ignition is observed for all filling pressure tested when the IRRRV is increased.

When the filling pressure increases, the arc voltage rises too. Consequently, the energy dissipated in the arc channel increases with increasing filling pressure. Moreover, due to the high filling pressure the arc radius decreases [13], [5]. In the absence of forced cooling near CZ, the hot core of the arc fails to dissipate the heat quickly. The relatively high temperature of the arc core at a high filling pressure after CZ

may result in a high number of charge carriers at a high filling pressure, especially when the cooling is not sufficient. The velocity of charge carriers also depends on the mobility of the charge carriers. Electrons being lighter, move faster than ions. A higher pressure, however, tends to reduce the mobility of the electrons due to its collision with neutral and charged particles [25]. The increase in temperature of the post-arc channel at a higher filling pressure may compensate for the reduced mobility of electrons caused by the high density [26]. As a result, the post-arc current may increase at a higher filling pressure and contribute to a faster re-ignition.

The thermal re-ignition characteristics of free-burning arc at 20 bar and 40 bar gas filling pressures are found to be quite similar. In previous work, for an arc peak current of 150 A at 350 Hz, the arc radius of the free-burning arc was calculated to be approximately 4 mm at atmospheric pressure [14]. In comparison, the calculated free-burning arc radius was 1.5 mm and 1.43 mm for an arc burning at 20 bar and 40 bar, respectively [14]. It was reported that the arc is constricted by filling pressure significantly at 20 bar filling pressure compared to at atmospheric pressure, whereas the constriction is not much greater when comparing an arc at 40 bar to one at 20 bar. This may explain the similarity in re-ignition properties for arcs burning at 20 bar and 40 bar filling pressure in the free-burning configuration.

When the arc burns inside the PTFE tube, the flow stagnation point lies near to the pin electrode as the pin electrode blocks any gas flow out. The axial pressure distribution in this configuration is parabolic where the maximum pressure lies at the stagnation point [27]–[29]. As a result, the plasma velocity reaches its maximum near the exit point through the ring electrode. It has been observed that the time to re-ignition increases when the arc burns inside a tube in comparison to the free-burning arc, which is expected. The PTFE ablates when the arc burns inside the PTFE tube. It has been reported that even after the arc is extinguished, the nozzle continues to ablate for a few milliseconds after CZ [24]. The PTFE vapor cools the arc which may contribute to the higher time to re-ignition when the arc burns inside the tube in comparison to the free-burning arc. For the lowest IRRRV, some successful current interruption is observed when the arc burns inside the tube.

The self-blast arrangement shows the best interruption performance among the three different arrangments investigated. The interruption performance improves at high filling pressure when the IRRRV is lowest in the self-blast arrangement. As the filling pressure increases, the density of the gas increases too. Under forced gas flow, due to the high density, the cooling is enhanced at a high-filling pressure. As a result, the post-arc current recorded is low and the interruption performance improves in the self-blast arrangement at lower IRRRV settings. However, when the IRRRV is high, the post-arc current increases rapidly which may initiate a thermal re-ignition. In self-blast arrangement, at 1 bar filling pressure, the percentage of successful interruption is less dependent on the IRRRV. The IRRRV plays an important role in the post-arc current and the thermal failures. Dielectric failures, however, are not dependent on IRRRV. The failures at 1 bar are of dielectric nature, as can be seen from the high breakdown voltage, see Figure 6 (c).

For the tube constricted and the self-blast arrangements, it is observed that the interruption performance is better at 40 bar than at 20 bar filling pressure. However, in the free-burning arc, the re-ignition time for 20 bar and 40 bar filing pressure was observed to be similar. The arc temperature near CZ varies at different filling pressures at different electrodes and nozzle arrangements. High filling pressure changes the material properties of the plasma. However, the material properties of the N_2 plasma in the range of up to several tens of bars is not available in the literature. As a result, the change of different parameters of the high pressure air plasma is summarized and shown in Table 3 [30], [31]. As the pressure is increased, the thermal conductivity peak of air shifts with the filling pressure. If the temperature of the arc just after CZ is such that the thermal conductivity is low, then the cooling will be affected. Moreover, increasing the pressure also increases the viscosity, which may shift the flow characteristics from being turbulent to more laminar, thus affecting the cooling. The reduced thermal conductivity together with increasing viscosity may inversely affect the interruption performance at 20 bar filling pressure.

Table 3. Effect of filling pressure on different parameters influencing the current interruption.

Parameters	**Effect of pressure**
Arc radius	Decreases non linearly.
Thermal conductivity	Increases with pressure after 18000 K. Shift of the thermal conductivity peak towards high temperature before 18000 K.
Viscosity	Increases with pressure. The viscosity peak as a function of temperature shifts towards high temperature.
Electrical conductivity	Increases with pressure after 15000 K, decreases with pressure for temperature less than 15000 K.
Energy density of the arc	Increases with pressure.

Almost identical current interruption characteristics are observed when the filling pressure is 30 bar (subcritical) and 35 bar (supercritical). Previously, it has been reported that the arc voltage does not change abruptly during the transition from gas to the SC state in N_2 [12]. The physical properties such as electrical conductivity, viscosity, thermal conductivity do not change abruptly for N_2 during the transition from gas to the SC state [31]. The effect of SC state on the interruption performance is not observed.

Among the failed current interruptions at high filling pressures (e.g., 20 bar, 40 bar), thermal re-ignition is observed to be the dominant failure mechanism. In the absence of forced cooling, the temperature decay rate in the post-arc channel may get affected by the high filling pressure. It has been observed that the post-arc dielectric strength increases rapidly with the increase of high filling pressure [32]. In the free-burning arc arrangement, just after CZ up to a critical time instants, the dielectric strength is observed to be low even at a high filling pressure [32]. As a result, if the cooling of the arc channel is not sufficient, a high filling pressure may result in higher post-arc current and in a subsequent thermal re-ignition. However, if the thermal phase is successfully passed, the temperature of the post-arc channel decreases below a critical value. The increased dielectric strength with the increase of filling pressure at a relatively low temperature helps to successfully pass the dielectric phase. As a result, all the failures at high filling pressure are observed as a thermal re-ignition type in this study. At 1 bar, however, both the dielectric restrike and thermal re-ignition type of failures are observed. Hence, the thermal phase seems to be the critical phase for the current interruption in ultra-high pressure N_2.

5. Conclusions

The current interruption performance of ultrahigh-pressure N_2, with or without forced gas flow, is reported in this paper. As the filling pressure increases, the arc voltage increases too. A comparison between different kinds of arcs (free-burning, tube constricted and self-blast type) at different filling pressure is inherently difficult as the arc voltage influences the amplitude of the arc current and the TRV. Nevertheless, based on the experimental investigation, some key conclusions are drawn from the study:

- In the absence of forced gas flow, the interruption performance deteriorates with increasing filling pressure.
- A high post-arc current is observed when the arc burns at higher filling pressures (i.e., 20 bar, 40 bar) compared to at atmospheric pressure. High post-arc current leads to thermal re-ignition when cooling is not sufficient.
- Forced gas flow improves interruption performance at all filling pressures. The improved cooling at high filling pressures reduces the post-arc current when the IRRRV is low. As a result, the interruption performance improves with the forced flow at high filling pressures for low IRRRV.
- For tube constricted and self-blast arrangements, current interruption performance at 20 bar is observed to be worse than that at 1 bar, whereas 40 bar shows the best performance. The temperature-dependent thermal conductivity at different filling pressures may affect the current interruption performance. A shift in the arc temperature near CZ due to the filling pressure may result in poor cooling if the thermal conductivity is low at that arc temperature.
- Among the failed interruptions, thermal re-ignition is observed to be the dominant failure mechanism at high filling pressures.
- No obvious improvement in interruption performance is observed when N_2 enters the supercritical region.

Acknowledgements

This work is supported by the Norwegian Research Council.

References

[1] Hazel T, Baerd H H, Legeay J J and Bremnes J J 2013 *IEEE Ind. Appl. Mag.* **19** no. 5 pp. 58–67
[2] Nordrum A, "Abb Siemens Test Subsea Power Grids For Underwater Factories - IEEE Spectrum." [Online]. Available: https://spectrum.ieee.org/energy/fossil-fuels/abb-siemens-test-subsea-power-grids-for-underwater-factories. [Accessed: 27-Sep-2019].
[3] Zhang J 2015 *PhD Thesis* Technical University of Eindhoven
[4] Zhang J, Heesch E M J, Beckers F J C M, Pemen A J M, Smeets R P P, Namihira T and Markosyan A H 2015 *IEEE Trans. Dielectr. Electr. Insul.* **22**, no. 4 pp. 1823–32
[5] Schmidt H P and Speckhofer G 1996 *IEEE Trans. Plasma Sci.* **24** no. 4 pp. 1229–38
[6] Speckhofer G and Schmidt H P 1996 *IEEE Trans. Plasma Sci.* **24**, no. 4, pp. 1239–48
[7] H. Tanoue *et al.* 2013 *19th IEEE Pulsed Power Conference*
[8] Tanoue H, Furusato T, Takahashi K, Hosseini S H R, Katsuki S and Akiyama H 2014 *IEEE Trans. Plasma Sci.* **42**, no. 10 pp. 3258–63
[9] Zhang J, Heesch B, Beckers F, Huiskamp T and Pemen G 2014 *IEEE Trans. Plasma Sci.*, **42**, no. 2, pp. 376–383
[10] Ito T and Terashima K 2002 *Appl. Phys. Lett.* **80** no. 16 pp. 2854–56
[11] Lock E H, Saveliev A V and Kennedy L A 2009 *IEEE Trans. Plasma Sci.* **37**, no. 6, pp. 1078–83
[12] Abid F, Niayesh K, Jonsson E, Stoa-Aanensen N S and Runde M 2018 *IEEE Trans. Plasma Sci.* **46** no. pp. 187–193
[13] Okuma T, Imatsuji T, Hashizume T, and Tanaka M 2018 *J of Fluid Science and Technology* **13**, no. 4
[14] Abid F, Niayesh K and Stoa-Aanensen N S 2019 *IEEE Trans. Plasma Sci.*, **47**, no. 1, pp. 754–761
[15] Niayesh K and Runde M 2017 *Power Switching Components* Springer
[16] Edels H and Ettinger Y 1962 *Proceedings of the IEE - Part A: Power Engineering* **109**, no. 43
[17] Garzon R D 2002 *High Voltage Circuit Breakers Design and Applications* Taylor & Francis
[18] Karimi A and Niayesh K 2009 *Electr. Eng.* **90**, no. 8, pp. 523–528
[19] Flurscheim C H 1982, *Power Circuit Breaker Theory and Design* IET
[20] Abid F, Niayesh K, Thimmappa S B, Espedal C and Stoa-Aanensen N S 2019 *Lecture Notes in Electrical Engineering* **599** pp 663-671 Springer.
[21] Barrault M, Bernard G, Maftoul J and Rowe S 1993 *IEEE Trans. Power Deliv.* **8**, no. 4, pp. 1782–1788
[22] Abid F, Niayesh K, and Støa-Aanensen N 2019, *Plasma Phys. Technol. J.*, **6**, no. 1, pp. 23–26.
[23] Lowke J J 1979, *J. Phys. D. Appl. Phys.*, vol. **12**, no. 11, pp. 1873–1886

[24] Babou Y, Corfdir P, and Suetterlin R P 2019,*Plasma Phys. Technol.*, vol. **6**, no. 2, pp. 148–151
[25] Chen F F 2018 *Introduction to Plasma Physics and Controlled Fusion* Springer
[26] Bisetti F and Morsli M E 2012 *Combust. Flame*, **159**, no. 12, pp. 3518–21
[27] Ruchti C B and Niemeyer L 1986 *IEEE Trans. Plasma Sci.*, **14**, no. 4, pp. 423–434
[28] L. Muller 1993 *J. Phys. D. Appl. Phys.* **26**, no. 8, pp. 1253–59
[29] Kovitya P and Lowke J J 1984 *J. Phys. D. Appl. Phys.* **17**, no. 6, pp. 1197–12
[30] C. Wang *et al*. 2016 *Plasma Sci. Technol.* **18**, no. 7.
[31] D'angola A, Colonna G, Gorse C, and Capitelli M, 2008 *Eur. Phys. J. D*, **46**, pp. 129–150
[32] Abid F, Niayesh K, and Stoa-Aanensen N 2019 *5th international conference on electric power equipment - switching technology, ICEPE-ST*

Paper V

Effect of Filling Pressure on Post-Arc Gap Recovery of N_2

Fahim Abid, Kaveh Niayesh and **Egil Viken**
Norwegian University of Science and Technology (NTNU)
Department of Electric Power Engineering
Trondheim, Norway

Nina Sasaki Støa-Aanensen, Erik Jonsson and **Hans Kristian Meyer**
SINTEF Energy Research
Trondheim, Norway

ABSTRACT

Experimental investigation of the effect of filling pressure on the post-arc dielectric recovery characteristics of nitrogen is reported in this paper. A half-cycle arc current duration of 540 µs followed by a 10 kV pulse with a rise rate of 150 V/µs is applied across the contact gap. The pulse is applied from 10 µs to 10 ms after the current zero. First, a free-burning arc is studied without any forced gas flow. The effect of the gap distance on the recovery process is studied by using two different inter-electrode gaps: 20 mm and 50 mm. The effect of arc current on the recovery process is investigated by using current amplitudes of 275 A and 425 A. Moreover, the effect of forced nitrogen flow near current zero is explored using two different arrangements: self-blast and puffer type. Four different nitrogen filling pressures are studied: 1, 20, 40, and 80 bar, the latter two being in the supercritical region. The experimental results show that, in the free-burning arc configuration, the breakdown voltage of the contact gap increases faster with the increase of the filling pressure. A gap of 50 mm recovers quicker than a 20 mm gap, whereas no strong current dependency is observed on the recovery characteristics in the investigated range. In the free-burning arc configuration, just after the current zero up to approximately 300 µs, the breakdown voltage at high filling pressure is found to be lower than at 1 bar. Forced gas flow, however, significantly enhances the dielectric recovery at a high filling pressure, also in the thermal phase.

Index Terms — **supercritical fluid, arc discharge, dielectric recovery, ultrahigh-pressure arc, switchgear**

1 INTRODUCTION

THE need to transfer power to and from offshore installations (wind farms and offshore mining) will lead to the development of offshore substations. To materialize such a substation, there are two possible paths to follow: one path is to place the electrical equipment on a platform or floater above sea level. Another path is to directly place the equipment on the seafloor and control it remotely. Among these two options, the latter is more economically viable [1]. The conventional solution is to place the power equipment (i.e., circuit breaker of vacuum or gas technology) inside a pressure-proof vessel [2]. Medium voltage gas circuit breakers are generally filled up to 1.3 bar filling pressure and sealed at the manufacturer site [3]. To transfer and control electrical power from the high-pressure water environment at seabed into the pressure-proof vessel, various feedthroughs and penetrators are required. All these arrangements used to cope with the high-pressure water environment, add considerable technical complexity and cost. A novel concept is developed, where the interruption chamber can be filled with high-pressure gas to reduce the differential pressure exerted on the encapsulation. Reducing the differential pressure will substantially reduce the cost and complexity of the encapsulations and feed-throughs.

If the pressure and temperature of a gas exceed a critical point, it enters the supercritical (SC) region [4]. In this SC region, liquid and gas states are united and indistinguishable. For example, an SC fluid has a high density, while the viscosity is low like a gas. The properties of an SC fluid are believed to be in favor of a successful current interruption medium [5]. In this paper nitrogen (N_2) is chosen for its low critical pressure (33.5 bar) [6]. Moreover, N_2 is abundant in air and hence, environmentally benign.

In order to successfully interrupt the current, the breakdown voltage of the contact gap must be higher than the transient recovery voltage at any time after the current zero (CZ) [7]. Many investigations are focused on the dielectric recovery of

Manuscript received on 8 February 2020, in final form 18 April 2020, accepted xx Month 20yy. Corresponding author: F.Abid.

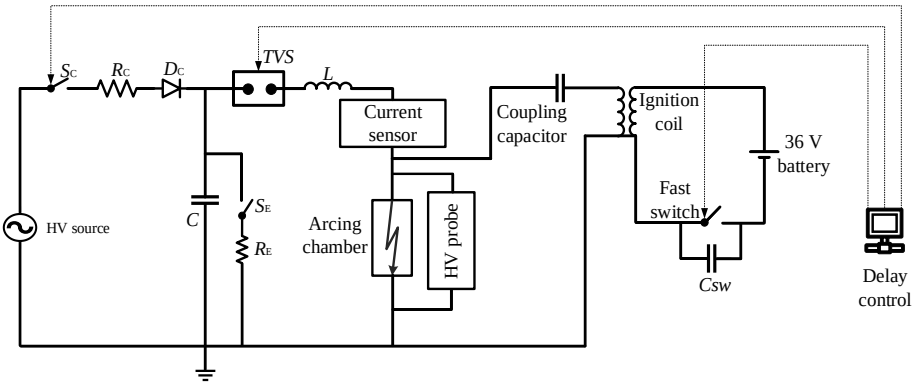

Figure 1. Schematics of the test circuit. An ignition coil is used to generate a 10-kV high voltage pulse which is applied at different instants after CZ.

the post-arc channel at 1 bar or slightly higher pressure arcs typical of land-based circuit breakers; e.g. [8–11]. In contrast, arc characteristics at an extremely high gas pressure including the SC region are not a well-explored area. Recently, a series of experiments have been conducted to study the arc properties at extremely high N_2 filling pressure in the SC region. First, a free-burning arc and the influence of tube constriction on the arc have been investigated in the SC state and beyond, up to 80 bar filling pressure during the high current phase [12,13]. Some further investigations were focused on the region near CZ, where the effect of N_2 filling pressure on the thermal interruption performance is evaluated [14–16]. The arc voltage is reported to increase with the filling pressure, whereas no abrupt change in arc voltage is observed during the transition of N_2 from gas to SC region [12]. As a result, the energy deposition in the arc channel increases at a higher filling pressure. The calculated arc diameter reduces with increasing pressure [13].

In this paper, the pressure dependence of the dielectric recovery characteristics of N_2 arcs is investigated including the SC region. To evaluate the dielectric recovery of the contact gap, a 10 kV high voltage (HV) pulse (rise time of approximately 70 µs) is applied between the electrodes at different instants after CZ. The time of the pulse is varied from 10 µs and 10 ms after CZ. The free-burning arc is studied at 1 (atmospheric pressure), 20, 40, and 80 bars, the latter two being in the SC region. Some of these results are reported in a conference paper [17]. In the free-burning arrangement, the effect of the contact gap and the current amplitude on the recovery characteristics is also studied at different filling pressures. In order to efficiently cool the arc near CZ and interrupt the current, the arc in a gas circuit breaker is generally subjected to a forced gas flow [7]. In commercial gas circuit breakers, two of the most commonly used techniques to cool the arc are self-blast and puffer type [7]. In this paper, two different mechanisms (self-blast and puffer arrangement) are adopted to evaluate the effect of forced gas flow on the post-arc dielectric recovery of N_2 at extremely high filling pressures. The breakdown voltages at different instants after CZ are used to analyze the recovery characteristics.

2 EXPERIMENTAL SETUP

The schematics of the test circuit and measurement system used in this study are shown in Figure 1. The high voltage (HV) energy storing capacitor, *C* is first charged to a preset value. It is then discharged by the triggered vacuum switch (TVS) through the inductor, *L* and further through the ignition copper wire inside the arcing chamber. The arcing chamber is a 15.7 liters, 500 bar rated pressure tank. The photo of the test setup and the corresponding value of the circuit parameters are shown in Figure 2 and Table 1 respectively. Once the TVS is closed, the current starts to flow, and the arc is initiated by the melting of the thin copper wire. The content of the copper in the atmospheric arcs at least seems to be in the range of 1-2% and therefore, the influence of metal vapor is not significant [18]. Furthermore, to reduce the effect of metal vapor between the different tests, all the tests are conducted using a 40 µm copper ignition wire. The current flow through the arc until the first CZ crossing, where the current is interrupted by the TVS. The right part of the test circuit in Figure 1 is a voltage pulse generator circuit using an ignition coil. An HV pulse of 10 kV (rise rate of 150 V/µs) is applied between the electrodes at different times after CZ. A coupling capacitor is placed between the ignition coil and the arcing chamber. The

Figure 2. Photographs of the lab setup; (a) HV source, (b) capacitor *C*, (c) inductor *L*, (d) arcing chamber, (e) N_2 cylinder.

Table 1. Test circuit parameters and their values.

Circuit Parameters	Value
HV Source	220V: 40 kV Transformer
Capacitor, *C*	4.8 µF
Inductor, *L*	6 mH
Coupling Capacitor	500 pF

coupling capacitor blocks the arc current to flow through the ignition coil while allowing the HV pulse to be applied across the electrodes. After applying the HV pulse, either the electrode gap withstands the applied voltage, or a breakdown occurs.

As the arc voltage increases with the filling pressure, for a given predefined charging voltage, the arc current amplitude varies with the filling pressure. While the arc current amplitude is 425 A at 1 bar, it is limited to 400 A at 80 bar filling pressure by the same charging voltage of the capacitor, *C*. One possible solution to overcome slightly different arc currents would be to increase the charging voltage of the capacitor. However, changing the charging voltage would also influence the stored energy of the capacitor. Hence, in this paper, the charging voltage of the capacitor is kept constant while the slight change of the arc current amplitude is considered as the property for arc burning at different filling pressures. The CZ crossing also changes by a few microseconds when the arc voltage varies. The timing of the application of HV pulse is compensated for different filling pressures to get the desired time to pulse after CZ.

Two HV probes with different voltage ranges are used to measure the HV pulse and the arc voltage. The arc current is measured by a shunt resistor. Both the HV probes and the current sensor are connected outside of the pressure tank and on the HV side of the arcing chamber. For the puffer arrangement, the movement of the piston is recorded by a linear displacement sensor while the blow pressure is recorded by a dynamic pressure sensor mounted at the throat of the puffer.

2.1 TEST OBJECTS

Three different test arrangements are used in this paper. The main bulk of the tests are conducted with a simple pin and ring electrode pair, resulting in a free-burning arc configuration, see Figure 3a. In the free-burning arrangement, the arc burns freely without any forced gas flow. At 50 mm inter-electrode gap and with a current of 425 A, the pressure dependence of the recovery characteristics is studied at four different filling pressures: 1, 20, 40, and 80 bar, as can be seen in Table 2. Then the inter-electrode gap is changed to 20 mm to study the distance dependency of the recovery process. For the 20 mm gap distance, three different filling pressures are investigated: 1, 20, and 40 bar. Finally, the current amplitude is varied to 275 A to investigate the current dependency of the dielectric recovery in the contact gap. For the current dependency, two different filling pressures are tested: 1 and 40 bar.

To study the effect of forced gas flow on the recovery process, two different arrangements are studied. A simple self-blast arrangement is adopted where the arc burns inside a PTFE tube with vents in the middle, see Figure 3b. Two opposite holes of 3 mm diameter in the middle of the inter-electrode gap act as the vents. The pin electrode is pushed inside the PTFE tube in such a way that it blocks the gas flow out through the pin

Table 2. Inter-electrode gap, corresponding arc current and the tested filling pressure for different test arrangements.

Test object	Inter-electrode gap [mm]	Arc current [A]	Filling pressure tested [bar]
Free-burning	50	425	1, 20, 40, 80
Free-burning	20	425	1, 20, 40
Free-burning	50	275	1, 40
Self-blast	50	425	1, 40
Puffer	20	425	1, 20, 40

electrode. A heating volume of 3.17 cm^3 is attached to the ring electrode. During the high current phase, a part of the ablated PTFE vapor directly leaves through the vent, while the rest is stored in the heating volume. As a result, the pressure in the heating volume increases. The high pressure in the heating volume forces a relatively cold gas flow through the vent of the tube and cools the arc near the CZ. For the self-blast arrangement, two different filling pressures are tested: 1 and 40 bar, see Table 2. The reference measurement in the self-blast arrangement is conducted without the heating volume, i.e., the arc burns inside the PTFE tube only without any backflow of gas near CZ. After every 10 experiments, the PTFE tube is changed, and a new tube is mounted.

The last test arrangement is a puffer-type configuration as shown schematically in Figure 3c. The puffer mechanism works by pre-charging a spring which is kept in position by an electromagnet. A 10 mm long PTFE nozzle with an inner diameter of 4 mm is mounted with the ring electrode. The total

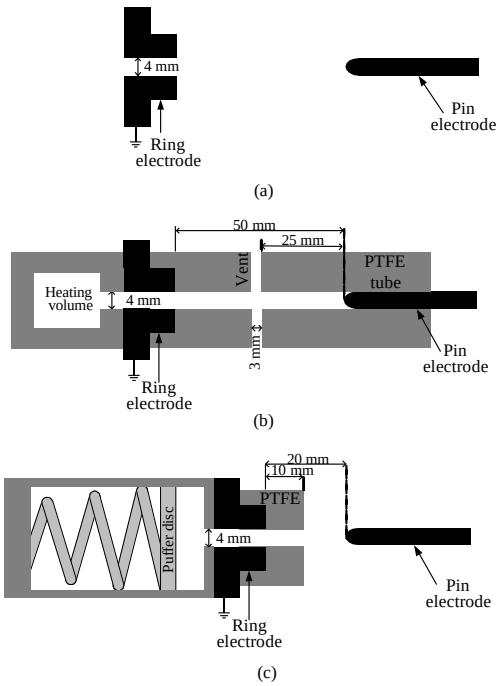

Figure 3. Test arrangement. (a) Free-burning arc, (b) self-blast arrangement, (c) puffer arrangement.

inter-electrode gap in the puffer setup is kept fixed at 20 mm. As the filling pressure increases, the density and the viscosity increase too. As a result, for the same pre-charging of the spring, the travel curve of the piston varies at different filling pressures. In this paper, the spring is released at instants that result in a similar upstream pressure difference at CZ for all filling pressures. To study the effect of forced gas flow on the same electrode and nozzle arrangement, reference measurements were also conducted. The reference measurement in the puffer arrangement is conducted without pre-charging the spring, i.e., the arc burns partly inside the PTFE nozzle and partly outside the nozzle without any forced gas flow.

2.2 PROCEDURE

All the experiments are conducted in a fixed electrode arrangement and the arc is initiated by the melting of a thin copper wire of 40 µm diameter. The ignition copper wire is mounted on the electrode by hand and then the flange of the pressure tank is closed. The pressure tank is first flushed and then filled with industrial-grade N_2 to ensure 99% N_2 inside the pressure tank. The energy storing capacitor, *C*, is charged to a predefined charging voltage of 15 kV to generate the arc current of 425 A. For the 275 A current settings, the charging voltage is reduced to 10 kV. Once *C* is charged to the predefined level, a computer program controls the timing of the switches S_C, TVS, HV pulse and release of the electromagnet (for the puffer arrangement). To investigate the breakdown or the hold voltage at different instants after CZ, the timing of the HV pulse is varied. After each test, the over-pressure in the pressure tank is released, and the ignition copper wire is mounted by hand. A total of 175 tests were conducted in this work.

3 EXPERIMENTAL RESULTS

A typical measurement of the arc current, the voltage across the contact gap at 20 bar pressure are shown in Figure 4. The arc is established by the melting of the copper wire (marked as the voltage peak at 0.5 ms before CZ). Once the arc is formed, the arc current continues to flow until CZ, where the current is interrupted by the TVS. Due to the application of the voltage pulse after CZ between the electrodes, a breakdown may occur

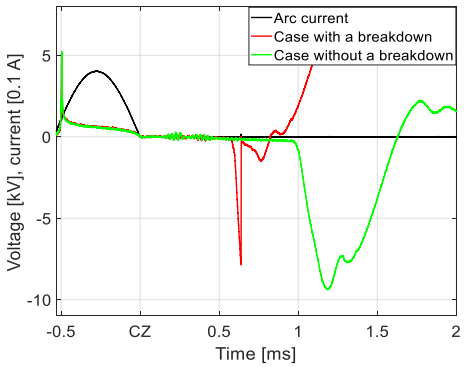

Figure 4. A measurement showing the arc current, a case with a breakdown (red line) and a case without a breakdown (green line).

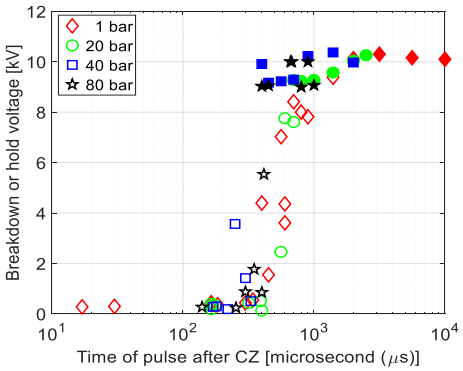

Figure 5. Breakdown or hold voltage at different instants after CZ for 50 mm gap distance at an arc current of 425 A in free-burning arrangement. The filled markers represent withstand voltages whereas the empty markers represent breakdown voltages.

in the hot, conductive channel. If a breakdown occurs, it is marked by a voltage collapse at 7.8 kV, see the red line at approximately 700 µs after CZ in Figure 4. In the case of without a breakdown, the contact gap withstands the applied HV pulse, as can be seen by the green line in Figure 4. For the case without a breakdown, the peak of the voltage pulse is recorded.

Just after CZ, voltage oscillations across the contact gap are recorded due to the stray capacitances, which is independent of the applied HV pulse. The peak of the voltage oscillations is approximately 400 V with a rise rate of approximately 125 V/µs. As the breakdown strength of the contact gap just after CZ is very low, such voltage oscillations may cause breakdowns. The breakdowns generated by these voltage oscillations are also considered to analyze the recovery characteristics.

3.1 FREE-BURNING ARC

Breakdown or hold voltages as a function of time after CZ in the free-burning arrangement for 50 mm gap distance at different pressures are shown in Figure 5. The filled and empty markers represent the hold voltage and the breakdown voltage respectively. At atmospheric pressure (1 bar) the measured breakdown voltages are close to 330 V between 10 µs and 300 µs after CZ for a 50 mm contact gap. The breakdown voltage gradually increases after 300 µs after CZ. At 1 bar pressure, the HV pulse does not generate a breakdown when the pulse is applied later than 2 ms after CZ.

The breakdown voltage between 10 to 300 µs after CZ at a high filling pressure (20, 40, and 80 bar), however, is around 100 V for 50 mm gap distance, see Figure 5. Before 300 µs, the breakdown voltage at a higher filling pressure is lower compared to the measured breakdown voltages at 1 bar filling pressure. After 300 µs, however, the breakdown voltage rises faster as the N_2 filling pressure is increased. The gap withstands the applied HV pulse after 800 µs and 400 µs for N_2 filling pressure of 20 and 40 bar, respectively.

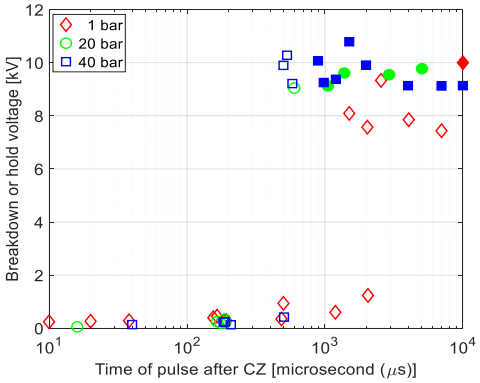

Figure 6. Breakdown or hold voltages at different instants after CZ for 20 mm long inter-electrode gap and an arc current amplitude of 425 A in free-burning arrangement. The filled markers represent withstand voltages whereas the empty markers represent breakdown voltages.

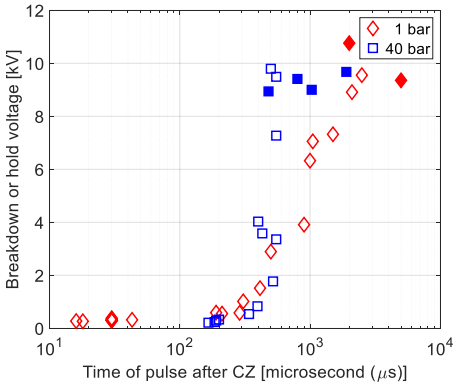

Figure 7. Breakdown or hold voltage at different instants after CZ for 50 mm inter-electrode gap distance for arc current of 275 A in free-burning arrangement. The filled markers represent withstand voltages whereas the empty markers represent breakdown voltages.

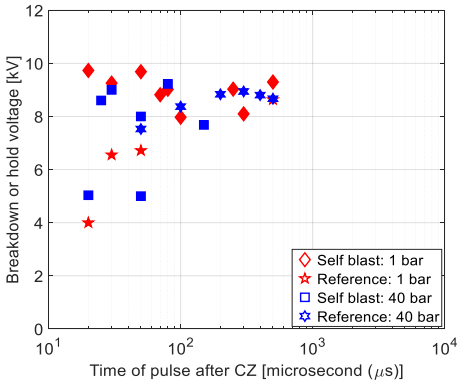

Figure 8. Breakdown or hold voltage at different instants after CZ in self-blast arrangement for 425 A arc current. The filled markers represent withstand voltages whereas the empty markers represent breakdown voltages.

3.1.1 INTER-ELECTRODE GAP

The gap dependency of the post-arc recovery process is studied in the free-burning arrangement by conducting the experiments at a 20 mm gap at 1, 20, and 40 bar N_2 filling pressures. The breakdown or hold voltages at different instants after CZ for different filling pressures are plotted in Figure 6. As was observed for the 50 mm case, the 20 mm gap recovers faster at 40 bar than at 1 bar. When compared between different gap distances, the 20 mm gap recovers more slowly than the 50 mm gap for all pressures (see Figure 5 and Figure 6). At 1 bar filling pressure at 50 mm gap, when the HV pulse was applied later than 2 ms after CZ, the gap withstood the voltage. When the inter-electrode gap is reduced to 20 mm, dielectric breakdowns were observed for pulses earlier than 10 ms after CZ. At 40 bar, the corresponding minimum times to hold the applied pulse are 400 µs and 700 µs for 50 mm and 20 mm gap distances, respectively.

3.1.2 ARC CURRENT

The effect of arc current amplitude on the recovery process is studied by carrying out experiments for an arc current amplitude of 275 A. In this case, the gap distance is kept fixed at 50 mm. Two different filling pressures are used: 1 and 40 bar. The breakdown or hold voltage at different instants after CZ is plotted in Figure 7. Similar to what is observed previously, at 275 A arc current a faster increase of the breakdown voltage at 40 bar is observed compared to 1 bar filling pressure. No significant change in recovery time is observed between the two tested current levels (see Figure 5 and Figure 7).

3.2 SELF-BLAST ARRANGEMENT

The breakdown or hold voltage at different instants after CZ for different filling pressures for the self-blast arrangement is shown in Figure 8. The time of HV pulse application after CZ was varied from 20 µs to 500 µs for both N_2 pressures (1 and 40 bar). In contrast to the free-burning arc arrangement, no breakdowns were observed neither at 1 bar nor at 40 bar filling pressures. For the cases without a heating volume, i.e. for the reference measurements, as the time to HV pulse is reduced, the amplitude of the applied pulse went down. Similarly, for the cases with the heating volume, i.e., self-blast type, few cases are observed at 40 bars when the amplitude of the applied pulse is reduced. The reduction of the amplitude of the HV pulse is perhaps linked with the high post-arc conductivity immediately after CZ.

3.3 PUFFER ARRANGEMENT

The viscosity and the density vary with the filling pressure. As a result, for the same spring setting, the travel curve and the subsequent upstream pressure difference vary for different filling pressures. The travel curve and the upstream pressure difference for different filling pressures are plotted in Figure 9. For the full stroke of the piston, it takes approximately 70, 83, and 110 ms at 20, 40, and 80 bar filling pressures, respectively. The arc experiments were conducted at the time when the piston remains roughly in the middle of its stroke and the upstream pressure difference is in the range of 80-90 mbar. The initiation of the arc can be seen by the sharp spike in the pressure curve

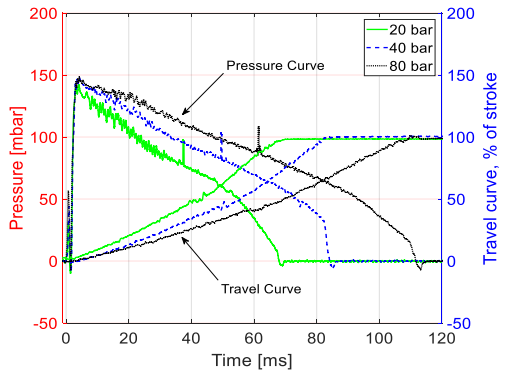

Figure 9. Travel curve and upstream pressure difference of the puffer for different filling pressure.

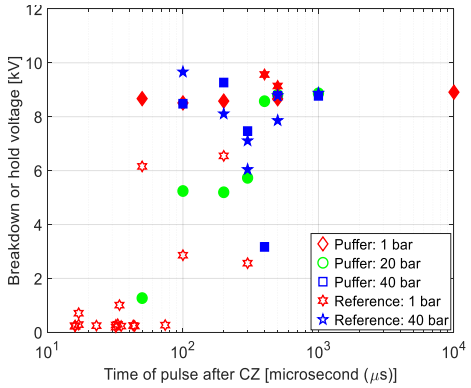

Figure 10. Breakdown or hold voltage at different instants after CZ for puffer arrangement for arc current of 425 A at 950 Hz. The filled markers represent withstand voltages whereas the empty markers represent breakdown voltages.

at 38 ms, 50 ms, and 62 ms at 20, 40, and 80 bar respectively, as shown in Figure 9. In this way, a similar upstream pressure difference can be ensured for all the different filling pressures.

The breakdown or the hold voltage at different instants after CZ for puffer arrangements at three different filling pressures are plotted in Figure 10. Reference measurements were conducted without any puffer movement, i.e., the arc burnt in the nozzle without any forced gas flow. No breakdowns were observed without forced gas flow, when the pulse was applied after 400 µs at 1 bar filling pressure. A voltage pulse before 400 µs caused a breakdown for reference measurements at 1 bar. For reference measurement at 40 bar filling pressure, however, no breakdown was observed even for the pulse at 100 µs. For the cases with a forced gas flow, no breakdown was observed at neither of the filling pressures.

The amplitude of the HV pulse is observed to go down as the time of pulse approaches CZ, as shown in Figure 11. This is perhaps due to the higher conductivity of the post-arc channel near CZ. At a high filling pressure (e.g., 20 and 40 bar), the damping of the applied HV pulse is greater than at 1 bar pressure. It has been observed that for some cases, the applied 10 kV pulse is limited to 1 kV when the time to pulse is 200 µs or less after CZ for 40 bar or 50 µs for 20 bar filling pressure. As a result, no test was possible to be carried out for a time to pulse of less than 50 µs.

4 DISCUSSION

As the current approaches zero, the arc temperature decreases. However, the temperature change in the arc channel at CZ is not instantaneous. After CZ, when the temperature of the post-arc channel continues to drop below a certain level, the ionized particles start to recombine, which reduces the number of free charge carriers [19], [20]. As a result, the post-arc breakdown voltage of the contact gap depends on the gap temperature. Many factors influence the temperature decay of the gap which includes the geometry of the gap and the physical properties of the medium e.g., thermal conductivity, density, specific heat and viscosity [21].

In the free-burning arrangement, just after CZ until several hundred microseconds, the breakdown voltage is observed to be the same for any particular filling pressure. For 1 bar, the breakdown voltage is approximately 330 V, whereas for the higher filling pressures (e.g., 20 bar, 40 bar, 80 bar) the breakdown voltage just after CZ is approximately 100 V. Just after CZ, a positive ion space charge layer is formed adjacent to the pulse cathode when the voltage stress appears across the

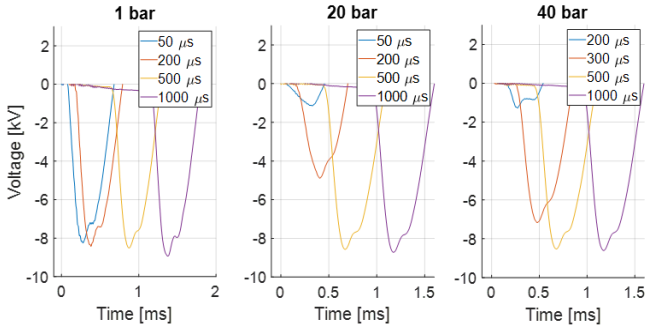

Figure 11. Change in the amplitude of the applied HV pulse at different instants after CZ in the puffer arrangement for different filling pressures.

contact gap. Due to the high mobility of electrons followed by a general drift of the charge in the gap in response to the applied voltage, the formation of the space charge layer adjacent to the electrodes is instantaneous. As a result immediately after CZ at 1 bar pressure, the breakdown voltage is close to the glow cathode-fall voltage [22]. Although no experimental data is found for glow cathode-fall voltage at a high filling pressure, an increase in the cathode-fall voltage is observed as the pressure is reduced [23].

For high filling pressures, the breakdown voltage until 300 µs is observed to be lower than at 1 bar. The energy deposition in the arc channel increases with the filling pressure due to high arc voltage. As the filling pressure is increased, the arc radius decreases [24]. Without forced gas flow, the thermal energy stored in the arc core fails to dissipate quickly. As a result, a relatively high post-arc current is observed for the arc burning at a high N_2 filling pressure [14]. A relatively high post-arc current may facilitate the glow to arc transition at high N_2 pressure, which would reduce the cathode-fall voltage [25]. In a recent study on the thermal interruption performance in the free-burning arc, the re-ignition voltage was observed to be lower at high filling pressures compared to at 1 bar [14]. In this paper, within the first 300 µs after CZ, the breakdown voltage is observed to be almost fixed. Such a plateau in the breakdown voltage with time just after CZ was also observed previously [22]. Another observation is that the duration of the plateau in the breakdown voltage is almost independent of the filling pressure.

For the free-burning arrangement, as the filling pressure increases, the breakdown voltage increases at a faster rate (after the critical time of approximately 300 µs after CZ). This critical time is probably linked with the temperature of the gap being close to the ionization temperature of N_2. Once the temperature of the gap falls below a certain level, the breakdown voltage will increase rapidly with the increase of the filling pressure, which is also observed in this paper. This fast increase in the breakdown voltage at higher pressures is also reported elsewhere [10].

The current, at least in the range investigated, has no significant effect on the dielectric recovery at any filling pressure. Perhaps the temperature of the arc core is not strongly dependent on the investigated arc currents. No strong current dependency of the arc voltage was observed during the high current phase between 150 to 450 A [12]. The inter-electrode gap, however, plays a bigger role in the recovery process. In the free-burning arc, natural convection is more efficient for a larger gap, resulting in faster arc cooling. Moreover, the breakdown voltage increases with increasing electrode gap once the temperature of the gap is below a certain level. As a result, the larger gap recovers faster and similar results have been previously reported.

In the free-burning arc arrangement, where natural convection is the dominant cooling mechanism after CZ, the resulting cooling of the electrode gap is not efficient. To increase the cooling of the gap, the forced convective cooling is adopted using two arrangements: a self-blast and a puffer type. As the cooling of the medium is enhanced, the recombination rate of the charge carriers after the extinction of the arc increases. The dielectric strength of the gap just after CZ is expected to be high under forced cooling. In this paper, no breakdown is observed for neither self-blast nor in the puffer setup under forced gas flow. At high pressure, however, the relatively high post-arc conductance is observed near CZ (seen as the damping of the applied HV pulse). No strong dependence of the SC state on post-arc dielectric recovery characteristics is observed. Nevertheless, forced gas flow significantly enhances the post-arc recovery at high filling pressures, also in the thermal phase. The blowing pressures for the self-blast and the puffer arrangements being different, no further comparison is made between the two blowing mechanisms.

5 CONCLUSIONS

The pressure dependence of the post-arc dielectric recovery characteristics is reported in this paper. To evaluate the recovery characteristics, an HV pulse is applied at different instants after CZ. The breakdown or hold voltage of the contact gap is analyzed as a function of time after CZ. First, the free-burning arc is investigated without forced gas flow. In the free-burning arrangement, the gap dependency and the current dependency is also studied. For the gap dependence of the recovery characteristics, a 20 and a 50 mm gap are compared for the arc current of 425 A. For the current dependence, two different amplitudes of current: 275 and 425 A are studied at 50 mm inter-electrode gap. Afterward, to investigate the effect of forced gas flow on the recovery process at different filling pressures, two different arrangements are used: a self-blast and a puffer arrangement. Depending on the experimental observations, the following conclusions are drawn:

- In the free-burning arrangement, the breakdown voltage of the contact gap increases faster with the increase of the filling pressure. However, in the thermal phase (just after CZ), the breakdown voltage is low for high filling pressure. A longer gap recovers quicker than a shorter gap. No strong current dependency of the post-arc dielectric recovery has been observed in the investigated current range.
- Forced gas flow significantly enhances the post-arc recovery at a high filling pressure, also in the thermal phase. No breakdown is observed even immediately after CZ under forced gas flow conditions for the applied currents and voltage pulses.

The experiments indicate that although the thermal phase is the critical phase of the ultrahigh-pressure N_2 arc, the dielectric phase is inherently superior as the filling pressure increases even without forced gas flow. A forced gas flow, however, also improves the performance of the thermal phase, which shows its prospects as a subsea current interruption medium.

ACKNOWLEDGMENT

This work is supported by the Research Council of Norway.

REFERENCES

[1] T. Hazel, H. H. Baerd, J. J. Legeay, and J. J. Bremnes, “Taking Power Distribution Under the Sea: Design, Manufacture, and Assembly of a Subsea Electrical Distribution System,” IEEE Ind. Appl. Mag., vol. 19, no. 5, pp. 58–67, Sep. 2013.

[2] A. Nordrum, “ABB Siemens Test Subsea Power Grids For Underwater Factories - IEEE Spectrum.” [Online]. Available: https://spectrum.ieee.org/energy/fossil-fuels/abb-siemens-test-subsea-

power-grids-for-underwater-factories. [Accessed: 27-Sep-2019].
[3] E. Jonsson, "Load Current Interruption in Air for Medium Voltage Ratings," PhD dissertation, Department of Electric Power Engineering, Norwegian University of Science and Technology, Norway, 2014.
[4] Z. B. Yang *et al*, "Post-breakdown dielectric recovery characteristics of high-pressure liquid CO_2 including supercritical phase," IEEE Trans. Dielectr. Electr. Insul., vol. 21, no. 3, pp. 1089–1094, Jun. 2014.
[5] J. Zhang, "Supercritical fluids for high power switching," PhD dissertation, Department of Electrical Engineering, Eindhoven University of Technology, Netherlands, 2015.
[6] J. Zhang *et al*, "Numerical and Experimental Investigation of Dielectric Recovery in Supercritical N_2," Plasma Sources Sci. Technol., vol. 24, no. 2, p. 025008, Feb. 2015.
[7] K. Niayesh and M. Runde, Power Switching Components. Springer International Publishing, 2017.
[8] K. D. Song, B. Y. Lee, and K. Y. Park, "Analysis of Thermal Recovery for SF_6 Gas-Blast Arc within Laval Nozzle," Jpn. J. Appl. Phys., vol. 42, no. Part 1, No. 11, pp. 7073–7079, Nov. 2003.
[9] M. Seeger **et al**, "Dielectric recovery in a high-voltage circuit breaker in SF_6," J. Phys. D. Appl. Phys., vol. 45, no. 39, p. 395204, Oct. 2012.
[10] M. Seeger *et al*, "Investigation of the Dielectric Recovery in Synthetic Air in a High Voltage Circuit Breaker," J. Phys. D. Appl. Phys., vol. 38, no. 11, pp. 1795–1804, Jun. 2005.
[11] T. Nakano *et al*, "Thermal Re-ignition Processes of Switching Arcs with Various Gas-blast Using Voltage Application Highly Controlled by Powersemiconductors," J. Phys. D. Appl. Phys., vol. 51, no. 21, p. 215202, May 2018.
[12] F. Abid *et al*, "Arc Voltage Characteristics in Ultrahigh-Pressure Nitrogen Including Supercritical Region," IEEE Trans. Plasma Sci., vol. 46, no. 1, pp. 187–193, Jan. 2018.
[13] F. Abid, K. Niayesh, and N. S. Stoa-Aanensen, "Ultrahigh-Pressure Nitrogen Arcs Burning Inside Cylindrical Tubes," IEEE Trans. Plasma Sci., vol. 47, no. 1, pp. 754–761, Jan. 2019.
[14] F. Abid *et al*, "Thermal Interruption Performance of Ultrahigh-Pressure Free-Burning Nitrogen Arc," in 21st International Symposium on High Voltage Engineering (ISH), Berlin, Heidelberg: SPRINGER, 2020, pp. 663–671.
[15] F. Abid, K. Niayesh, and N. Støa-Aanensen, "Nozzle Wear And Pressure Rise In Heating Volume of Self-Blast Type Ultra-High Pressure Nitrogen Arc," Plasma Phys. Technol. J., vol. 6, no. 1, pp. 23–26, 2019.
[16] F. Abid, K. Niayesh, and N. Støa-Aanensen, "Arc Voltage Distribution Measurement in Tube Constricted Ultrahigh-Pressure Nitrogen Arc," in International Symposium on High Voltage Engineering (ISH), Budapest, Hungary: Springer Nature, 2020, pp. 672–679.
[17] F. Abid, K. Niayesh, and N. Stoa-Aanensen, "Post-arc Dielectric Recovery Characteristics of Free-burning Ultrahigh-Pressure Nitrogen Arc," in 2019 5th International Conference on Electric Power Equipment - Switching Technology (ICEPE-ST), 2019, pp. 105–108.
[18] A. Kadivar and K. Niayesh, "Two-way interaction between switching arc and solid surfaces: distribution of ablated contact and nozzle materials," J. Phys. D. Appl. Phys., vol. 52, no. 40, p. 404003, Oct. 2019.
[19] H. Edels, D. Whittaker, K. G. Evans, and A. B. Shaw, "Experiments and Theory on Arc Reignition by Spark Breakdown," Proc. Inst. Electr. Eng., vol. 112, no. 12, p. 2343, 1965.
[20] G. Farrall and J. Cobine, "Recovery Strength Measurements in Arcs from Atmospheric Pressure to Vacuum," IEEE Trans. Power Appar. Syst., vol. PAS-86, no. 8, pp. 927–932, Aug. 1967.
[21] H. Edels and J. C. Holme, "Measurements of the Decay of Arc Column Temperature Following Interruption," Br. J. Appl. Phys., vol. 17, no. 12, pp. 1595–1606, Dec. 1966.
[22] F. W. Crawford and H. Edels, "The Reignition Voltage Characteristics of Freely Recovering Arcs," Proc. IEE Part A Power Eng., vol. 107, no. 32, p. 202, 1960.
[23] J. P. Novak, "Electric field and electrode potential drops of arcs and glow discharges in air," J. Appl. Phys., vol. 62, no. 12, pp. 4719–4724, Dec. 1987.
[24] T. Okuma *et al*, "Effects of Working Pressure on Temperature Characteristics in Multiphase AC Arc," J. Fluid Sci. Technol., vol. 13, no. 4, pp. JFST0024–JFST0024, 2018.
[25] W. A. Gambling and H. Edels, "The high-pressure glow discharge in air," Br. J. Appl. Phys., vol. 5, no. 1, pp. 36–39, Jan. 1954.

Fahim Abid was born in Jamalpur, Bangladesh in 1990. He completed the B.Sc. degree in Electrical and Electronic Engineering in 2012 from the Islamic University of Technology (IUT), Bangladesh. He received the M.Sc. degree in 2015 on Electrical Engineering from the Royal Institute of Technology (KTH), Sweden. He is currently working on his Ph.D. degree at the Department of Electric Power Engineering at Norwegian University of Science and Technology (NTNU), Norway.

Kaveh Niayesh (S'98–M'01–SM'08) completed the B.Sc. and M.Sc. degree in Electrical Engineering from the University of Tehran, Iran, in 1993 and 1996 respectively. In 2001, he completed the Ph.D. degree from the RWTH-Aachen University of Technology in Electrical Engineering. In the last 19 years, he held different academic and industrial positions including Principal Scientist with the ABB Corporate Research Center, Baden-Dattwil, Switzerland; Associate Professor with the University of Tehran; and Manager, Basic Research, with AREVA T&D, Regensburg, Germany. Currently, he is a Professor in the Department of Electric Power Engineering at Norwegian University of Science and Technology (NTNU), Norway. He is the holder of 16 patents and has more than 120 journal and conference publications on current interruption and limitation, vacuum and gaseous discharges, plasma modeling and diagnostics, and pulsed power technology.

Egil Viken is currently working with his M.Sc. in electrical power engineering from the Norwegian University of Science and Technology (NTNU), Trondheim, Norway. He is in the final year of his master and is planning to graduate summer 2020. He worked in SINTEF with current interruption as an intern the summer 2018 and 2019.

Nina Sasaki Støa-Aanensen completed the M.Sc. degree in Applied Physics and Mathematics in 2011 and the Ph.D. degree in Electrical Power Engineering in 2015 from the Norwegian University of Science and Technology (NTNU), Trondheim, Norway. Currently, she is working as a research scientist in SINTEF Energy Research, Trondheim, Norway.

Erik Jonsson received the M.Sc. degree in physics in 2005 from Uppsala University, Sweden. He completed the Ph.D. degree in Electrical Power Engineering in 2014 from Norwegian University of Science and Technology (NTNU), Trondheim, Norway. He worked with ABB Corporate Research, Västerås, Sweden from 2006 to 2007. Currently, he is working as a research scientist in SINTEF Energy Research, Trondheim, Norway.

Hans Kristian Meyer completed his M.Sc. degree in 2015 and Ph.D. degree in 2019 on Electric Power Engineering from the Norwegian University of Science and Technology (NTNU) in Trondheim, Norway. Currently he is working as a research scientist in SINTEF Energy Research, Trondheim, Norway.

Paper VI

THERMAL INTERRUPTION PERFORMANCE OF ULTRAHIGH-PRESSURE FREE-BURNING NITROGEN ARC

Fahim Abid[1][0000-0001-8570-491X], Kaveh Niayesh[1], Shashidhara Basavapura Thimmappa[1], Camilla Espedal[2], Nina Støa-Aanensen[2]

[1] Norwegian University of Science and Technology, Trondheim, Norway
[2] SINTEF Energy Research, Trondheim, Norway
fahim.abid@ntnu.no

Abstract. In this paper, an experimental investigation of the thermal interruption performance of free-burning nitrogen arcs at 1 bar, 20 bar, and 40 bar filling pressures is reported. This work contributes to the fundamental understanding of arc characteristics at very high gas filling pressures. A resonant circuit is used to generate an arc peak current of 130 A at a frequency of 190 Hz. An ignition copper wire initiates the arc between a 4 mm diameter pin electrode and a ring electrode. The arc burns freely at a fixed inter-electrode gap of 50 mm without any forced gas flow. A resistive-capacitive branch parallel to the arc controls the initial rate of rise of recovery voltage. By changing the parallel resistance, the rate of rise of recovery voltage is varied from 9.8 V/µs to 84.8 V/µs. Time to re-ignition and the corresponding re-ignition voltages are considered as the primary parameters to characterize the thermal interruption performance. It is observed that the re-ignition time rises with the decrease of rate of rise of recovery voltage at all pressure levels, which is expected. However, in the absence of a forced gas flow, high gas filling pressure results in a reduction of the time to re-ignition and the re-ignition voltage in contrast to atmospheric pressure nitrogen arc.

Keywords: Supercritical fluid, Arc discharge, Free-burning arc.

1 Introduction

When the temperature and pressure of any fluid exceed its critical point, the fluid enters into a supercritical (SC) state [1]. Supercritical fluids exhibit properties of the gaseous phase and the liquid phase simultaneously. High density, high heat conductivity, high diffusivity, the absence of vapor bubbles and self-healing properties are some of the unique features of an SC fluid [2]. Insulation and current quenching fluids in power switching devices must hold a specific set of properties: high insulation strength during off time, low resistance during on time, large current handling capability, high voltage rating, fast recovery after switching, long lifetime, etc. For gas circuit breakers, the properties of SC fluid are believed to enhance the current interruption performance [2].

Nitrogen (N_2) reaches a supercritical state beyond its critical pressure (33.5 bar) and critical temperature (126 K). Nitrogen is chosen in this work due to its environmentally benign nature, good insulation strength and low critical pressure. The amount of published works on arc discharge inside supercritical fluid is scarce. Nonetheless, it has

been reported that the free-burning arc voltage increases with filling pressure of nitrogen, without any abrupt change during the transition from gas to SC state [3], [4]. A higher arc voltage results in a higher energy deposition in the arc channel. To the knowledge of the authors, no work has been reported on the current interruption performance of supercritical nitrogen for switchgear applications.

Current interruption can be described as a race between the cooling of the arcing channel and the voltage that builds up across the contacts. When the cooling of the arc channel is not sufficient, thermal re-ignition may occur [5]. Thermal re-ignition happens immediately after current zero (CZ) (up to a few microseconds) when the contact gap is still hot and with remaining electrical charge carriers. In contrast, dielectric re-strike happens at a much longer timescale (hundreds of microseconds) when the contact gap is fairly cold [6]. This study focuses on the influence of filling pressure on thermal re-ignition of free-burning nitrogen arcs in a fixed electrode arrangement.

Thermal re-ignition is strongly dependent on the initial rate of rise of recovery voltage (IRRRV) after CZ and the slope of the current curve before CZ [5]. In this study, the steepness of the current before CZ is kept constant. Moreover, a simplified test method is adopted by adding an impedance branch parallel to the arcing contact. A more detailed description of the method can be found in the literature [7]. By changing the resistance parallel to the arc, the IRRRV is varied from 9.8 V/µs to 84.8 V/µs. The arc is left to burn freely in N_2 at 1-40 bar without any forced cooling. The thermal interruption performance will be evaluated by measuring the time to re-ignition and the voltage at re-ignition.

The test setup and the method are outlined in chapter 2. The measured time to re-ignition and re-ignition voltages as a function of IRRRV at various gas filling pressures are presented in chapter 3. Finally, in chapter 4, the conclusions are drawn from the study.

2 Experiment Setup

The electrical setup is shown schematically in Fig. 1. The test circuit consists of the charging and discharging sections of a 7.2 µF high voltage (HV) capacitor bank, *C*. The inductance, *L*, and the charging voltage of *C* are kept constant to generate a fixed current amplitude of 130 A at a frequency of 190 Hz. Once the switch, S_D, is closed, the current flows through the inductor and further through a copper ignition wire (25 µm diameter) inside the arcing chamber. An ignition wire is mounted between two copper tungsten (Cu-W) electrodes (pin and ring electrodes) that are kept at a fixed distance of 50 mm. Once the current flows, the ignition wire melts due to adiabatic heating and initiates the arc. The arc is allowed to burn freely between the electrodes without any forced N_2 flow.

The arc current continues to flow until CZ, where the current is momentarily interrupted. Because of this momentary interruption, the energy storing elements in the circuit generate a voltage stress across the arcing contacts, known as the transient recovery voltage (TRV). In this paper, a known impedance (C_{TRV} and R_{TRV}) parallel to the arc controls the TRV. The TRV shaping part comprises a capacitor, C_{TRV} of 1.2 µF and a resistor, R_{TRV}. By changing R_{TRV}, the initial rate of rise of recovery voltage is controlled. Five different values of the R_{TRV} is used to generate IRRRVs in the range of 9.8 V/µs to 84.8 V/µs. The circuit is simulated in MATLAB Simulink to calculate the IRRRV.

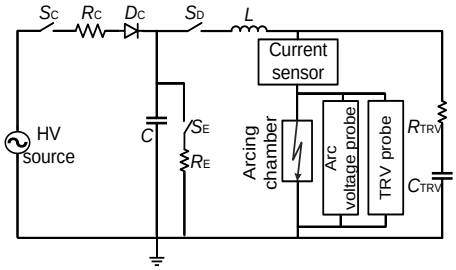

Fig. 1. Electrical setup consisting of a resonant circuit to generate the arc current and a TRV shaping part.

From the simulation, it is found that the charging voltage and the R_{TRV} are the two most important parameters influencing the IRRRV. The circuit parameters and the resulting IRRRV are shown in Table 1.

Two high voltage (HV) probes with different voltage range and frequency responses are used to measure the arc voltage and TRV across the electrodes. The HV probes are connected outside the pressure tank. A shunt resistor is used to measure the arc current. The current sensor is connected on the high voltage side of the arcing chamber on a floating potential. All the data are sent to the control room via optical fiber and stored in a digital oscilloscope for further analysis. The sampling rate of the measurement is ten samples per microsecond.

Photos of the lab setup are shown in Fig. 2. The high voltage transformer, the capac-

Table 1. Circuit parameters and the calculated current steepness and IRRRV.

L [mH]	dI/dt [A/ms]	R_{TRV} [Ω]	IRRRV [V/µs]
96	152	47	9.8
		140	22.4
		280	43.0
		420	63.9
		560	84.8

itors, and the inductor can be seen in Fig. 2(a). A pressure tank of 15.7-liters rated for 500 bars, shown in Fig. 2(b), is used as arcing chamber. A 24 kV HV cable is fed through the flange of the pressure tank. The HV cable is terminated to the pin electrode and held in position inside the pressure tank by insulators. The experimental setup is put inside an explosion-safe room. The pressure tank is pressurized through the valves from the nitrogen gas bottles (black bottles in Fig. 2(b)). Before each experiment, the pressure vessel is flushed with industrial grade nitrogen, to ensure at least 99% pure nitrogen for all the experiments conducted. The ignition wire is mounted by hand for each test and is kept in the same position to reduce the experimental uncertainty. For all five circuit settings, experiments at three different pressures are conducted: 1, 20 and 40 bar. When the filling pressure is 40 bar, the fluid is in the supercritical state. Ten tests are conducted for all three pressure levels for the case where R_{TRV} is 47 Ω. For the

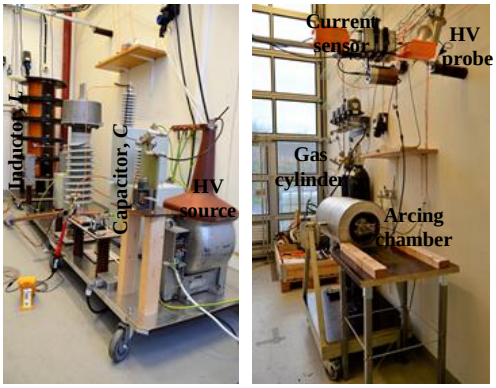

(a) (b)

Fig. 2. Photos of lab setup. (a) Electrical components. (b) Arcing chamber.

rest of the R_{TRV} values, at least five tests are performed for each test pressure. All the operations are controlled from a separate room located at a safe distance.

3 Experimental Results and Discussions

A typical measurement of the arc voltage and the arc current is shown in Fig. 3. The ignition voltage peak marks the initiation of the arc. Due to the high voltage rise during ignition, some of the energy in C goes to charging C_{TRV}. Such a case of charging the TRV shaping capacitor can be seen in Fig. 3 by the collapse of the arc current during the melting of the ignition wire. However, the charging of the C_{TRV} did not have any effect on the IRRRV.

The current is interrupted momentarily at CZ (at approximately 2.6 ms). Just after CZ, the remaining charge carriers are accelerated by the rise of the TRV. Such a movement of charge carriers after CZ is often called post-arc current. If the post-arc current is high enough, sufficient energy may remain in the hot column to re-establish the arc, seen as re- ignition in Fig. 3. The re-ignition is marked by the collapse of the TRV and by the sudden increase of the arc current. In this paper, the time between CZ and the re-ignition is defined as the time to re-ignition (Δt), as shown in Fig. 3. The voltage at which the re-ignition happens is named as re-ignition voltage.

3.1 Time to Re-ignition as a Function of IRRRV

The time to re-ignition (Δt) as a function of IRRRV at various filling pressures is plotted in Fig. 4. Data points at an IRRRV of 9.8 V/μs for all three filling pressures represent the average of ten tests while the rest of the points are the average of at least five tests. The error bar corresponds to the highest and lowest measured values of Δt. When the IRRRV is increased, a faster time to re-ignition is observed for all filling pressures, as expected. A higher IRRRV causes the remaining charge carriers in the arc channel after

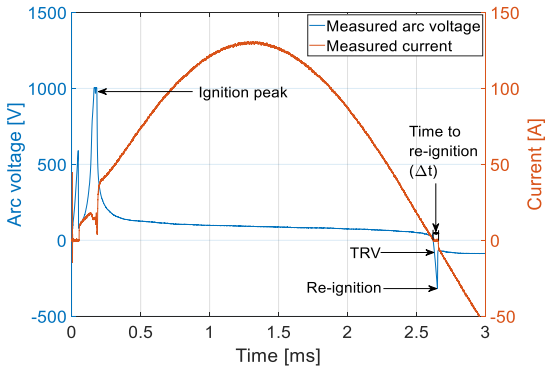

Fig. 3. Measured arc voltage and arc current for atmospheric pressure nitrogen arc with an arc peak current of 130 A and an IRRRV of 9.8 V/µs.

CZ to accelerate faster, which speeds up the re-ignition process. The variation in Δt is high when the IRRRV is low and is believed to be due to the stochastic nature of the arc discharge.

The average time to re-ignition for arcs at atmospheric pressure and an IRRRV of 9.8 V/µs is approximately 35 µs. The re-ignition time goes down to approximately 13 µs when the filling pressure is 20 bar or 40 bar. A quicker re-ignition at a high filling pressure (20 bar or 40 bar) compared to atmospheric pressure arc is also observed for all the measured IRRRV values. However, the difference in re-ignition time for arc burning in 20 bar and 40 bar gas filling pressure is less apparent.

3.2 Re-ignition Voltage as a Function of IRRRV

The re-ignition voltage as a function of IRRRV for different gas filling pressures is shown in Fig. 5. The average re-ignition voltage in atmospheric pressure arcs is about

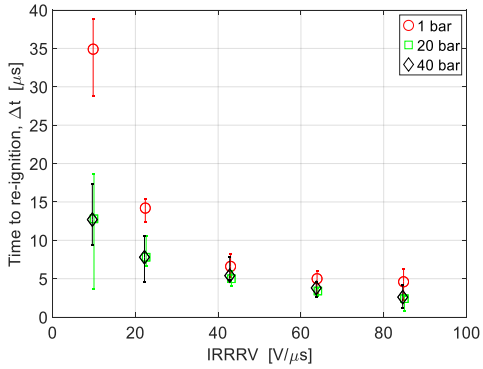

Fig. 4. Time to re-ignition as a function of IRRRV at different gas filling pressure.

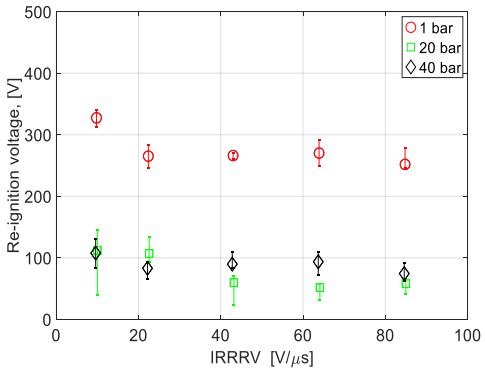

Fig. 5. Re-ignition voltage as a function of IRRRV at different gas filling pressures.

250-350 V, almost irrespective of measured IRRRV ranges. The fluctuation in re-ignition voltage is less at atmospheric pressure, as indicated by fluctuation bars. The effect of high filling pressure (i.e., 20 bar or 40 bar) on the re-ignition voltage compared to atmospheric pressure is evident from Fig. 5. The average arc re-ignition voltage in 20 bar and 40 bar gas filling pressure is in the range of 50-110 V, almost irrespective of the values of the IRRRV (over the range of 9.8–84.8 V/µs).

3.3 Current and Voltage Waveform Near CZ

The measured current and voltage waveforms for two different IRRRV settings at three different gas filling pressures are shown in Fig. 6. The current and arc voltage for arcs burning at different filling pressures for the IRRRV of 9.8 V/µs are shown in Fig. 6 (a). The time to re-ignition is longer at atmospheric pressure compared to 20 and 40 bar filling pressures. At atmospheric pressure (IRRRV = 9.8 V/µs), the thermal re-ignition happens approximately 35 µs after CZ, at a re-ignition voltage of 330 V.

For the experiments at atmospheric pressure, the re-ignition is easily detected by a distinct voltage collapse. In contrast, no sudden change in voltage can be seen at 20 and 40 bar. Here, the re-ignition is identified by a change in the slope of the measured voltage. At high pressures, the current starts to flow almost instantly after CZ. The measured arc current and the voltage waveform of the arc burning at different filling pressures for IRRRV of 43 V/µs is shown in Fig. 6 (b). At 1 bar, the thermal re-ignition occurs approximately 7 µs after CZ at a re-ignition voltage of 290 V. For the arc burning at 20 bar and 40 bar; the current flows almost immediately after CZ.

The time constant of an arc is an indication of how fast the arc goes from a conducting state to an insulating state. A smaller time constant is observed as a fast change of arc voltage just before CZ. From Fig. 6, the change of arc voltage just before CZ is observed to be slower at a high gas filling pressure (i.e., 20 bar, 40 bar) compared to at 1 bar. This indicates that the time constant for free-burning arcs at higher filling pressures is larger than that at atmospheric pressure.

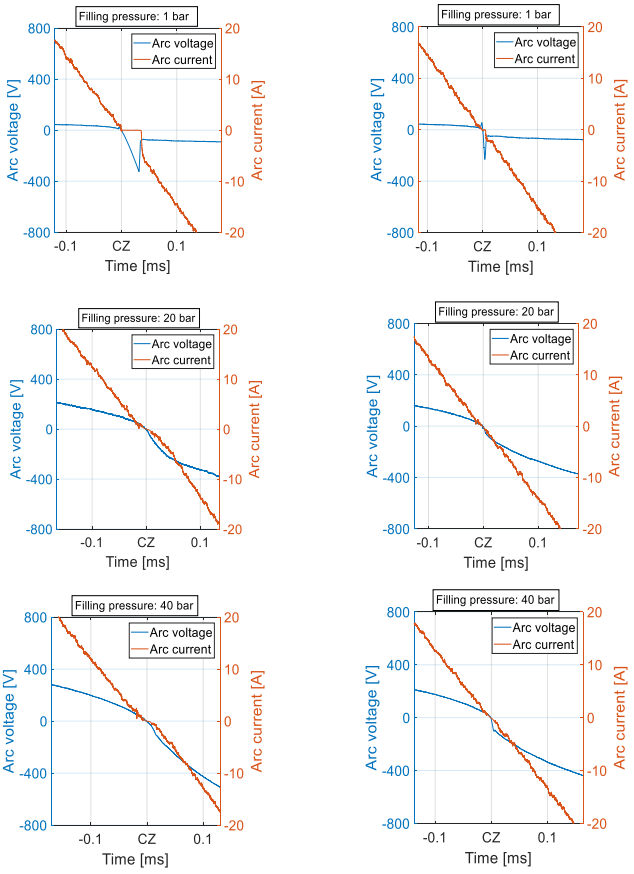

(a) (b)

Fig. 6. Measured arc voltage and current waveform near CZ for different filling pressures at two different IRRRV settings. (a) IRRRV is 9.8 V/µs. (b) IRRRV is 43 V/µs.

3.4 Discussions

The thermal interruption performance of free-burning nitrogen arcs is observed to worsen at high filling pressures compared to at atmospheric pressure. The current starts to flow almost immediately after CZ for arcs burning at high filling pressures (i.e., 20 bar, 40 bar). When the filling pressure increases, the arc voltages rises too. Consequently, the energy dissipation in the arc channel increases at high filling pressures. Moreover, the arc radius decreases with increasing pressure. In the absence of forced

cooling near CZ, the hot core of the arc fails to dissipate the heat fast enough. The relatively high temperature of the arc core after CZ results in a high number of charge carriers which may facilitate the faster re-ignition of the arc.

The re-ignition voltage is observed to be independent of the investigated IRRRV values for a specific filling pressure. It is reported in the literature that a free-burning air arc takes almost a second to recover entirely at atmospheric pressure [8]. Under free-recovery conditions of air arcs, often the recovery voltage does not linearly increase with time. A fixed recovery voltage for some duration of time is reported in the literature [8]. In this paper, the measured re-ignition voltage of 250-350 V at atmospheric pressure is observed. The measured re-ignition voltage at atmospheric pressure is in line with the reported re-ignition voltage of nitrogen arcs of 340-350 V in the works of Nakano et al. with a different method [9].

The thermal re-ignition characteristics at 20 bar and 40 bar gas filling pressures are found quite similar. In a previous work, for arc peak current of 150 A at 350 Hz, the arc radius of the free-burning arc was calculated to be approximately 4 mm at atmospheric pressure [10]. In comparison, the calculated free-burning arc radius was 1.5 mm and 1.43 mm for arc burning at 20 bar and 40 bar respectively [10]. It was reported that the arc is constricted significantly at 20 bar filling pressure compared to at atmospheric pressure, whereas the constriction is not much when compared between the arc burning at 20 bar and 40 bar filling pressure [10]. This may explain the similarity in re-ignition properties for arcs burning at 20 bar and 40 bar filling pressure.

4 CONCLUSIONS

The thermal interruption performance of free-burning nitrogen arcs as a function of N_2 filling pressure is reported in this paper. By adding a resistive-capacitive branch parallel to the arc, the IRRRV is controlled, whereas the slope of the current decay before CZ is fixed. The time to re-ignition and the re-ignition voltages are analyzed as a function of IRRRV at different filling pressures. Based on the experimental investigations, the following conclusions have been drawn:

- The time to re-ignition increases when the IRRRV decreases for all gas filling pressures, as expected.
- High nitrogen filling pressures (i.e., 20 bar, 40 bar) reduce the time to re-ignition compared to atmospheric pressure arc.
- The re-ignition voltage is not strongly dependent on the investigated IRRRV values. The re-ignition voltage is found to decrease at high filling pressures (i.e., 20 bar, 40 bar) compared to free-burning arcs in atmospheric pressure.
- The thermal interruption performance of free-burning arcs worsen at high nitrogen filling pressures compared to atmospheric pressure arc.

Acknowledgement

This work is supported by the Norwegian Research Council.

References

1. D. Banuti, M. Raju, P. C. Ma, M. Ihme, and J.-P. Hickey, "Seven questions about supercritical fluids - towards a new fluid state diagram," presented at the 55th AIAA Aerospace Sciences Meeting, 2017.
2. J. Zhang, A. Markosyan, M. Seeger, E. van Veldhuizen, E. van Heesch, and U. Ebert, "Numerical and experimental investigation of dielectric recovery in supercritical N_2," Plasma Sources Science and Technology, vol. 24, no. 2, p. 025008, 2015.
3. F. Abid, K. Niayesh, E. Jonsson, N. S. Støa-Aanensen, and M. Runde, "Arc Voltage Characteristics in Ultrahigh-Pressure Nitrogen Including Supercritical Region," IEEE Transactions on Plasma Science, vol. 46, no. 1, pp. 187-193, 2018.
4. F. Abid, K. Niayesh, E. Jonsson, N. S. Støa-Aanensen, and M. Runde, "Arc Voltage Measurements Of Ultrahigh Pressure Nitrogen Arcs In Cylindrical Tubes," presented at the 22nd International Conference on Gas Discharges and their Applications, Novi Sad, Serbia, 2-7 September 2018.
5. K. Niayesh and M. Runde, Power Switching Components. Springer, 2017.
6. H. Edels, A. Halder, A. Shaw, and D. J. N. Whittaker, "Convection-free post-arc gap recovery," vol. 193, no. 4812, p. 263, 1962.
7. A. Karimi and K. Niayesh, "A simple evaluation method of the thermal interruption limit of power circuit breakers," Electrical Engineering, vol. 90, no. 8, pp. 523-528, 2009.
8. F. Crawford and H. Edels, "The reignition voltage characteristics of freely recovering arcs," Proceedings of the IEE-Part A: Power Engineering, vol. 107, no. 32, pp. 202-212, 1960.
9. T. Nakano, Y. Tanaka, K. Murai, Y. Uesugi, T. Ishijima, K. Tomita, K. Suzuki and T. Shinkai, "Thermal re-ignition processes of switching arcs with various gas-blast using voltage application highly controlled by powersemiconductors," Journal of Physics D: Applied Physics, vol. 51, no. 21, p. 215202, 2018.
10. F. Abid, K. Niayesh, and N. Støa-Aanensen, "Ultrahigh-Pressure Nitrogen Arcs Burning inside Cylindrical Tubes," IEEE Transactions on Plasma Science, vol. 47, no. 1, pp. 754-761, Jan. 2019.

Paper VII

Arc Voltage Distribution Measurement in Tube Constricted Ultrahigh-Pressure Nitrogen Arc

Fahim Abid[1][0000-0001-8570-491X], Kaveh Niayesh[1], Nina Støa-Aanensen[2]

[1] Norwegian University of Science and Technology, Trondheim, Norway
[2] SINTEF Energy Research, Trondheim, Norway
fahim.abid@ntnu.no

Abstract. This work contributes to the fundamental understanding of axial voltage distribution of the arc burning inside polytetrafluoroethylene (PTFE) tube at very high filling pressures of nitrogen. The arc peak current of 85 A at a frequency of 190 Hz with a fixed initial rate of rise of recovery voltage (IRRRV) of approximately 50 V/µs is used throughout the study. Arc burning at three different filling pressures are studied: 1 bar, 20 bar, and 40 bar. To examine the axial voltage distribution in the arc, the arc voltage at three different axial position of the arc is independently measured. For some cases, a 3 cubic centimeter heating volume is attached to the ring electrode, which produces a back flow. For the cases with a heating volume, the pressure rise in the heating volume is also measured. It is observed that the pressure rise in the heating volume increases with the filling pressure. In the presence of the heating volume at a high filling pressure (i.e., 20 bar, 40 bar), the voltage drop increases significantly near the vent due to the relatively cold gas flow.

Keywords: Supercritical Fluid, Arc Discharge, Free-burning Arc.

1 Introduction

Nitrogen (N_2) enters into a supercritical (SC) state when the temperature and pressure exceed the critical point (126 K and 33.5 bar) [1]. High density, high heat conductivity, high diffusivity, the absence of vapor bubbles and self-healing properties are some of the unique features of an SC fluid [2]. For gas circuit breakers, the properties of SC fluid are believed to enhance the current interruption performance [2]. Arc discharges inside SC medium are a relatively new field of research. It has been reported that the free-burning arc voltage increases with filling pressure without any abrupt change during the transition of N_2 from gas to SC state [3]. As the filling pressure increases, the energy dissipation in the arc also increases [4]. The arc radius is reported to decrease as a result of the high filling pressure [5]. A successful current interruption must facilitate a quick transition of the arc column from a conducting state to an insulating state near current zero (CZ). To avoid a thermal re-ignition, it is necessary to cool the arc effectively near CZ [6].

The test circuit used in this paper generates an arc peak current of 85 A at a frequency of 190 Hz. This result in a current steepness of 100 A/ms just before CZ. A fixed

IRRRV of 50 V/µs is applied across the arcing contacts just after CZ. Arc burning at three different filling pressures are investigated: 1bar (atmospheric pressure), 20 bar, and 40 bar. At room temperature and 40 bar filling pressure, nitrogen is in SC state. The conductivity of the switching arc is often not homogeneous axially, leading to some areas of the arc column being more critical in the interruption process [6]. In this paper, a direct measurement of the voltage drop in three axial positions of the arc is independently measured. To study the effect of the gas flow on the axial voltage distribution at different filling pressures, some of the tests are conducted with a heating volume. For the cases with a heating volume, the pressure rise (Δp) in the heating volume is also measured. The voltage distribution across the different sections of the arc are analyzed together with the pressure rise measurements in the heating volume.

2 Experiment Setup

The test setup shown in Fig. 1 is used to generate the arc current and the IRRRV. The capacitor, C is charged from a high voltage (HV) source to a charging voltage of 10 kV. Once the capacitor is charged, it is disconnected from the grid by the switch S_C. The capacitor, C is discharged by a knife switch S_D, the inductor, L and further through the arcing chamber. The opening of the switch S_C and closing of the switch S_D are synchronized by a control circuit to have the same energy in the capacitor, C for all the experiments.

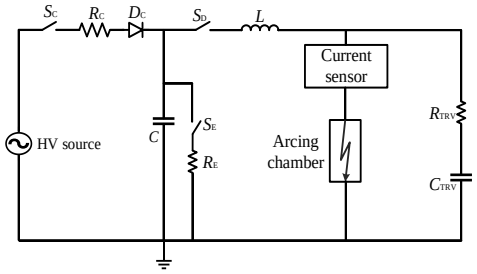

Fig. 1. Electrical setup consisting of a resonant circuit to generate the arc current and a TRV shaping part.

A pressure tank of 15.7-liters rated for 500 bar is used as the arcing chamber. The purity of the nitrogen is maintained to at least 99% in all the tests. Arc-resistant copper-tungsten. electrodes (pin and a ring electrode) are kept at a fixed inter-electrode gap of 50 mm, see Fig. 2. A PTFE tube with a vent (2 opposite holes of 3 mm diameter passing through the tube) is firmly mounted on the electrode. A 40 µm diameter copper wire is passed through the PTFE tube and fixed with the electrodes. The arc is initiated by melting of the copper wire. Once the arc is initiated, the current continues to flow

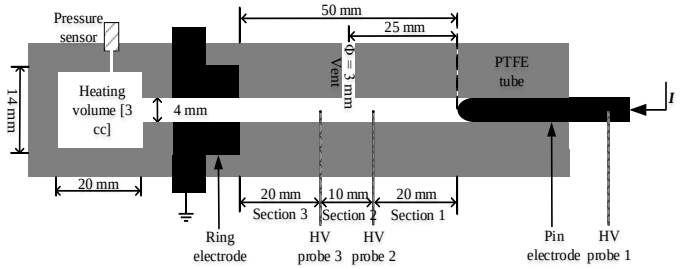

Fig. 2. The configuration of the electrode, heating volume and the PTFE tube. The pressure sensor is mounted on one side of the heating volume. The HV probes 2, 3 and the pressure sensor are put inside the pressure tank. For some cases heating volume is removed and for some cases heating volume is attached.

through the arc until CZ, where the current is momentarily interrupted. During this momentary interruption, a controlled voltage stress is applied across the electrodes, depending on the values of R_{TRV} and C_{TRV}. In this paper, the R_{TRV} and C_{TRV} are kept constant to 560 Ω and 1.2 µF respectively to generate a fixed IRRRV of 50 V/µs after CZ.

An HV probe 1 is connected across the electrodes from the outside of the pressure tank to measure the total arc voltage. Two other HV electrodes are used to measure the voltage drop at a distance of 20 mm and 30 mm from the pin electrode with respect to ground, as shown in Fig. 2. For this purpose, a thin tungsten wire is inserted into the tube by tiny holes. To avoid the gas flow through the tiny holes, the holes are closed from outside of the tube. These two HV probes are put inside the pressure tank to measure the voltage distribution inside the tube. To measure the arc current, a resistive shunt for the range of ±500 A is used.

Arc burning inside three different gas filling pressures is studied: 1 bar (atmospheric pressure), 20 bar and 40 bar. For the arc voltage distribution tests, total six tests are conducted: one test at each pressure levels, with or without the heating volume. A 3 cc heating volume is mounted behind the ring electrode, as shown in Fig. 2. A piezoelectric pressure sensor is mounted on a side wall of the heating volume to measure the pressure rise in the heating volume. The pressure sensor is recess mounted, and a vinyl electric tape is used to protect it from the thermal blast. Due to the limitation of the available channels in the oscilloscope, three tests with the heating volume is repeated to measure the pressure rise. The same PTFE tube with the vent is used for all the performed tests. The measured signals from HV probe 2, 3 and the pressure sensor inside the pressure tank are sent out via a signal penetrator. All data are transferred via optical fiber link and stored in oscilloscope for further analysis.

3 Experimental Results and discussions

The measured voltages and current for arc burning at 1 bar nitrogen with the heating volume are shown in Fig. 3. In this case, the current was interrupted successfully at the first CZ. The voltage peak around 0.4 ms marks the melting of the copper wire and the initiation of the arc. Before the initiation of the arc, the voltage measured from HV probe 2, and 3 may give an erroneous result as the tungsten wire connected to probes may or may not have touched the copper wire before melting. Near current zero, due to the different frequency response of the voltage probes the measurements from HV probe 2, and 3 are not trusted. The arc voltage distribution analysis in this paper only considers from 1 ms to 50 microseconds before CZ. The voltage drop in section 1 is calculated as the difference in measured voltages of HV probe 1 and 2, section 2 as the difference between HV probe 2 and 3, and section 3 as the measured voltages in HV probe 3.

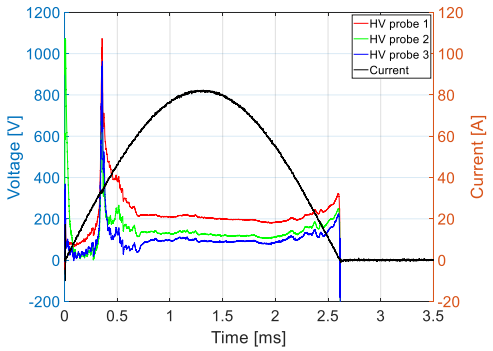

Fig. 3. Measured voltages in three probes and measured current for arc burning in PTFE tube with the heating volume at 1 bar nitrogen.

3.1 Without Heating Volume

The voltage distribution across three sections of the arc together with the total arc voltage for the cases without a heating volume at three different filling pressures are presented in Fig. 4. It can be seen that the total arc voltage increases from approximately 200 V for arc burning in 1 bar to approximately 550 V and 750 V at the current peak (at 1.3 ms) for arc burning in 20 bar and 40 bar filling pressures respectively. Due to the fixed pin electrode inside the PTFE tube, the stagnation point is near the pin electrode. As there is no heating volume attached, the ablated PTFE vapor leaves the tube without any backflow. At 1 bar more or less homogenous voltage distribution is observed across three sections (section 2 is half the length of section 1 and 3). Approximately 55% of the total voltage drops are measured across section 2 and section 3 at

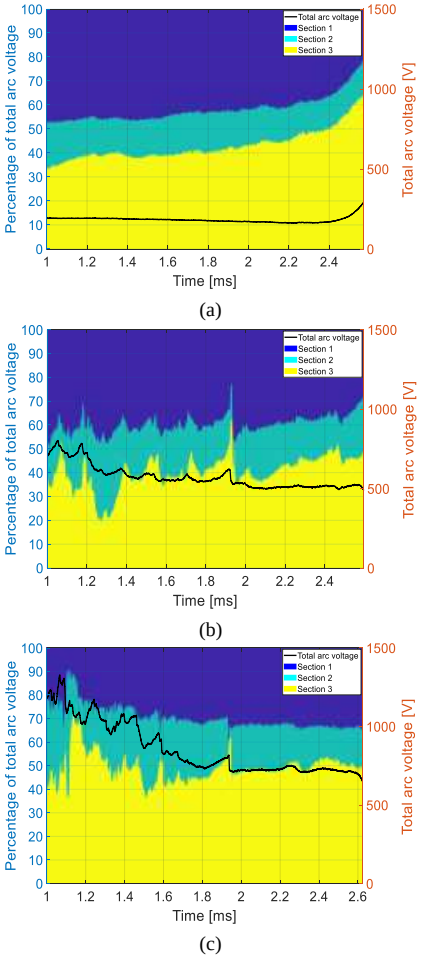

Fig. 4. Arc voltage distribution across three sections of the arc for the cases without heating volume. (a) 1 bar. (b) 20 bar. (c) 40 bar.

the current peak for arc burning in 1 bar filling pressure. At 20 and 40 bar filling pressure, the voltage drop across section 2 and 3 corresponds to approximately 60% and 75% respectively during current peak. With the increase of filling pressure, the voltage drop across section 2 increases slightly. At 20 bar and 40 bar filling pressures, the measured voltages show fluctuations compared to atmospheric pressure arc.

3.2 With Heating Volume

The voltage distribution across three sections of the arc together with the measured arc voltage for the cases with a heating volume attached to the ring electrode at three different filling pressures are presented in Fig. 5. At atmospheric pressure in Fig. 5 (a), the voltage drop across section 2 and 3 increases to approximately 60% compared to 55%

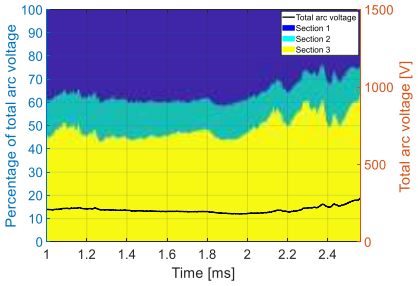

(a)

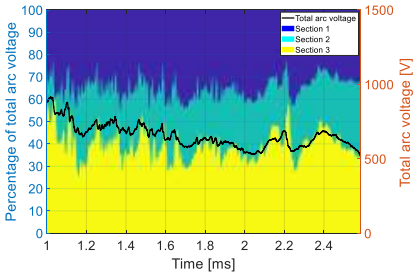

(b)

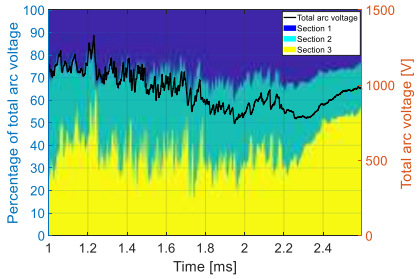

(c)

Fig. 5. Arc voltage distribution across three sections of the arc for the cases with heating volume. (a) 1 bar. (b) 20 bar. (c) 40 bar.

in Fig. 4 (a). At 20 and 40 bar filling pressures, the voltage drop across section 2 and 3 are approximately 65% and 75% respectively. However, the voltage distribution across section 2 at 20 bar filling pressure are comparable and at 40 bar are higher than the drop in section 1 and 3 although section 2 is half the length of section 1 and 3. The total arc voltages are also observed to increase with the attachment of heating volume at all three filling pressures compared to without any heating volume. The total arc voltage at 20 and 40 bar with a heating volume show more fluctuations compared to without a heating volume.

3.3 Pressure Rise in Heating Volume

The pressure rise in the heating volume for arc burning at three different filling pressures is plotted in Fig. 6. The pressure rise in the heating volume increases to 5 bar and 8 bar when burning at 20 and 40 bar filling pressures respectively compared to an increase of 1 bar at atmospheric pressure arc. The increase in pressure rise is in line with the energy dissipation in the arc at different filling pressures respectively. Fig. 6 shows that at 20 and 40 bar filling pressure the pressure rise goes to a negative value at approximately 1.5 ms, which is probably due to cold gas intake through the vent to the heating volume.

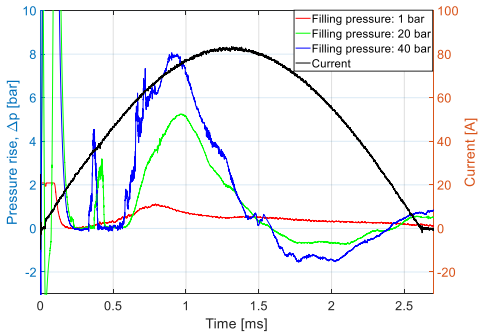

Fig. 6. Pressure rise in the heating volume for three different filling pressures.

The increased gas flow due to the presence of the heating volume at 20 and 40 bar filling pressures can be responsible for the relatively high voltage drop near the vent. It is observed that at a high filling pressure, the arc voltage shows unsteady nature by fluctuations in the measured arc voltage. Erratic gas flow can cause turbulence near the arc boundary which can explain the fluctuations in the arc voltage [7].

4 CONCLUSIONS

The arc voltage distribution for arc burning inside 4 mm diameter PTFE tube between a fixed inter-electrode gap of 50 mm at three different filling pressures (1 bar, 20 bar,

and 40 bar) of nitrogen are reported in this paper. For that purpose, a direct measurement of voltage drop at three axial positions of the arc is independently conducted. For some of the cases, a heating volume is attached to the ring electrodes. For the cases with a heating volume, the pressure rise in the heating volume is also measured.

It has been observed that without a heating volume as the ablated gas axially leaves the PTFE tube, the axial voltage distribution in the arc is more or less homogenous. At a high filling pressure, the pressure rise in the heating volume increases due to increased energy dissipation at high filling pressures. The presence of heating volume forces gas flow outwards or inwards through the vent, depending on the pressure on the heating volume. This flow of relatively cool gas near the vent causes significantly high voltage drop near the vent at a high gas filling pressure.

Acknowledgement

This work is supported by the Norwegian Research Council.

References

1. J. L. Sengers, G. Morrison, G. Nielson, R. Chang, and C. Everhart, "Thermodynamic behavior of supercritical fluid mixtures," *International Journal of Thermophysics*, vol. 7, no. 2, pp. 231-243, 1986.
2. J. Zhang, A. Markosyan, M. Seeger, E. van Veldhuizen, E. van Heesch, and U. Ebert, "Numerical and experimental investigation of dielectric recovery in supercritical N_2," *Plasma Sources Science and Technology*, vol. 24, no. 2, p. 025008, 2015.
3. F. Abid, K. Niayesh, E. Jonsson, N. S. Støa-Aanensen, and M. Runde, "Arc Voltage Characteristics in Ultrahigh-Pressure Nitrogen Including Supercritical Region," *IEEE Transactions on Plasma Science*, vol. 46, no. 1, pp. 187-193, 2018.
4. F. Abid, K. Niayesh, E. Jonsson, N. S. Støa-Aanensen, and M. Runde, "Arc Voltage Measurements Of Ultrahigh Pressure Nitrogen Arcs In Cylindrical Tubes," presented at the 22nd International Conference on Gas Discharges and their Applications, Novi Sad, Serbia, 2-7 September, 2018.
5. F. Abid, K. Niayesh, and N. Støa-Aanensen, "Ultrahigh-Pressure Nitrogen Arcs Burning inside Cylindrical Tubes," *IEEE Transactions on Plasma Science*, vol. 47, no. 1, pp. 754-761, Jan. 2019.
6. H. Taxt, T. R. Settendal, and K. Niayesh, "Arc voltage distribution measurement in a medium voltage ablation-dominated switch," in *22 nd International conference on Gas discharge and their applications*, Novi Sad, Serbia, 2018.
7. A. Howatson and D. J. J. o. P. D. A. P. Topham, "The instability of electric arcs burning axially in accelerated flow," vol. 9, no. 7, p. 1101, 1976.

Paper VIII

Paper IX

Post-arc Dielectric Recovery Characteristics of Free-burning Ultrahigh-Pressure Nitrogen Arc

F. Abid[1]*, K. Niayesh[1], and N. Støa-Aanensen[2]

[1] Norwegian University of Science and Technology, Trondheim, Norway
[2] SINTEF Energy Research, Trondheim, Norway
* fahim.abid@ntnu.no

***Abstract*—This work contributes to the fundamental understanding of post-arc dielectric recovery characteristics of free-burning nitrogen arcs as a function of gas filling pressure. Arc peak current of 425 A at a frequency of 925 Hz is used throughout the experiment. The arc burns freely between two fixed electrodes without any forced gas flow. Three different filling pressures are investigated: 1 bar (atmospheric pressure), 20 bar, and 40 bar, the latter being in the supercritical region. To investigate the effect of inter-electrode gap on the recovery process, two different gap distances are used: 20 mm and 50 mm. A 10 kV high voltage pulse with a rate of rise of 150 V/µs is applied across the electrodes after current zero. To evaluate the recovery process, the time between current zero and the start of the pulse is varied from 10 µs to 10 ms. Experimental results show that the dielectric recovery performance improves with the filling pressure even in the absence of a forced gas flow. The breakdown strength is observed to recover faster for a longer electrode gap.**

I. Introduction

Nitrogen undergoes phase transition to a supercritical state (SC) above a critical pressure (33.5 bar) and a critical temperature (126 K). An SC fluid exhibits properties of both the liquid (high dielectric strength, high heat capacity) and the gaseous phase (self-healing, no vapor bubbles). Current interruption medium in power switching devices must hold a specific set of properties; such as high insulation strength during off time, low resistance during on time, fast recovery after switching, long lifetime etc. For gas circuit breakers, the properties of SC fluids are believed to enhance the current interruption performance [1], [2].

At present, the gas circuit breakers are filled at the atmospheric pressure or slightly elevated pressure. It is well known that the dielectric strength is high at high filling pressures. Nonetheless, there are few publications reported on gas discharge at extremely high filling pressure and in supercritical region. Among the published works, none of them covers high energy arc discharges typical for power switching applications [1], [2]. Recently, some efforts have been made to investigate arc discharges in SC N_2 at tens of bars filling pressure. Nitrogen is chosen due to its environmentally benign nature, good insulation strength and low critical pressure. It has been reported that the free-burning arc voltage increases with filling pressure of nitrogen, without any abrupt change during the transition from gas to SC state [3], [4]. A higher arc voltage results in a higher energy deposition in the arc channel.

Current interruption can be described as a race between the cooling of the arcing channel and the voltage that builds up across the contacts [5]. To have a successful current interruption, the dielectric strength between the electrodes should be higher than the transient recovery voltage stress imposed by the network. Hence, the post-arc dielectric recovery characteristics of the arcing medium is of importance. To the knowledge of the authors, no work has been reported on the post-arc dielectric recovery characteristics of supercritical nitrogen for switchgear applications.

This study focuses on the influence of filling pressure on the dielectric recovery characteristics of free-burning nitrogen arcs in a fixed electrode arrangement. Three different filling pressures are investigated in this study: 1 bar (atmospheric pressure), 20 bar, and 40 bar (supercritical region). To evaluate the recovery of dielectric strength as a function of time, a 10 kV high voltage (HV) pulse with a rise time of approximately 70 µs is applied across the electrodes after CZ. The time between CZ and the pulse is varied from 10 µs to 10 ms. Finally, to investigate the effect of inter-electrode gap on the recovery process, the gap distance between the electrodes is varied. The breakdown voltage as a function of time after current zero crossing is reported to evaluate the dielectric recovery characteristics of the arc channel at different filling pressures.

II. Experiment Setup

The test circuit is shown schematically in Fig. 1. It consists of a charging and a discharging section of a 4.8 µF high voltage (HV) capacitor bank, *C*. The capacitor, *C* is charged from the HV source and through the diode-resistor unit (R_C-D_C). Once the capacitor, *C* is fully charged to a predefined charging voltage, the switch S_C is opened to disconnect the rest of the circuit from the grid. The inductance, *L*, is chosen in such a way that a fixed current amplitude of 425 A at a frequency of 925 Hz can be generated. Once the triggered vacuum switch (*TVS*) is closed, the current flows through the inductor and further through a copper ignition wire (40 µm diameter) inside the arcing chamber. After the current starts flowing, the ignition wire melts due to adiabatic heating and an arc is initiated. The arc burns freely between the electrodes without any forced N_2 flow.

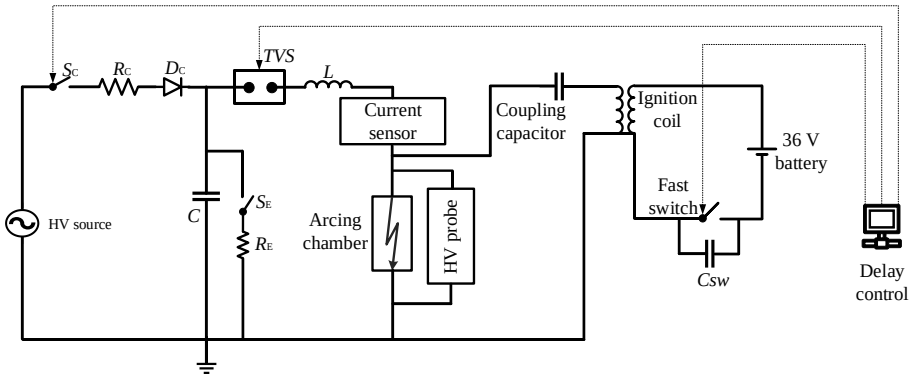

Fig. 1. Test circuit.

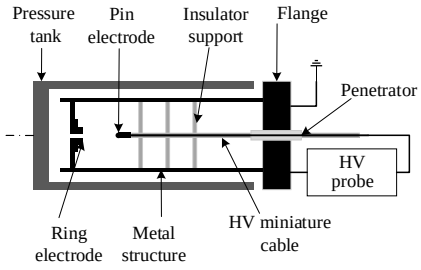

Fig.2. Interior connection of the pressure tank.

The arc current continues to flow until current zero crossing (CZ), when the TVS interrupts the current. A 10 kV high voltage (HV) pulse is applied between the arcing electrodes after a predefined time delay. The HV pulse is generated from a car ignition coil by opening the current flowing through its primary windings. A coupling capacitor is connected between the high current circuit and the ignition coil. The time delay of the pulse after CZ can be precisely controlled in the order of few microseconds by a computer-controlled synchronization unit. In this paper, the time between CZ and the start of the HV pulse is varied from 10 µs to 10 ms. When the dielectric strength of the electrode gap is not high enough to withstand the HV pulse, a breakdown occurs, marked by a collapse of the applied pulse voltage.

A pressure tank of 15.7-liters rated for 500 bars, shown schematically in Fig. 2 is used as arcing chamber. A 24 kV HV cable is fed through the flange of the pressure tank. The HV cable is terminated to the pin electrode, and held in position inside the pressure tank by insulators. The experimental setup is put inside an explosion-safe room. All the operations are controlled from a separate room located at a safe distance.

A high voltage (HV) probe is used to measure the arc voltage and voltage pulse after CZ across the electrodes. The HV probe is connected outside the pressure tank. A shunt resistor is used to measure the arc current. The current sensor is connected on the high voltage side of the arcing chamber on a floating potential. All the data are sent to the control room via optical fiber and stored in a digital oscilloscope for further analysis.

III. Experimental Results and Discussions

A typical measurement of the arc voltage, arc current and the HV pulse after CZ at 1 bar filling pressure is shown in Fig. 3. The initial voltage peak at approximately 0.5 ms before CZ marks the melting of the ignition wire and initiation of the arc. The current continues to flow until CZ, where the TVS interrupts the current. Just after the CZ, the temperature of the arc channel is still high. As a result, some of the charged carriers are present between the arcing contacts. When a HV pulse is applied between the contacts, a breakdown may occur.

Two different cases, with one breakdown and one without breakdown, are shown in Fig. 3. The red line represents a test where the HV pulse was applied approximately 700 µs after CZ, resulting in a breakdown. The breakdown is recognized by a voltage collapse at 7.8 kV. The test without a breakdown (pulse applied at 2 ms after CZ) shows the full HV pulse and following oscillations from the ignition coil (green line). For the cases where a breakdown occurred, the value of the breakdown voltage is considered for further analysis. For the cases without having a breakdown due to the pulse, it

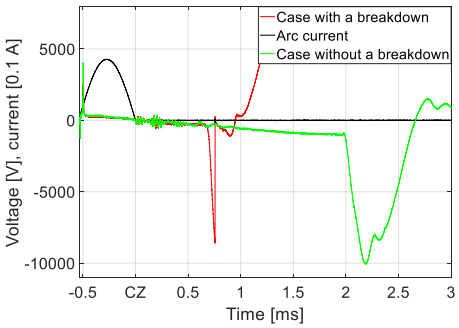

Fig. 3. Typical measurement showing a case of a breakdown (red line) and a case of not breakdown (hold) occurs (green line).

is termed as a hold voltage. Due to the stray capacitance in the setup, there are voltage oscillations with a voltage peak of approximately 400 V just after CZ, which are not part of the applied HV pulse. The rate of rise of these voltage oscillations are 125 V/µs, which is comparable to the rate of rise of 10 kV HV pulse. When the breakdown strength of the medium is less than the voltage oscillations then breakdown occurs. In this paper the breakdown caused by the voltage oscillations are also considered to evaluate the recovery characteristics.

A. Effect of filling pressure

The effect of gas filling pressure on the dielectric recovery performance of free-burning nitrogen arcs is illustrated in Fig. 4. The filled markers indicate a not breakdown (hold voltage) due to the HV pulse, while the empty markers indicate the breakdown voltage. At 1 bar filling pressure and 50 mm gap distance, the withstand voltage is approximately 330 V from 10 µs up to approximately 400 µs after CZ. After 400 µs, the gap gradually recovers its dielectric strength, which can be seen by the increase of the breakdown voltage for pulses starting later than 500 µs. After approximately 2 ms, no breakdowns were observed for the applied pulse at 1 bar gas pressure.

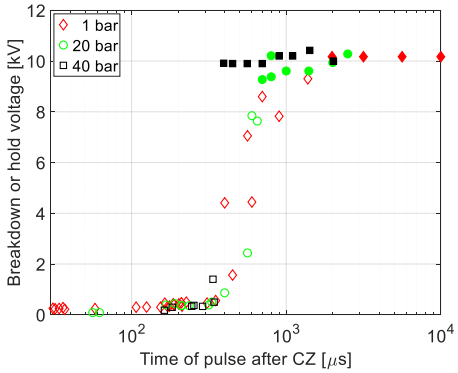

Fig. 4. Breakdown or hold voltage as a function of time to pulse after CZ for 50 mm inter-electrode gap distance. The filled marker represents the withstand voltage whereas the empty marker represents the breakdown voltage.

For 20 bar and 40 bar at an inter-electrode gap of 50 mm, the breakdown voltage after CZ from 10 µs to approximately 300 µs is approximately 100 V, which is low compared to 1 bar filling pressure during that time. However, after 300 µs the gap recovery process was observed to be faster as the filling pressure increases. Compared to the case with 1 bar filling pressure; no breakdowns occurred for 50 mm gap distance for pulses after 800 µs and 400 µs for 20 bar and 40 bar filling pressures, respectively.

B. Inter-electrode gap

To investigate the effect of inter-electrode gap distance on the recovery process, similar experiments were conducted at a gap distance of 20 mm at two different

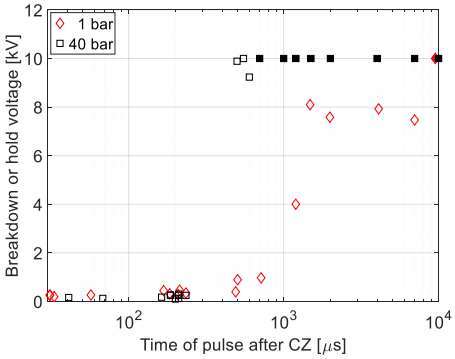

Fig. 5. Breakdown or hold voltage as a function of time to pulse after CZ at an interelectrode gap of 20 mm. The filled marker represents the hold voltage whereas the empty marker represents the breakdown voltage.

filling pressures: 1 bar and 40 bar. The breakdown or hold voltage as a function of the time of the start of the pulse after CZ are plotted in Fig. 5. The observed trend of a faster recovery of the post-arc channel for 40 bar in contrast to 1 bar filling pressure is also observed at 20 mm gap distance. When compared between the two inter-electrode gap distances, it is observed that the smaller gap distance takes longer time to recover, see Fig. 4 and Fig. 5. For 1 bar at 50 mm gap distance, no breakdown is observed when a pulse is applied after 2 ms of CZ. However, when the gap distance is 20 mm, the gap recovers slowly, resulting in a minimum time to hold the pulse at 10 ms. At 40 bar, the minimum time after CZ for having a not breakdown (hold) of the pulse is 400 µs and 700 µs for 50 mm and 20 mm, respectively.

C. Discussions

The post arc dielectric recovery performance of free-burning nitrogen arc indicates that after a certain time (several hundreds of microsecond) the recovery performance improves with the filling pressure. However, just after CZ, the breakdown voltage measured for high filling pressure arcs is lower than that for the atmospheric pressure arcs. Thermal interruption performances of the free-burning nitrogen arc also show a reduced breakdown voltage for high filling pressure (i.e., 20 bar, 40 bar) in comparison to atmospheric pressure. When the filling pressure is high, the energy deposition in the arc channel also increases because of increased arcing voltage. The arc at high filling pressure gets constricted due to the filling pressure and the temperature of the arc core increases as a result. In free burning arc, in the absence of forced cooling, the arc core fails to dissipate the stored thermal energy. As a result, the breakdown voltage just after CZ is found to be low at high filling pressure in comparison to atmospheric pressure. The time just after CZ is hence very crucial for free-burning arc at an extremely high filling pressure.

For power switching applications, to cool the arc effectively near CZ, some sort of forced gas flow is applied as a form of puffer or self-blast principle. A forced gas flow at a high filling pressure can increase the mass flow

rate and hence, the cooling can be enhanced. But as was seen, increasing the distance did not lead to significant changes in the recovery rate (up to 10 kV, at least). The difference was much greater for 1 bar, which indicates that faster moving contacts are perhaps more important at low pressures. As the dielectric recovery characteristic improves at a high filling pressure, with forced cooling and moving contact arrangement, the ultrahigh-pressure nitrogen has the potential to be used as a current interrupting medium.

IV. Conclusions

The post-arc dielectric recovery performance of free-burning nitrogen arcs as a function of filling pressure is reported in this paper. A 10 kV HV pulse is applied with a controlled time delay after CZ. Based on the experimental investigations, the following conclusions have been drawn:

- The dielectric recovery performance of free-burning arcs improves with the filling pressure, and a faster dielectric recovery is observed as the filling pressure is increased. However, just after CZ (in the thermal phase) the withstand voltage is lower for higher filling pressures.
- As the inter-electrode gap distance is decreased, the recovery process takes more time, as expected.

Acknowledgment

This work is supported by the Research Council of Norway, Project number 280539.

References

[1] Z. Yang, S. Hosseini, T. Kiyan, S. Gnapowski, and H. Akiyama, "Post-Breakdown Dielectric Recovery Characteristics Of High-Pressure Liquid CO_2 Including Supercritical Phase," *IEEE Transactions on Dielectrics and Electrical Insulation*, vol. 21, no. 3, pp. 1089-1094, 2014.

[2] J. Zhang, A. Markosyan, M. Seeger, E. van Veldhuizen, E. van Heesch, and U. Ebert, "Numerical and experimental investigation of dielectric recovery in supercritical N_2," *Plasma Sources Science and Technology*, vol. 24, no. 2, p. 025008, 2015.

[3] F. Abid, K. Niayesh, E. Jonsson, N. S. Støa-Aanensen, and M. Runde, "Arc Voltage Characteristics in Ultrahigh-Pressure Nitrogen Including Supercritical Region," *IEEE Transactions on Plasma Science*, vol. 46, no. 1, pp. 187-193, 2018.

[4] F. Abid, K. Niayesh, E. Jonsson, N. S. Støa-Aanensen, and M. Runde, "Arc Voltage Measurements Of Ultrahigh Pressure Nitrogen Arcs In Cylindrical Tubes," presented at the 22nd International Conference on Gas Discharges and their Applications, Novi Sad, Serbia, 2-7 September, 2018.

[5] K. Niayesh and M. Runde, *Power Switching Components*. Springer, 2017.

5. Summary of the Results and Conclusions

Papers I, II and VIII deal with the ultrahigh-pressure N_2 arc characteristics during the high-current phase. The thermal phase of the arc is presented in Papers III, IV, VI and VII. Finally, the findings from the post-arc dielectric recovery characteristics of the ultrahigh-pressure N_2 arc are presented in Papers V and IX. The summary of the main findings at different phases of the ultrahigh-pressure N_2 arc is presented here.

5.1 High-current Phase

The free-burning arc voltage as a function of the filling pressure for the 20 mm interelectrode gap is shown in Fig. 5.1. Each point represents the arc voltage at the current peak of 150 A, for a half cycle duration of 1.43 ms. The arc voltage increases from about 60–65 V at 1 bar to approximately 450 V at 98 bar. The gas enters into the SC state at 33.5 bar. The arc voltage is observed to increase with the filling pressure without any abrupt change during the transition from gas to SC state.

As the filling pressure is increased, the arc radius reduces resulting in an

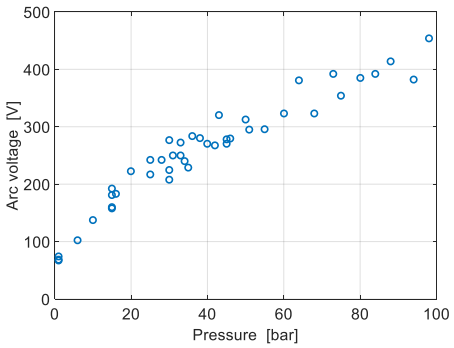

Fig. 5.1. Arc voltage for arc current of 150 A, for half cycle current duration of 1.43 ms, at 20 mm inter-electrode gap for different filling pressures.

increased current density. Constriction of the arc due to high pressure contributes significantly to the rise of the arc voltage. Due to scarcity of high-pressure material data for N_2 at high temperature, thermodynamic and transport properties of high-pressure air are analysed. The physical properties of air (which consists of approximately 80% N_2) do not change abruptly near the arc temperature and critical pressure of N_2 [43], [44]. As the arc properties are dictated by the physical properties of the arc temperature and pressure and

not the room temperature, no abrupt change in the arc voltage is observed when the gas to SC transition happens.

In contrast to the free-burning arc, when the arc burns inside a tube, depending on the diameter of the tube and the nitrogen filling pressure, the arc gets constricted. The arc voltage is depicted as a function of the inner diameter of the tube for different filling pressures in Fig. 5.2, together with the free-burning arc. As the inner diameter decreases, a gradual increase of the arc voltage is observed for both alumina and PTFE tubes at 1 bar. As the N_2 filling pressure is increased, the arc voltage also increases, as expected. The arc voltages measured for arcs burning inside 15 mm wide tubes are similar to those of corresponding free-burning arcs. The variation in arc voltage for a given case seems to somewhat increase with increasing pressure and decreasing diameter, although the data is limited. The arc voltage dependency on the tube material is not strong at 20, 40 and 80 bar N_2 filling pressures. At a filling pressure of 20 bar, the arc voltage (approximately 300 V) seems to be more or less independent of both tube inner diameter and tube material. At 40 and 80 bar N_2, the maximum arc voltage is observed not for the smallest inner diameter of the tubes, but rather for 4 mm or 8 mm tube inner diameters.

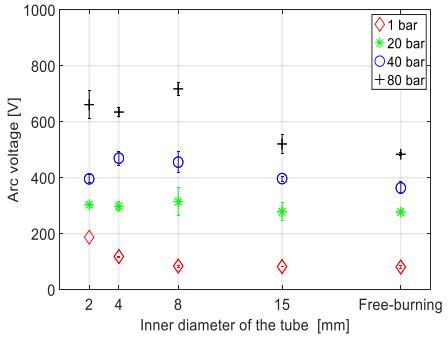

(a)

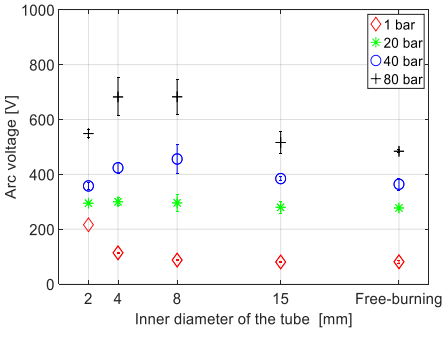

(b)

Fig. 5.2, Arc voltages at the current peak of 150 A at 350 Hz as a function of inner diameters of the tubes at different filling pressures. (a) Alumina. (b) PTFE.

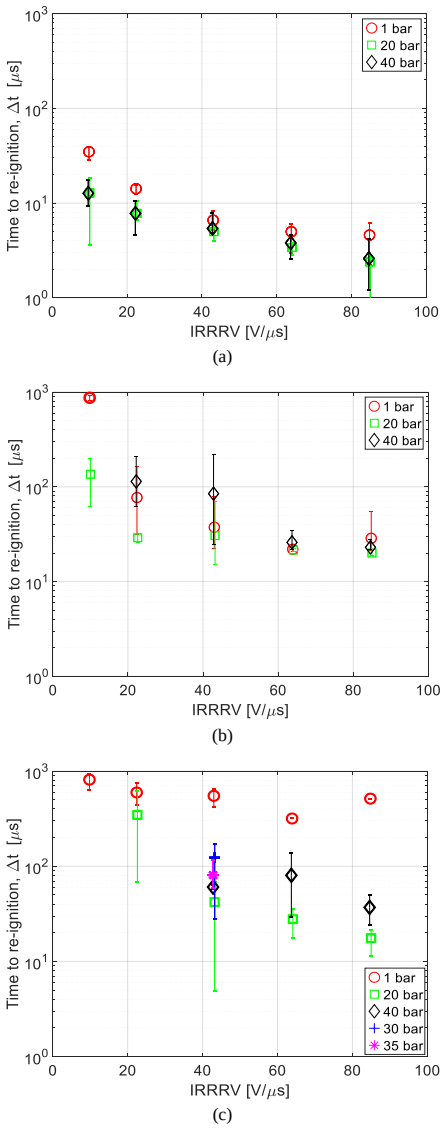

Fig. 5.3. Re-ignition time as a function of IRRRV for different filling pressures and at different electrode and nozzle configurations for arc current of 130 A. (a) Free-burning arc. (b) Tube constricted arc. (c) Self-blast arrangement.

Due to the physical constriction, the arc voltage increases as the tube diameter is reduced, as can be seen for 1 bar filling pressure case, see Fig. 5.2. As the arc radius decreases with the filling pressure, the interaction of the arc with the tube is limited. Moreover, the absorption of radiation at high filling pressures is high. As a result, the effect of tube constriction at a higher filling pressure is less obvious compared to the 1 bar case.

5.2 Thermal Interruption Performance

The investigation was later focused on the behaviour near CZ and the thermal interruption performance of the ultrahigh-pressure N_2 arc was studied. As the IRRRV is increased, the remaining charge carriers are accelerated faster, which would result in earlier re-ignition, as can be seen in Fig. 5.3. A higher filling pressure, however, increases the energy deposition in the arc as a result of high arcing voltage. The arc at high filling pressure gets constricted due to the filling pressure, and the temperature of the arc core consequently increases. In the free-burning arc, in the absence of forced cooling, the arc core fails to dissipate the stored thermal energy quickly. As a result, a relatively high post-arc current is observed for the arc burning at a high N_2 filling pressure. It turns out that without the forced gas flow the thermal interruption performance at higher filling pressure is worse than at atmospheric pressure, see Fig. 5.3(a). The time to re-ignition decreases in the free-burning arrangement at a higher filling pressure. No successful current interruption was observed for the free-burning arc at any of the IRRRVs investigated.

When the arc burns inside the PTFE tube, the flow stagnation point lies near to the pin electrode, as the pin electrode blocks any gas flow out. When the arc burns inside a tube, the average time to re-ignition increases at all IRRRVs compared to the free-burning arc, see Fig. 5.3(b). The PTFE ablates when the arc burns inside the PTFE tube. It has been reported that even after the arc is extinguished, the nozzle continues to ablate for a few milliseconds after CZ [45]. The PTFE vapour cools the arc, which may contribute to the longer time to re-ignition than when the arc burns inside the tube, in comparison to the free-burning arc. For the lowest IRRRV, some successful current interruptions are observed when the arc burns inside the tube, see Table 5.1.

The self-blast arrangement shows the best interruption performance among the three different arrangements investigated, see Table 5.1. The interruption performance improves at high filling pressure when the IRRRV is lowest in the self-blast arrangement. As the filling pressure increases, the density of the

Table 5.1. Number of successful current interruptions compared to the number of tests conducted at different IRRRVs for different filling pressures and test arrangements.

Test arrangement	**Filling Pressure [bar]**	**Number of successful interruptions / the number of tests conducted for arc current of 130 A**				
		IRRRV 9.8 V/µs	**IRRRV 22.4 V/µs**	**IRRRV 43 V/µs**	**IRRRV 63.9 V/µs**	**IRRRV 84.8 V/µs**
Free burning	1	0/10	0/5	0/5	0/5	0/5
	20	0/10	0/5	0/5	0/5	0/5
	40	0/10	0/5	0/5	0/5	0/5
Tube constricted	1	5/10	0/5	0/5	0/5	0/5
	20	0/10	0/5	0/5	0/5	0/5
	40	10/10	0/5	0/5	0/5	0/5
Self-blast (with heating volume)	1	3/5	2/5	6/10	3/5	2/5
	20	5/5	1/5	1/10	1/5	1/5
	40	5/5	5/5	6/10	2/5	2/5
	30	-	-	5/10	-	-
	35	-	-	5/10	-	-

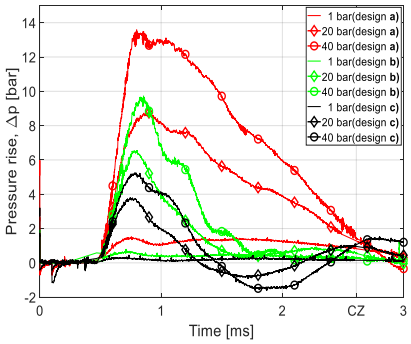

Fig. 5.4. Pressure rise in heating volume at different filling pressures for different vent designs. Design **a** (2 opposite holes of 2 mm diameter), design **b** (2 opposite holes of 3 mm diameter), and design **c** (4 opposite holes of 3 mm diameter) for an arc current of 130 A.

gas also increases. Under a forced gas flow, due to the high density, the cooling is enhanced at a high filling pressure. As a result, the post-arc current recorded is low, and the interruption performance improves in the self-blast arrangement at lower IRRRV settings. However, when the IRRRV is high the post-arc current again increases rapidly, which may initiate a thermal re-ignition. No significant change in the interruption performance and the time to re-ignition is observed between the subcritical (30 bar) or supercritical (35 bar) phase of N_2, as can be seen in Fig. 5.3(c).

In the case of a self-blast arrangement, the pressure rise in the heating volume increases as the filling pressure is increased, as shown in Fig. 5.4. The high density of the gas at a higher filling pressure together with the ablated mass from the PTFE tube are responsible for the pressure rise in the heating volume. The pressure in the heating volume, however, is heavily dependent on the design (corresponding to different vent sizes), as expected. Most of the ablated material leaves through a bigger vent (design ***c***) compared to a smaller vent (design ***a***), resulting in a lower pressure rise in the heating volume in design ***c***, see Fig. 5.4. Furthermore, a high filling pressure also increases the viscosity. As a result, designs suitable for 1 bar may become inappropriate for a high filling pressure.

5.3 Post-arc Dielectric Recovery Characteristics

After investigating the thermal interruption performance, the post-arc dielectric recovery characteristics are studied. The breakdown or hold voltage at different N_2 filling pressures at different instants after CZ are shown in Fig. 5.5. The filled markers indicate a hold voltage (not breakdown) during the HV pulse, while the empty markers indicate the breakdown voltage. At 1 bar filling pressure and 50 mm gap distance, the breakdown voltage is approximately constant at 330 V from 10 µs up to approximately 300 µs after CZ. After 300 µs, the gap gradually recovers its dielectric strength, which can be seen by the increase of the breakdown voltage for pulses starting later than 300 µs. After approximately 2 ms, no breakdowns were observed for the applied pulse at 1 bar gas pressure.

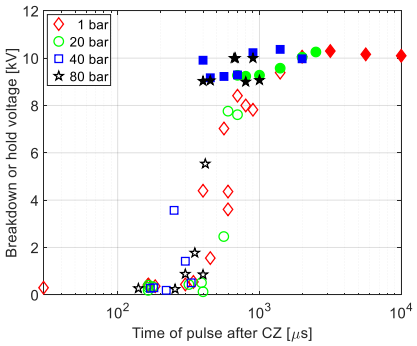

Fig. 5.5. Breakdown or hold voltage as a function of time to pulse after CZ for 50 mm inter-electrode gap distance. The filled markers represent withstand voltages whereas the empty markers represent breakdown voltages.

For 20 bar, 40 bar and 80 bar filling pressure and an interelectrode gap of 50 mm, the breakdown voltage after CZ from 10 µs to 300 µs is approximately 100 V, which is low compared to 1 bar filling pressure during that time. However, after 300 µs the dielectric strength was observed to increase at a faster rate as the filling pressure increases. Compared to the case with 1 bar filling pressure, no breakdowns occurred for pulses after 800 µs and 400 µs for 20 bar and 40 bar filling pressures, respectively.

In the free-burning arrangement, from just after CZ until several hundred microseconds, the breakdown voltage is observed to be the same for all filling pressures. What occurs during this early recovery period will depend on several conditions. Because of the residual plasma and space charges present, the application of voltage to the gap will involve the formation of a positive ion space charge layer adjacent to the pulse cathode. This occurs almost instantaneously due to the high mobility of electrons, and is followed by a general drift of charge in the gap in response to the applied voltage. As a result, the breakdown voltage just after CZ at atmospheric pressure is reported to be close to the glow cathode-fall voltage [46]. Although no experimental data are found for glow cathode-fall voltage at an extremely high filling pressure, an increase in the cathode-fall voltage is observed as the pressure is reduced [47]. More importantly, the high post-arc current observed at a high filling pressure may facilitate the glow to arc transition at high N_2 pressure, which would reduce the cathode fall-voltage [48]. A similar reduction in the re-ignition voltage for the free-burning arc at high N_2 pressure is also observed when the thermal interruption performance is studied.

For the free-burning arrangement, as the filling pressure increases, the breakdown voltage increases at a faster rate (after the critical time of approximately 300 µs after CZ). This critical time is probably linked to the temperature of the gap being close to the ionisation temperature of N_2. Once the temperature of the gap falls below a certain level, the breakdown voltage will rapidly increase with the increase of the filling pressure, which is also observed in this thesis. This fast increase in the breakdown voltage at higher pressures is also reported elsewhere [49].

In the free-burning arc arrangement, where natural convection is the dominant cooling mechanism after CZ, the resulting cooling of the electrode gap is not efficient. To increase the cooling of the gap, the forced convective cooling is adopted using two arrangements: a self-blast and a puffer type. As the cooling of the medium is enhanced, the recombination rate of the charge carriers after the extinction of the arc increases. As a result, the dielectric strength of the gap just after CZ is high, and no breakdown is observed for either the self-blast or the puffer setup. No strong dependence of the SC state on post-arc dielectric recovery characteristics is observed. The forced gas flow significantly enhances the dielectric recovery of the arc channel at high filling pressures, which is also the case in the thermal phase.

5.4 Conclusions

Experimental investigation of the arc properties at extremely high N_2 filling pressure and in the supercritical state has been undertaken. The investigated arc current amplitude was varied from 85 A to 450 A at a frequency of 190 Hz to 950 Hz. To categorically study the different phases of the ultrahigh-pressure N_2 arc, the focus of this thesis is split into three distinct parts: the high-current phase, the thermal phase and the dielectric phase. Based on the experimental results the following conclusions have been drawn:

- The arc voltage increases with N_2 filling pressure without any abrupt change during the transition from gas to the supercritical state. The arc duration dependence on the arc voltage is not significant for current durations of 0.59–2.17 ms for the tested filling pressures up to 45 bar. The current dependence of the arc voltage is not significant for currents of 150–450 A for the tested filling pressures up to 45 bar.

- At atmospheric pressure, the arc voltage increases with decreasing inner diameter of the tube, as expected. The measured arc voltage at high filling pressures inside a tube does not have a simple relationship with the inner diameter of the tube. The optical micrographs show reduced ablation traces in a 4-mm-wide tube at 80 bar, compared to the 1-bar ambient pressure arcs. The increase in the absorption of radiation by the gas surrounding the arc core at very high-pressure may reduce the ablation. Moreover, the constriction of the arc channel due to the filling pressure limits the interaction of the arc core with the tube.

- In a free-burning arrangement the time to re-ignition reduces as the filling pressure increases, and a lower re-ignition voltage is observed at high filling pressures (i.e. 20 bar and 40 bar) compared to atmospheric pressure. In the absence of forced cooling, the post-arc current increases at higher filling pressures (i.e. 20 bar and 40 bar) compared to atmospheric pressure, which leads to thermal re-ignition. The thermal interruption performance of free-burning arcs worsens at high nitrogen filling pressures compared to atmospheric pressure arcs. Forced gas flow, however, improves interruption performance at all filling pressures. For tube-constricted and self-blast arrangements, current interruption performance at 20 bar is observed to be worse than that at 1 bar, whereas 40 bar shows the best

performance. The temperature-dependent thermal conductivity at different filling pressures may affect the current interruption performance. A shift in the arc temperature near CZ due to the filling pressure may result in poor cooling if the thermal conductivity is low at the arc temperature. Among the failed interruptions, thermal re-ignition is observed to be the dominant failure mechanism at high filling pressures. No obvious improvement in interruption performance is observed when N_2 enters the supercritical region.

- Without a heating volume as the ablated gas axially leaves the PTFE tube, the axial voltage distribution in the arc is found to be more or less homogenous. The heating volume forces a gas flow outward or inwards through the vent, depending on the pressure of the heating volume. This flow of relatively cool gas causes a significantly high voltage drop near the vent at a high filling pressure.

- The pressure rise in the heating volume increases with the filling pressure. The outlet vent dimension plays a decisive role in both the pressure rise in the heating volume and the back-flow near CZ. With proper designing, the interruption performance can be improved for ultrahigh-pressure N_2 arcs. Total nozzle mass loss is found to increase with the filling pressure. A high filling pressure also constitutes high energy deposition in the arc, as a result of high arcing voltage. Nevertheless, the mass loss per unit energy deposition in the arc is found to be less dependent on filling pressures.

- In the free-burning arrangement, in the absence of forced gas flow the dielectric strength of the contact gap recovers faster with the increase of the filling pressure. However, just after CZ (in the thermal phase), the breakdown voltage is low for higher filling pressures. As the interelectrode gap distance is reduced, the recovery process takes a longer time. No strong current dependency of the post-arc dielectric recovery has been observed in the investigated current range.

- Forced gas flow significantly enhances the dielectric recovery of the arc channel at a high filling pressure, which is also the case in the thermal phase. No breakdown is observed, even immediately after CZ, under forced gas flow conditions for the applied currents and voltage pulses.

Although the thermal phase is the critical phase of the ultrahigh-pressure N_2 current interruption, the dielectric behaviour is inherently superior at a high filling pressure even in the absence of forced cooling. A forced gas flow, however, also improves performance during the thermal phase, which shows the potential of ultrahigh-pressure N_2 to be used as a subsea current interruption medium.

5.5 Suggestions for Future Work

The characteristics of the switching arc as a function of N_2 filling pressure is studied in this thesis. However, the arc current amplitude is fairly low compared to that of the MV applications, and the frequency of the current in

the experiments is not a normal power frequency. It would be interesting to study the interruption performance of the ultrahigh-pressure N_2 arc under more common MV switching duties. Moreover, throughout this thesis, a fixed electrode arrangement is used, in comparison to the moving electrode arrangement in an actual circuit breaker. Hence, it would be interesting to use a moving electrode arrangement for further study. The moving electrode will allow for the performing of more tests without opening the pressure vessel, which may in turn make it possible to explore the limit of the interruption capability of the N_2 arc as a function of filling pressure.

In this thesis, no optical diagnostics of the arc are conducted. By utilising a high-speed camera, or using spectroscopic analysis of the spectrum, it is possible to gain valuable insight into the plasma. One possibility is to use a pressure tank with an optical window or to use fibre optical feedthrough into the pressure tank to carry out optical diagnostics.

It would be interesting to study the interruption performance in other gases at extremely high filling pressures, e.g. CO_2, which displays better current interruption characteristics.

The last suggestion for further work is to bring theory closer to the experimental results by developing numerical models for the current interruption process. The test switch has a very simple axisymmetric design. By developing multi-physics models that can reproduce the results seen in the experiments, a more complete understanding of the current interruption process could be obtained than that which it is possible to achieve through empirical investigations alone.

References

[1] G. P. Glasby, “Deep Seabed Mining: Past Failures and Future Prospects,” *Mar. Georesources Geotechnol.*, vol. 20, no. 2, pp. 161–176, Apr. 2002.

[2] T. Hazel, H. H. Baerd, J. J. Legeay, and J. J. Bremnes, “Taking Power Distribution Under the Sea: Design, Manufacture, and Assembly of a Subsea Electrical Distribution System,” *IEEE Ind. Appl. Mag.*, vol. 19, no. 5, pp. 58–67, Sep. 2013.

[3] A. Nordrum, “ABB Siemens Test Subsea Power Grids For Underwater Factories - IEEE Spectrum.” [Online]. Available: https://spectrum.ieee.org/energy/fossil-fuels/abb-siemens-test-subsea-power-grids-for-underwater-factories. [Accessed: 27-Sep-2019].

[4] J. V Sengers and J. M. H. L. Sengers, “Thermodynamic Behavior of Fluids Near the Critical Point,” *Annu. Rev. Phys. Chem.*, vol. 37, no. 1, pp. 189–222, Oct. 1986.

[5] J. Zhang, “Supercritical fluids for high power switching,” Eindhoven University of Technology, 2015.

[6] C. Shon, K. Song, Y. Oh, and H. Oh, “Investigation of the Supercritical Fluids as an Insulating Medium for High Speed Switching,” vol. 11, pp. 1–4, 2016.

[7] J. Zhang, A. H. Markosyan, M. Seeger, E. M. van Veldhuizen, E. J. M. van Heesch, and U. Ebert, “Numerical and Experimental Investigation of Dielectric Recovery in Supercritical N2,” *Plasma Sources Sci. Technol.*, vol. 24, no. 2, p. 025008, Feb. 2015.

[8] E. Jonsson, “Load Current Interruption in Air for Medium Voltage Ratings,” Norwegian University of Science and Technology, 2014.

[9] Z. Guo *et al.*, “Study of the Arc Interruption Performance of CO2 Gas in High-Voltage Circuit Breaker,” *IEEE Trans. Plasma Sci.*, vol. 47, no. 5, pp. 2742–2751, 2019.

[10] C. Green, *Switching Equipment*. Cham: Springer International Publishing, 2019.

[11] L. G. Christophorou, J. K. Olthoff, and R. J. Van Brunt, “Sulfur Hexafluoride and the Electric Power Industry,” *IEEE Electr. Insul. Mag.*, vol. 13, no. 5, pp. 20–24, Sep. 1997.

[12] H. P. Schmidt and G. Speckhofer, “Experimental and Theoretical Investigation of High-Pressure Arcs-Part I: the Cylindrical Arc Column (Two-Dimensional Modeling),” *IEEE Trans. Plasma Sci.*, vol. 24, no. 4, pp. 1229–1238, 1996.

[13] G. Speckhofer and H.-P. Schmidt, “Experimental and Theoretical Investigation of High-pressure Arcs. II. The Magnetically Deflected Arc (Three-dimensional Modeling),” *IEEE Trans. Plasma Sci.*, vol. 24, no. 4, pp. 1239–1248, 1996.

[14] E. H. Lock, A. V. Saveliev, and L. A. Kennedy, “Influence of Electrode Characteristics on DC Point-to-Plane Breakdown in High-Pressure Gaseous and Supercritical Carbon Dioxide,” *IEEE Trans. Plasma Sci.*, vol. 37, no. 6, pp. 1078–1083, Jun. 2009.

[15] H. Tanoue *et al.*, “Shock Wave Generated by Negative Pulsed Discharge in Supercritical Carbon Dioxide,” in *2013 19th IEEE Pulsed Power Conference (PPC)*, 2013, pp. 1–5.

[16] H. Tanoue, T. Furusato, K. Takahashi, S. H. R. Hosseini, S. Katsuki, and H. Akiyama, “Characteristics of Shock Waves Generated by a Negative Pulsed Discharge in Supercritical Carbon Dioxide,” *IEEE Trans. Plasma Sci.*, vol. 42, no. 10, pp. 3258–3263, Oct. 2014.

[17] H. Muneoka, K. Urabe, S. Stauss, and K. Terashima, “Breakdown Characteristics of Electrical Discharges in High-density Helium Near the Critical Point,” *Appl. Phys. Express*, vol. 6, no. 8, 2013.

[18] J. Zhang, B. van Heesch, F. Beckers, T. Huiskamp, and G. Pemen, “Breakdown Voltage and Recovery Rate Estimation of a Supercritical Nitrogen Plasma Switch,” *IEEE Trans. Plasma Sci.*, vol. 42, no. 2, pp. 376–383, Feb. 2014.

[19] J. Zhang *et al.*, “Breakdown Strength and Dielectric Recovery in a High Pressure Supercritical Nitrogen Switch,” *IEEE Trans. Dielectr. Electr. Insul.*, vol. 22, no. 4, pp. 1823–1832, Aug. 2015.

[20] K. Niayesh and M. Runde, *Power Switching Components*. Springer International Publishing, 2017.

[21] © 2018 IEEE. Reprinted, with permission from F. Abid, K. Niayesh, E. Jonsson, N. S. Stoa-Aanensen, and M. Runde, “Arc Voltage Characteristics in Ultrahigh-Pressure Nitrogen Including Supercritical Region,” *IEEE Trans. Plasma Sci.*, vol. 46, no. 1, pp. 187–193, Jan. 2018.

[22] © 2019 IEEE. Reprinted, with permission from F. Abid, K. Niayesh, and N. S. Stoa-Aanensen, "Ultrahigh-Pressure Nitrogen Arcs Burning Inside Cylindrical Tubes," *IEEE Trans. Plasma Sci.*, vol. 47, no. 1, pp. 754–761, Jan. 2019.

[23] F. Abid, K. Niayesh, N. Støa-Aanensen, E. Jonsson, and M. Runde, "Arc Voltage Measurements of Ultrahigh Pressure Nitrogen Arcs in Cylindrical Tubes," in *22nd international conference on gas discharge and their application*, 2018, pp. 91–94.

[24] F. Abid, K. Niayesh, S. B. Thimmappa, C. Espedal, and N. Støa-Aanensen, "Thermal Interruption Performance of Ultrahigh-Pressure Free-Burning Nitrogen Arc," in *21st International Symposium on High Voltage Engineering (ISH)*, Berlin, Heidelberg: SPRINGER, 2020, pp. 663–671.

[25] F. Abid, K. Niayesh, and N. Støa-Aanensen, "Arc Voltage Distribution Measurement in Tube Constricted Ultrahigh-Pressure Nitrogen Arc," in *International Symposium on High Voltage Engineering (ISH)*, Budapest, Hugary: Springer Nature, 2020, pp. 672–679.

[26] F. Abid, K. Niayesh, C. Espedal, and N. Støa-aanensen, "Current Interruption Performance of Ultrahigh- Pressure Nitrogen Arc," *Submitt. to J. Phys. D Appl. Phys.*

[27] F. Abid, K. Niayesh, and N. Støa-Aanensen, "Nozzle Wear And Pressure Rise In Heating Volume Of Self-Blast Type Ultra-High Pressure Nitrogen Arc," *Plasma Phys. Technol. J.*, vol. 6, no. 1, pp. 23–26, 2019.

[28] © 2019 IEEE. Reprinted, with permission from F. Abid, K. Niayesh, and N. Stoa-Aanensen, "Post-arc Dielectric Recovery Characteristics of Free-burning Ultrahigh-Pressure Nitrogen Arc," in *5th international conference on electric power equipment - switching technology, ICEPE-ST 2019*, 2019.

[29] F. Abid, K. Niayesh, E. Viken, N. Støa-aanensen, E. Jonsson, and H. K. Meyer, "Post-arc Dielectric Recovery Characteristics of Ultrahigh- Pressure Nitrogen Arc," *Submitt. to IEEE Transcations Dielectr. Electr. Insul.*

[30] D. Garzon, *High Voltage Circuit Breakers Design and Applications*. 2002.

[31] J. J. Lowke, "Simple Theory of Free-burning Arcs," *J. Phys. D. Appl. Phys.*, vol. 12, no. 11, pp. 1873–1886, Nov. 1979.

[32] K. C. Hsu and E. Pfender, "Modeling of a Free-burning, High-intensity Arc at Elevated Pressures," *Plasma Chem. Plasma Process.*, vol. 4, no. 3, pp. 219–234, Sep. 1984.

[33] P. Kovitya and J. J. Lowke, "Theoretical Predictions of Ablation-stabilised Arcs Confined in Cylindrical Tubes," *J. Phys. D. Appl. Phys.*, vol. 17, no. 6, pp. 1197–1212, Jun. 1984.

[34] C. B. Ruchti and L. Niemeyer, "Ablation Controlled Arcs," *IEEE Trans. Plasma Sci.*, vol. 14, no. 4, pp. 423–434, 1986.

[35] N. Osawa and Y. Yoshioka, "Analysis of Nozzle Ablation Characteristics of Gas Circuit Breaker," *IEEE Trans. Power Deliv.*, vol. 25, no. 2, pp. 755–761, 2010.

[36] L. Muller, "Modelling of an Ablation Controlled Arc," *J. Phys. D. Appl. Phys.*, vol. 26, no. 8, pp. 1253–1259, Aug. 1993.

[37] H. Edels, A. K. Halder, A. B. Shaw, and D. Whittaker, "Convection-free Post-arc Gap Recovery," *Nature*, vol. 193, no. 4812, pp. 263–264, Jan. 1962.

[38] A. Karimi and K. Niayesh, "A Simple Evaluation Method of the Thermal Interruption Limit of Power Circuit Breakers," *Electr. Eng.*, vol. 90, no. 8, pp. 523–528, Feb. 2009.

[39] H. Edels, D. Whittaker, K. G. Evans, and A. B. Shaw, "Experiments and Theory on Arc Reignition by Spark Breakdown," *Proc. Inst. Electr. Eng.*, vol. 112, no. 12, p. 2343, 1965.

[40] J. Aakervik, G. Berg, and S. Hvidsten, "Design of a High Voltage Penetrator for High Pressure and Temperature Laboratory Testing," in *2011 Annual Report Conference on Electrical Insulation and Dielectric Phenomena*, 2011, pp. 267–270.

[41] H. Taxt, K. Niayesh, and M. Runde, "Medium-Voltage Load Current Interruption in the Presence of Ablating Polymer Material," *IEEE Trans. Power Deliv.*, vol. 33, no. 5, pp. 2535–2540, Oct. 2018.

[42] M. Barrault, G. Bernard, J. Maftoul, and S. Rowe, "Post-arc Current Measurement Down to the Ten Milliamperes Range," *IEEE Trans. Power Deliv.*, vol. 8, no. 4, pp. 1782–1788, 1993.

[43] C. Wang *et al.*, "Thermodynamic and Transport Properties of Real Air Plasma in Wide Range of Temperature and Pressure," *Plasma Sci. Technol.*, vol. 18, no. 7, 2016.

[44] A. D'angola, G. Colonna, C. Gorse, and M. Capitelli, "Thermodynamic and transport properties in equilibrium air plasmas in a wide pressure and temperature range," *Eur. Phys. J. D*, vol. 46, pp. 129–150, 2008.

[45] Y. Babou, P. Corfdir, and R.-P. Suetterlin, “Experimental Assesment of PTFE Post-arc Ablation,” *Plasma Phys. Technol.*, vol. 6, no. 2, pp. 148–151, 2019.

[46] F. W. Crawford and H. Edels, “The Reignition Voltage Characteristics of Freely Recovering Arcs,” *Proc. IEE Part A Power Eng.*, vol. 107, no. 32, p. 202, 1960.

[47] J. P. Novak, “Electric Field and Electrode Potential Drops of Arcs and Glow Discharges in Air,” *J. Appl. Phys.*, vol. 62, no. 12, pp. 4719–4724, Dec. 1987.

[48] W. A. Gambling and H. Edels, “The High-pressure Glow Discharge in Air,” *Br. J. Appl. Phys.*, vol. 5, no. 1, pp. 36–39, Jan. 1954.

[49] M. Seeger, G. Naidis, A. Steffens, H. Nordborg, and M. Claessens, “Investigation of the Dielectric Recovery in Synthetic Air in a High Voltage Circuit Breaker,” *J. Phys. D. Appl. Phys.*, vol. 38, no. 11, pp. 1795–1804, Jun. 2005.